AD-A065 783 FOREIGN TECHNOLOGY DIV WRIGHT-PATTERSON AFB OHIO F/G 20/4
SCIENTIFIC NOTES FROM THE CENTRAL AEROHYDRODYNAMIC INSTITUTE.(U)
JUL 78
UNCLASSIFIED FTD-ID(RS)T-0680-78 NL

1 OF 3
AD
A065783

FTD-ID(RS)T-0680-78

1

FOREIGN TECHNOLOGY DIVISION

SCIENTIFIC NOTES FROM THE CENTRAL
AERO-HYDRODYNAMIC INSTITUTE

Approved for public release;
distribution unlimited.

UNEDITED MACHINE TRANSLATION

FTD-ID(RS)T-0680-78 6 July 78

MICROFICHE NR: FTD-78-C-000925

SCIENTIFIC NOTES FROM THE CENTRAL AERO-HYDRODYNAMIC INSTITUTE

English pages: 260

Source: Uchenyye Zapiski TsAGI, Moscow, Vol. 1, No. 2, 1970, pp. 1-124, foreign pages 46-52 originally translated under FTD-MT-24-0006-72 and FTD-HT-23-708-73, foreign pages 111-114 originally translated under FTD-MT-24-21-72

Country of origin: USSR
Requester: FTD/TQTA

PREPARED BY:

TRANSLATION DIVISION
FOREIGN TECHNOLOGY DIVISION
WP-AFB, OHIO.

Table of Contents

U. S. BOARD ON GEOGRAPHIC NAMES TRANSLITERATION SYSTEM

Block	Italic	Transliteration	Block	Italic	Transliteration
А а	*А а*	A, a	Р р	*Р р*	R, r
Б б	*Б б*	B, b	С с	*С с*	S, s
В в	*В в*	V, v	Т т	*Т т*	T, t
Г г	*Г г*	G, g	У у	*У у*	U, u
Д д	*Д д*	D, d	Ф ф	*Ф ф*	F, f
Е е	*Е е*	Ye, ye; E, e*	Х х	*Х х*	Kh, kh
Ж ж	*Ж ж*	Zh, zh	Ц ц	*Ц ц*	Ts, ts
З з	*З з*	Z, z	Ч ч	*Ч ч*	Ch, ch
И и	*И и*	I, i	Ш ш	*Ш ш*	Sh, sh
Й й	*Й й*	Y, y	Щ щ	*Щ щ*	Shch, shch
К к	*К к*	K, k	Ъ ъ	*Ъ ъ*	"
Л л	*Л л*	L, l	Ы ы	*Ы ы*	Y, y
М м	*М м*	M, m	Ь ь	*Ь ь*	'
Н н	*Н н*	N, n	Э э	*Э э*	E, e
О о	*О о*	O, o	Ю ю	*Ю ю*	Yu, yu
П п	*П п*	P, p	Я я	*Я я*	Ya, ya

*ye initially, after vowels, and after ъ, ь; e elsewhere.
When written as ё in Russian, transliterate as yё or ё.

RUSSIAN AND ENGLISH TRIGONOMETRIC FUNCTIONS

Russian	English	Russian	English	Russian	English
sin	sin	sh	sinh	arc sh	$\sinh^{-1}$
cos	cos	ch	cosh	arc ch	$\cosh^{-1}$
tg	tan	th	tanh	arc th	$\tanh^{-1}$
ctg	cot	cth	coth	arc cth	$\coth^{-1}$
sec	sec	sch	sech	arc sch	sech^{-1}
cosec	csc	csch	csch	arc csch	csch^{-1}

Russian	English
rot	curl
lg	log

Page A.

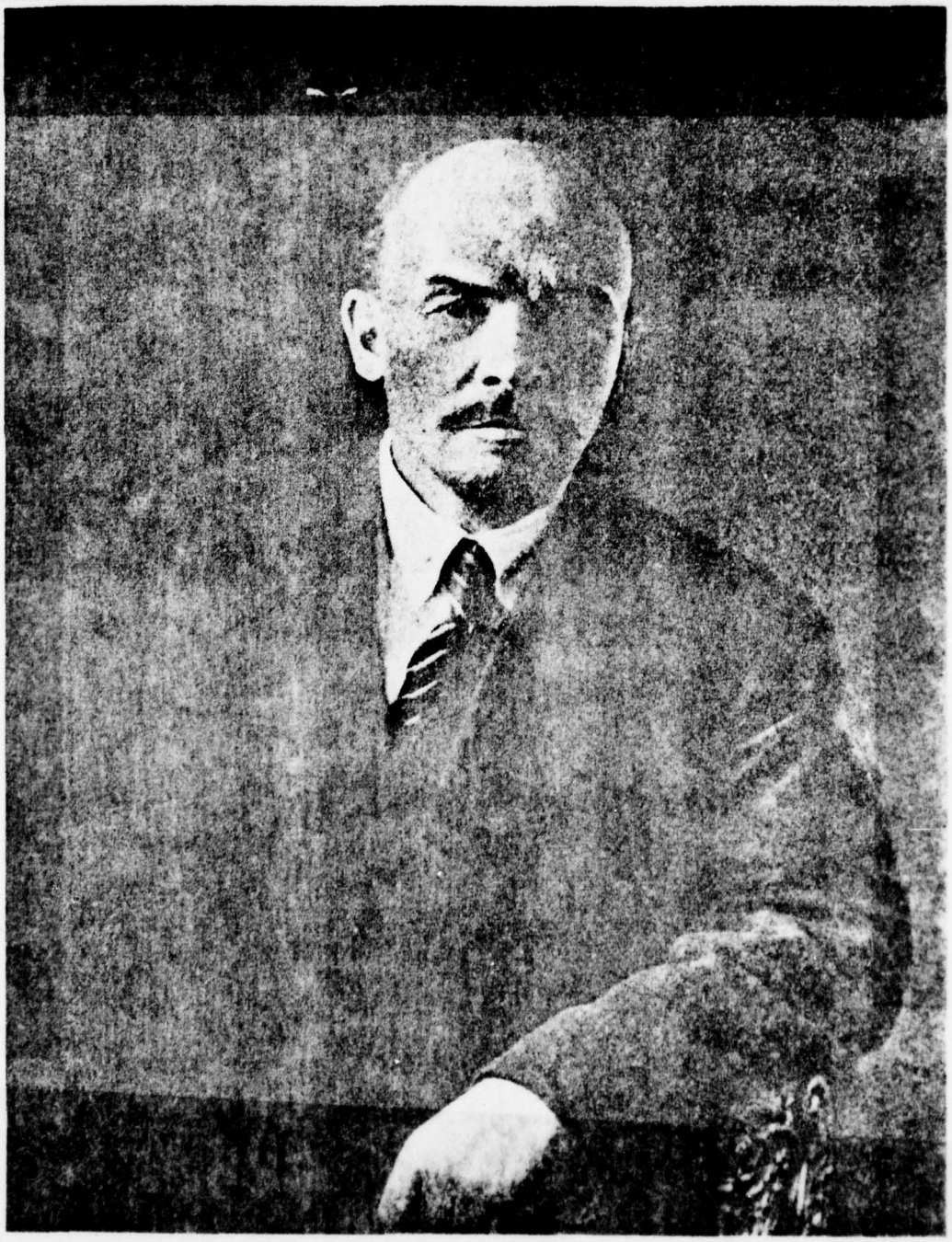

Were carried out 100 years from the birthday of Vladimir Ilyich Lenin - greatest revolutionary, leader of the Communist Party, founder of the first in the world socialist state.

"With name and Lenin's activity is connected whole revolutionary epoch in humanity's life. Lenin gave answer/responses to the most urgent questions, placed by the course of historical development, he thoroughly developed the theory of the Socialist Revolution and building Communist society, it armed russian, all the international revolutionary movement by scientifically substantiated strategy and tactics, it headed the fight of class for the conversion of the ideals of socialism in life. Socialism, converted by Marx and Engels from utopia into science and enriched by Lenin by new conclusion/derivations and discovery/openings, was personified into the social practice of world-wide historical scales, it became basic revolutionary force of our time". (Theses of the CC of KPSS [CPSU] to the 100th anniversary from the birthday of V. I. Lenin).

Lenin, the greatest scientist in revolution and revolutionary in science, gave enormous value to questions of the scientific-technical progress of our country. From the first days of the existence of Soviet state, all possible and comprehensive development of science

and technology became one of the most important and systematic directions of the activity of the Communist Party and Soviet government.

In heavy 1918, when young Soviet republic in lethal fight reflected the brightness onset of counter revolution, Lenin writes the "sketch of the plan of scientific-technical work" for the Academy of Sciences, in which he scientifically assigned the mission of developing the plan/layout of the reorganization of industry and economic lift of Russia. This plan/layout strikes with its depth, newness of posing of problems, with organic communication/connection with life. Under Vladimir Ilyich's management/manual in the same period, was developed the plan/layout of the electrification of Russia - plan/layout GOELRO [State Commission for the Electrification of Russia], to realization of which Lenin gave enormous value.

Vladimir Ilyich paid great attention to development of Soviet aviation and technology. Lenin supported great Russian scholarly professor N. E. Joukowski's proposition about the organization of central aerohydrodynamic institute. TsAGI [' Central Institute of Aerohydrodynamics im. N. Ye Zhukovskiy is the authentic creation of Great October. Because of the daily concerns of the Communist Party and Soviet government of TsAGI, it became the world famous

scientific research aviation center, equipped with modern research equipment, disposing of the highly skilled scientific personnel/frames.

Following Lenin's legacy, Soviet people under the management/manual of the Communist Party carried out an industrialization of the country, they converted our native land into mighty socialist power, the reliable stronghold of peace, progress and socialism.

Page C.

Science in our country ever more and more is converted into the direct productive force of society. The Communist Party takes all measures for realizing the Leninist precept about that, "so that the science for us would not remain a dead letter or fashionable phrase ... so that the science real/actually would enter in the flesh and the blood, it was converted into the component element of mode of life completely and by present form". (Coll. works, Vol. 45, page 391).

Published during October 1968. The resolution by the CC of the CPSU and Council of Ministers of the USSR "about measures for the increase of the effectiveness of the work of scientific organizations

and the acceleration of use in the national economy of the achievements of science and technology" is directed toward further increase in the effectiveness of scientific investigations.

Soviet scientists, accurate to Lenin's legacy, direct their efforts for the solution of stated before them by party/batch and government most important problems in further increase in the effectiveness of scientific investigations for purpose of the provision for technical progress.

Page 1.

METHOD OF CALCULATION OF FLOW AROUND A BODY OF REVOLUTION OF ANY FORM DURING ARBITRARY MOTION IN IDEAL FLUID.

L. A. Maslov.

Is proposed the method of calculation of distribution of the speed, pressure and potential on surface, and also in any point of space around the body of revolution, which accomplishes arbitrary motion in ideal fluid. In comparison with known methods in this case to the form of body of revolution, are superimposed no limitations and sufficient accuracy/precision of calculations is reached at the considerably smaller expenditures of time EVM [computer]. Examples of calculations are compared with known exact solutions and with the experimental values of pressures on the surface of different bodies.

At present the potential flow around the bodies of revolution of any form during arbitrary motion can be designed only with the aid of method [1]. However, method [1] it is very laborious, and more effective proves to be the method of calculation of flow about body of revolution during arbitrary motion, presented in works [2] and

[3]. Method [2], furthermore, easily it is spread to the case of the calculation of three-dimensional body during arbitrary motion [4]. However, during its use on surface are superimposed some limitations.

In this article is proposed the calculation method, which represents by itself the generalization of method [2]. In this case, the method of the assignment to body surface makes it possible to examine the bodies of revolution of any form during arbitrary motion.

1. Fundamental principles. If v_1, v_2, v_3 - projection of vector $\vec{v}$ of the forward velocity of pole A of solid body, and Ω_1, Ω_2, Ω_3 - to the projection of angular velocity vector $\vec{\Omega}$, on the connected with the body axes of coordinates xyz, then for the potential of the disturbed velocities of liquid it is possible to write

$$\Phi(x, y, z, t) = \sum_{i=1}^{6} v_i(t)\Phi_i(x, y, z),$$

where are introduced designations $v_4 = l\Omega_1$; $v_5 = l\Omega_2$; $v_6 = l\Omega_3$ (l - length of body).

Page 2.

For determining each of six single potentials $\Phi_i(x, y, z)$ it is required to solve the exterior problem of Neumann

$$\Delta\Phi_i = 0; \quad \left.\frac{\partial\Phi_i}{\partial n}\right|_{\infty} = \frac{\vec{v}_i \cdot \vec{n}}{v_i} \quad (i = 1, 2, \ldots, 6) \qquad (1.1)$$

with zero conditions at infinity. Here v_i - the velocity of the points of body surface in the appropriate simple motion; ω - surface, which limits solid body; n - normal to the surface ω, directed inside liquid. If we the solution search for in the form of the potential of the simple layer

$$\Phi_i(P) = -\iint_{\omega} \mu_i(Q) \frac{d\omega}{R}, \qquad (1.2)$$

the boundary condition (1.1) is reduced to the integral second-order of Fredholm equation relative to the intensity of layer μ

$$2\pi\mu_i(P) + \iint_{\omega} \mu_i(Q) \frac{\vec{R}\cdot\vec{n}(P)}{R^3} d\omega = \vec{v}_i(P)\cdot\vec{n}(P), \qquad (1.3)$$

where P - an arbitrary calculation point; Q - current point of surface ω; $\vec{R} = \overrightarrow{QP}$.

Equation (1.3) has unique solution, if surface ω belongs to the class of Lyapunov's surfaces [5].

The longitudinal X-axis of the Cartesian system of coordinates xyz with unit vectors $\vec{i}\vec{j}\vec{k}$ coincides with the axis of the symmetry of body of revolution. The origin of coordinates is placed in the leading edge/nose of body (Fig. 1). Together with Cartesian system is examined the system of cylindrical coordinates xrθ (u = r cos θ, z =

r sin θ). To the calculation point P appropriate themselves coordinates xrθ, to the current point Q - ccordinate ξρϑ; $\vec{R}$ = (x-ξ) $\vec{i}$ + (r cos θ - ρ sin ϑ) $\vec{j}$ + (r sin θ - ρ sin ϑ) $\vec{k}$.

If pole A is selected on X-axis at a distance x_A from carrying body, then for the velocity of the points of body surface during its arbitrary motion it is possible to write

$$\vec{v} = (v_5 r \sin\theta - v_6 r \cos\theta - v_1)\vec{i} + [v_6(x - x_A) - v_4 r \sin\theta - v_2]\vec{j} + \\ + [v_4 r \cos\theta - v_5(x - x_A) - v_3]\vec{k}, \qquad (1.4)$$

where the linear dimensicns are referred to the length of body 1.

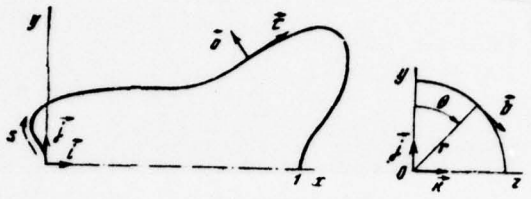

Fig. 1.

Page 3.

Equation of generatrix of body of revolution

$$r = r(x) \tag{1.5}$$

is represented in the parametric form:

$$r = r(s);\ x = x(s), \tag{1.6}$$

where s - an arc length of generatrix, calculated off the origin of ccordinates. The value of parameter s, characterizing the current point Q of body surface, is designated by letter σ.

Por the representation of the differential cell/elements of surface, are introduced the designations

$$r' = \frac{\partial r}{\partial s};\quad x' = \frac{\partial x}{\partial s}. \tag{1.7}$$

The element of area of surface is equal to

$$d\omega = rdsd\theta.$$

At each point of body surface, is introduced the connected with this pcint rectangular coordinate system whose unit vectors are equal to

$$\left.\begin{aligned} \vec{n} &= -r'\vec{i} + x'\cos\theta\vec{j} + x'\sin\theta\vec{k}; \\ \vec{\tau} &= x'\vec{i} + r'\cos\theta\vec{j} - r'\sin\theta\vec{k}; \\ \vec{b} &= -\sin\theta\vec{j} + \cos\theta\vec{k}; \end{aligned}\right\} \qquad (1.8)$$

here $\vec{n}$ - standard; vector $\vec{\tau}$ it is directed tangentially toward generatrix to the side of an increase in the arc length s; vector $\vec{b}$ lie/rests at transverse plane and forms with $\vec{n}$ and $\vec{\tau}$ right-handed coordinate system.

Unlike method [2], where the surface is assigned in the form of (1.5) and is utilized tle derivative dr/dx, in this case form (1.6) makes it possible to present any the curve, which limits simply connected region.

As a result of substitutions, fundamental integral equation (1.3) takes the form

$$2\pi\mu_i(s,\theta) = \vec{v}_i\vec{n}(s,\theta) - \int_0^L\int_0^{2\pi}\mu_i(\sigma,\vartheta)\frac{[x'r - r'(x-\xi) - x'\rho\cos(\theta-\vartheta)]\rho d\sigma d\vartheta}{[(x-\xi)^2 + r^2 + \rho^2 - 2r\rho\cos(\theta-\vartheta)]^{3/2}}, \qquad (1.9)$$

where L - complete arc length of generatrix frcm forepart/nose point x = 0, r = 0) to the tailed (x = l, r = 0).

Analogous expressions are obtained for velocities and potentials.

2. Calculation formulas. as it follows from the considerations cf symmetry, for the characteristic of the arbitrary motion of body of revolution in ideal fluid, it suffices tc know the parameters of flcw only for three simple motions:

- forward/progressive along X-axis with a velocity of v_1 = 1 (i = 1).

- forward/progressive along y axis with a velocity of v_2 = 1 (i = 2).

- rotary around transverse axis, for example the parallel z axis and passing through pole A, with angular is velocity v_6 = 1 (i = 6).

The total values of relative velocity and potential on the body surface of rotation it is possible to present in the form

$$\vec{U} = \vec{\tau}[u_{1\tau}v_1 + u_{2\tau}(v_2\cos\vartheta + v_3\sin\vartheta) + u_{6\tau}(v_6\cos\vartheta - v_5\sin\vartheta)] + \\ + \vec{b}[u_{2b}(v_2\sin\vartheta - v_3\cos\vartheta) + u_{6b}(v_6\sin\vartheta + v_5\cos\vartheta) - rv_4]; \quad (2.1)$$

$$\Phi = l[\varphi_1 v_1 + \varphi_2(v_2\cos\vartheta + v_3\sin\vartheta) + \varphi_6(v_6\cos\vartheta - v_5\sin\vartheta)], \quad (2.2)$$

where u_{ir} and u_{ib} - dimensionless components of relative velocities on axes r and b. φ_i - the dimensionless potentials in the appropriate simple motion, which are subject to further determination.

Solution μ_i of integral equation (1.9) for the simple motions indicated should be searched for in the form

$$\mu_1(s, \theta) = \mu_1(s); \quad \mu_2(s, \theta) = \mu_2(s)\cos\theta; \quad \mu_6(s, \theta) = \mu_6(s)\cos\theta. \qquad (2.3)$$

Instead of source strength $\mu_i(s)$ it is convenient to examine other unknown functions $g_i(s)$, connected with μ_i the relationship/ratios

$$g_i = 2\pi r \frac{\mu_i}{v_i}, \qquad (2.4)$$

and all the calculations of news in a dimensionless form, accepting as characteristic linear dimension the length of body 1.

After the substitution of values (2.3) and (2.4) into equation (1.9) and the prolonged conversions, analogous given in work [2], integral equations for each simple motion (i = 1, 2, 6) they take the form

$$g_i(s) = f_{i0}(s) - \int_0^L g_i(\sigma) K_{i0}(s, \sigma)\, d\sigma. \qquad (2.5)$$

Here for known functions $f_{l0}(s)$, equal to the product of the normal component of the velocity of following to a radius of body at the particular point, are utilized the relationship/ratios

$$f_{10} = rr'; \quad f_{20} = -rx'; \quad f_{60} = r[rr' + x'(x - x_A)]. \tag{2.6}$$

The nuclei of integrals are designated:

$$\left.\begin{aligned} &K_{10}(s, \sigma) = (BG_1 + x'G_2)A; \quad K_{20}(s, \sigma) = K_{60}(s, \sigma) = (BH_1 + x'H_2)A; \\ &A = \frac{1}{\pi\sqrt{(x-\xi)^2 + (r+\rho)^2}}; \quad B = \frac{2r[x'(r-\rho) - r'(x-\xi)]}{(x-\xi)^2 + (r-\rho)^2}; \\ &G_1 = E(k^2); \quad G_2 = K(k^2) - E(k^2); \\ &H_1 = \frac{1}{k^2}[(1+k'^2)E(k^2) - 2k'^2K(k^2)]; \\ &H_2 = \frac{1}{k^2}[(1+3k'^2)K(k^2) - (3+k'^2)E(k^2)], \end{aligned}\right\} \tag{2.7}$$

where K(k²) and E(k²) - complete elliptical integrals of the first and second kind with the module/modulus

$$k^2 = \frac{4r\rho}{(x-\xi)^2 + (r+\rho)^2} \quad \text{and} \quad k'^2 = 1 - k^2.$$

Page 5.

Analogously are obtained calculated relationship/ratios for the components of the dimensionless velocities and potentials, indicated in formulas (2.1) and (2.2):

$$\left.\begin{aligned} u_{i\tau}(s) &= f_{i1}(s) + \int_0^L g_i(\sigma) K_{i1}(s, \sigma)\, d\sigma; \\ u_{ib}(s) &= f_{i2}(s) + \frac{1}{r}\int_0^L g_i(\sigma) K_{i2}(s, \sigma)\, d\sigma; \end{aligned}\right\} \tag{2.8}$$

$$\varphi_i(s) = -\int_0^L g_i(\sigma) K_{i2}(s, \sigma)\, d\sigma; \tag{2.9}$$

$$f_{11} = x'; \quad f_{21} = r'; \quad f_{61} = rx' - r'(x - x_A);$$
$$f_{22} = -1; \quad f_{62} = x - x_A;$$

$$\left.\begin{aligned} K_{11}(s, \sigma) &= \left(CG_1 + \frac{r'}{r} G_2\right) A; \quad K_{12}(s, \sigma) = G_3 A; \\ K_{21}(s, \sigma) = K_{61}(s, \sigma) &= \left(CH_1 + \frac{r'}{r} H_2\right) A; \; K_{22}(s, \sigma) = K_{62}(s, \sigma) = H_3 A. \end{aligned}\right\} \tag{2.10}$$

where besides the values, determined to formulas (2.7), are introduced the designations

$$\left.\begin{aligned} C &= \frac{2x'(x - \xi) + r'(r - \rho)}{(x - \xi)^2 + (r - \rho)^2}; \quad G_3 = 2K(k^2); \\ H_3 &= \frac{2}{k^2}\left[(1 + k'^2) K(k^2) - 2E(k^2)\right]. \end{aligned}\right\} \tag{2.11}$$

At the end points where x = 0, r = 0, or x = 1, r = 0, are not difficult to show that integral of equation (2.5) always have zero solution and do not require special examination, as is done in method [2]. During the determination of the values of the velocities and potentials in end points, it suffices to calculate the components of dimensionless velocity during transverse and rotary motions (i = 2.6) along y axis

$$u_{iy} = c_i - \int_0^L \frac{g_i(\sigma)\rho\, d\sigma}{2\left|(x - \xi)^2 + \rho^2\right|^{3/2}} \tag{2.12}$$

and dimensionless potential during the longitudinal flow

$$\varphi_1 = -\int_0^L \frac{g_1(\sigma)\,d\sigma}{[(x-\xi)^2+\rho^2]^{1/2}}, \qquad (2.13)$$

where $C_2 = 1$, for forepart/nose turn/sharpen one should place $x = 0$ and $c_6 = x_A$, but for the tailed point $x = 1$ and $c_6 = x_A - 1$. The remaining components of the velocities and potentials in these points are equal to zero.

Page 6.

The velocities in the points of space, which do not belong to body surface, are conveniently calculated in cylindrical coordinate system $xr\theta$. For the components of the dimensionless velocity in each simple motion, it is not difficult to obtain

$$\left.\begin{aligned} u_{ix}(x, r) &= f_{i3}(x) + \int_0^L g_i(\sigma) K_{i3}(x, r, \sigma)\,d\sigma; \\ u_{ir}(x, r) &= f_{i4}(x) + \int_0^L g_i(\sigma) K_{i4}(x, r, \sigma)\,d\sigma; \\ u_{i\theta}(x, r) &= f_{i2}(x) + \frac{1}{r}\int_0^L g_i(\sigma) K_{i2}(x, r, \sigma)\,d\sigma. \end{aligned}\right\} \qquad (2.14)$$

In this case, to formula for u_{i6} it ccincides with formula (2.8) for u_{ib}, and for the nuclei of the integrals of first two formulas (2.14) are introduced the designations

$$K_{13}=\frac{2(x-\xi)}{r_1^2}G_1A;\quad K_{14}=\left(2\frac{r-\rho}{r_1^2}G_1+\frac{1}{r}G_2\right)A;$$
$$K_{23}=K_{63}=\frac{2(x-\xi)}{r_1^2}H_1A;\ K_{24}=K_{64}=\left(2\frac{r-\rho}{r_1^2}H_1+\frac{1}{r}H_2\right)A.$$

Here $r^2_1 = (x-\xi)^2 + (r-\rho)^2$, and for remaining values are used designations (2.7) and (2.10). The dimensionless components of velocity of following $f_{i3}(x)$ and $f_{i4}(x)$ are equal to $f_{13} = f_{24} = 1$; $f_{14} = f_{23} = f_{63} = 0$; $f_{64} = x_A - x$.

For the calculations of pressure coefficients in the case of arbitrary motion, one should use Lagrange's integral. During the calculation of apparent additional masses, it is necessary to bear in mind, that for a body of revolution independent variables and not equal to zero are identically four apparent additional masses: λ_{11}, λ_{22}, λ_{26} and λ_{66}. By analogy with work [3] it is not difficult to obtain

$$\left.\begin{aligned}
\lambda_{11} &= -2\pi\rho_0\int_0^L rr'\varphi_1\,ds;\\
\lambda_{22} &= \pi\rho_0\int_0^L rx'\varphi_2\,ds;\\
\lambda_{26} &= -\pi\rho_0\int_0^L r\,|rr'+x'(x-x_A)|\,\varphi_2\,ds;\\
\lambda_{66} &= -\pi\rho_0\int_0^L r\,|rr'+x'(x-x_A)|\,\varphi_6\,ds,
\end{aligned}\right\}\qquad(2.15)$$

where ρ_0 - mass density of liquid.

3. Methods of calculations. The sclutien of the fundamental integral equation of problem (2.5) is determined in the finite number of discrete calculation points of body surface. The the intricate shape of body, the greater the calculation points it is necessary to select for the sufficiently precise description of generatrix. So, in that comprised for computers "Minsk-2" to the program, according to which were fulfilled examples of calculations, can be utilized to 160 calculation points, arbitrarily arrange/located on by generatrix bodies of revolution. For example, for smooth bodies sufficient accuracy/precision is reached at 50 calculation points.

Page 7.

The proposed method allow/assumes the presence of the finite number of salient points of the enclosures of generatrix. At very salient point for formal satisfaction of Lyapunov's conditions, one should assume a small bending radius. In the process of calculations, the rounding is realize/accomplished automatically applying quadratic interpolation between calculation points. In the places of an abrupt change in the enclosures, is necessary the packing/seal of calculation points.

Basic difficulty is the calculation of improper integrals in equations and formulas for velocities and potentials. By analogy with work [2] improper integrals are calculated with the aid of the replacement of variables:

$$\sigma - s = \operatorname{sign}(h)\frac{0{,}5\,Lh^2}{1-h^2}. \tag{3.1}$$

Inverse dependence will be determined by relationship/ratio

$$h(s,\sigma) = \operatorname{sign}(\sigma - s)\sqrt{\frac{|\sigma - s|}{|\sigma - s| + 0{,}5\,L}}; \tag{3.2}$$

$$d\sigma = \frac{dh}{h'}; \quad \frac{1}{h'} = \frac{4}{L}\sqrt{|\sigma - s|(|\sigma - s| + 0{,}5\,L)^3}. \tag{3.3}$$

Reference point alternating/variable h coincides with the special feature/peculiarity of integral, which is located in the calculation point whose coordinate s projects in this formula as parameter. Functions (3.2) and (3.3) are continuous and different frcm zero everywhere, with the exception/elimination of most singular pcint where (3.3) it vanishes as $|s-\sigma|^{1/2}$.

By analogy with work [4] replacement is utilized only on the section

$$|s-\sigma| \leqslant 0{,}05\,L, \tag{3.4}$$

i.e. near singular point. Integrals are represented in the form

$$\int_0^L g(\sigma)\,K(s,\sigma)\,d\sigma = \int_0^{s-0.05L} g(\sigma)\,K d\sigma + \int_{s+0{,}05\,L}^{L} g(\sigma)\,K d\sigma + \int_{-1/\sqrt{11}}^{1/\sqrt{11}} g(\sigma)\,K\frac{dh}{h'}. \tag{3.5}$$

In formula (3.5) with $s \leqslant 0.05L$ first term, but with $s \geqslant 0.95L$ second term they are not considered, since in these cases they are

included in the third. In this case, the limits of the third integral respectively change and are calculated directly from formula (3.2), where one should place $\sigma = 0$ in the first case and $\sigma = L$ in the second.

The first two integrals of formula (3.5) do not have a special feature/peculiarity and are calculated with the aid of trapezoidal rule on the node/units of integration, arrange/located in calculation points. Last/latter integral is calculated from trapezoidal rule with the constant space in new alternating/variable h. In this case replacement (3.2) provides the symmetrical location of the node/units of integration relative to special feature/peculiarity with an increase of the density of the location of node/units in its vicinity, which corresponds to the conditions for existence of principal value for Cauchy and it makes it possible to calculate improper integrals according to trapezoidal rule with the constant space in new variables. necessary in this case values $g(\sigma)$, $\varepsilon(\sigma)$ and $\rho(\sigma)$ in the node/units of integration, which prove to be between calculation points, are determined by quadratic interpolation according to Newton [6].

Integral equations are solved by the method of successive approximations according to the following diagrams:

for i = 1

$$g_{10} = \frac{1}{2} f_{10}; \quad g^*_{1k} = f_{10} - \int g_{1,k-1} K_{10}\, d\sigma; \quad g_{1k} = \frac{1}{2}(g^*_{1k} + g_{1,k-1});$$

for i = 2.6

$$g_{i0} = f_{i0}, \quad g_{ik} = f_{i0} - \int g_{i,k-1} K_{i0}\, d\sigma,$$

where k - a number of approach/approximatien.

Page 8.

Solution is considered found, if

$$|g_{ik}(s) - g_{i,k-1}(s)|_{\max} < 0{,}005\, |f_{i0}|_{\max},$$

i.e. boundary conditions (1.3) are fulfilled with accuracy/precision by 0.5o/o. The number of approach/approximatiens oscillates from 4 for smooth bodies to 10-15 for the bodies of intricate shape.

Information about body is assigned by the tables of values x and r calculation points. Derivatives (1.7) are calculated with the aid of Newton's formulas from values of x and r at three calculation points [6]. Integrals in the formulas of apparent additional masses (2.15) are calculated from trapezoidal rule. Space alternating/variable h was selected as being equal to $\Delta h = 1/\sqrt{1536}$.

4. Examples of calculations. For purpose of checking the method presented on computers "Minsk-2" for ellipscids of revolution are carried out the calculations of apparent additional masses and relative velocities for which are known precise analytical expressions [7]. The applicability of method to the determination of pressures in real liquid is shown based on the example of the calculation of the body, which has the vertical section of generatrix, for which could not be obtained the solution by method [2], or bodies in the form of the combination of the cone with cylinder, having a local abrupt change in the enclosures.

In Fig. 2 and 3 points plotted/applied the results of calculation by the proposed method of dimensionless velocities on the surface of the elliptical disk, which has the relationship/ratio of semi-axes a/b = ◄ 0.1, and the ellipscid which has a/b = 9. By solid lines are constructed precise values of velocities. Calculation of velocity field is checked on the example of the flow around the sphere of single diameter of forward/progressive flow along X-axis. Table 1 gives corrected values of velocity u_{1x} the points of vertical diameter (x = 0.5), also, in the points of horizontal diameter (y = 0), arrange/located on different distances from the surface of sphere.

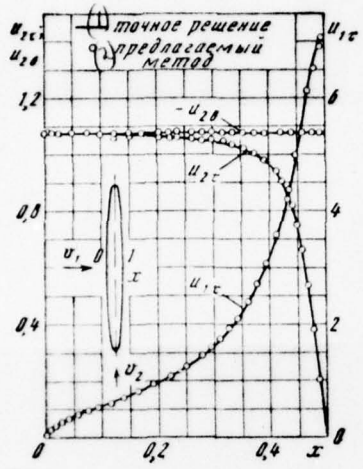

Fig. 2.

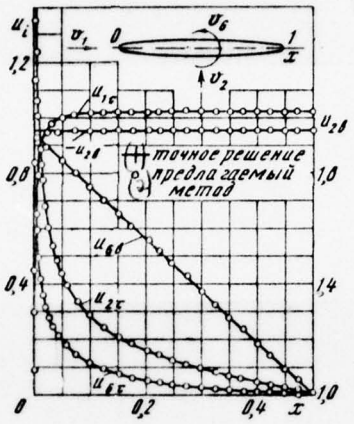

Fig. 3.

Fig. 2.

Key: (1). Exact solution. (2). proposed method.

Fig. 3.

Key: (1). Exact solution. (2). proposed method.

Page 9.

Results of the calculation of the coefficients of apparent

additicnal masses for three ellipsoids by the proposed method are given in comparison with precise values in table 2.

The comparison of precise velccities and apparent additional masses with the results of calculaticns acccrding to the proposed method they testify to sufficient accuracy/precision of the latter. The disagreement of precise and calculated values comprises less than 1c/o.

Fig. 4 and 5, show the comparison of the calculated and experimental values of the coefficient of pressure $\bar{p}$ in the nose section of the body surface, which contain the vertical section of duct/contour. Fig. 4, shows the enclosures of bodies of revolution 1-3 and is given distribution $\bar{p}$ at zero angle of attack [1].

FOOTNOTE [1]. Bodies of revolution 1-3 correspond to engine nacelles No. 25, 85 and 87, investigated experimentally in work [8].
ENDFOOTNOTE.

In Fig. 5, is constructed distributicn p according to one meridian of body of revolution 3 at the angle of attack $\alpha = -10°$, when this meridian is windward, and the angle of attack $\alpha = 10°$, when this meridian becomes leeward. The agreement of the results of calculation with experiment proves to be sufficiently good.

table 1.

(1) Отстояние от поверхности	(2) Значения скорости u_{1x}		(1) Отстояние от поверхности	(2) Значения скорости u_{1x}	
	(3) по предлагаемому методу	(4) точные значения		(3) по предлагаемому методу	(4) точные значения
(5) По вертикальному диаметру			(6) По горизонтальному диаметру		
0,01	1,470	1,471	0,01	0,0587	0,577
0,1	1.288	1,289	0,1	0,4213	0,4213
2,0	1,004	1,004	2,0	0,9920	0,9920

Key: (1). Distance from surface. (2). Values of velocity. (3). according to proposed method. (4). precise values. (5). According to vertical diameter. (6). According to horizontal diameter.

Table 2.

$\frac{a}{b}$	K_{11}	K_{22}	K_{66}	K_{11}	K_{22}	K_{66}
	(1) по предлагаемому методу			(2) точные значения		
0,1	6,130	0,0751	—	6,184	0,0748	—
1,0	0,499	0,500	—	0,500	0,500	—
9.0	0,0244	0,950	0,860	0,0244	0,954	0,864

Key: (1). according to the proposed method. (2). precise values.

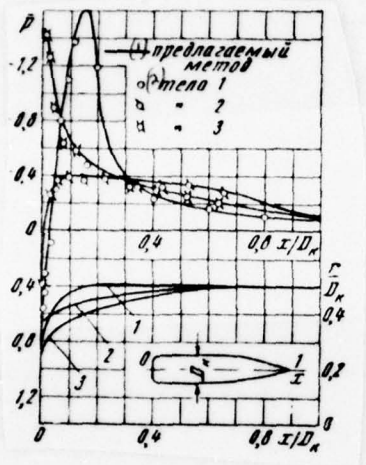

Fig. 4.

Key: (1). the proposed method. (2). body.

Page 10.

The same good convergence of the calculated and experimental values of pressure is obtained for the nose section of the body, which represents by itself to the combination of cone with cylinder (Fig. 6).

It must be noted that the results, given to Fig. 4, for a body with the vertical sections of generatrix at zero angle of attack can be obtained with the aid of methods [1] and [9], while the case of

flow at angle of attack it can be designed only according to method [1]. In method [9] by virtue of the use of function of current, can be examined only axial motion of body of revolution. Examples of the calculations of the bodies of revolution, which have the local abrupt changes in the form of enclosures, given to Fig. 2 and 6, they are encountered only of the authors of work [1]. However, in method [1] the volume of calculations proves to be considerably greater than in this case.

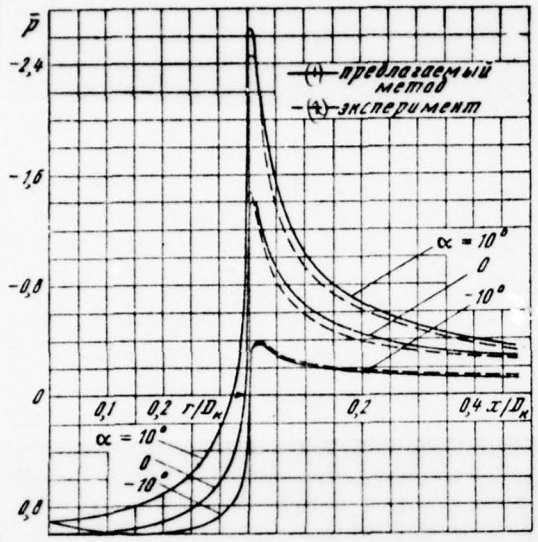

Fig. 5

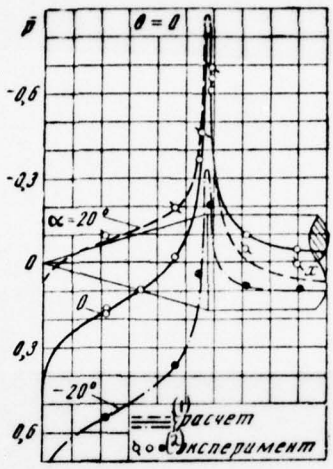

Fig. 6.

Fig. 5.

Key: (1). the proposed methcd. (2). experiment.

Fig. 6.

Key: (1). calculation. (2). experiment.

[redacted]S.

References.

1. J L Hess, A M O Smith. Calculation of potential flow about arbitrary body shapes. International Symposium on Analogue and Digital Techniques Applied to Aeronautics, Liege, 1963, Bruxelles, 1964.

2. F Vandrey. A method for calculating the pressure distribution of a body of revolution moving in a circular path through a perfect incompressible fluid. ARS R and M, 1960, No. 3139.

3. L. A. Maslov. Use of one method of determining the velocity potential the flow around body of revolution of ideal fluid for the calculation of apparent additional masses. "engineering journal", 1965, Vol. 5, No. 4.

4. L. A. Maslov. Arbitrary motion of oblong body in ideal fluid. Publ. of the AS USSR, MZhG, 1966, No. 6.

5. S. G. Mikhlin. Lectures on linear integral equations. Fizmatgiz, 1959.

6. I. S. Berezin, N. P. Zhidkov. Methods of calculations. T. 1. Fizmatgiz, 1959.

7. G. Lamb. Hydrodynamics. OGIZ, 1948.

8. P. M. Kanter. Pressure distribution according to the cowlings of the motors of air cocling. The technical reports of TsAGI, iss. 5, 1941.

9. O. P. Sidorov. Solution of the problem of the flow around body of revolution, transactions of KAI, iss. XXIII, 1949.

The manuscript entered 21/V 1969.

Page 11.

HYDRODYNAMICS OF THIN FLEXIBLE BODY. (Estimation of hydrodynamics of rippled surfaces).

G. V. Logvinovich.

For purpose of the explanation of the mechanism of the floating of fishes by the method of flat/plane sections is studied the hydrodynamics of the fine/thin body being deformed. Are obtained the simple formulas, which make it possible to evaluate thrust/rod and the spent power during the sinuscidal wave strains of the axle/axis of body.

Are estimated the hydrodynamic characteristics of fishes. Is given the comparison of the results of theory with experimental materials.

Hydrodynamics of the fine/thin body being deformed, which accomplishes during forward/progressive uniform motion small undulations, can be sufficiently simply studied via the application of the method of flat/plane sections with the use of a concept of the "pierced layer" [1]. Two-dimensional problems of such kind were

theoretically examined by Sikman [2], that also placed some experiments, and by V. A. Eroshin [3], that developed the theory of the airfoil/profile being deformed in L. I. Sedov's setting [4]. However, the study of spatial problem, apparently, in larger measure approaches us understanding of the mechanism of floating of fishes and marine animals, than the solution of two-dimensional problems. The use in this case of a method of flat/plane sections is justified by the fact that the bodies of many marine animals are very elongated lengthwise.

1. Let us examine motion of slender body in inertial system of coordinates xyz, which moves in unlimited volume of liquid along axle/axis Ox with a constant velocity of v (Fig. 1). The longitudinal curvilinear axle/axis of the body s being deformed weakly differs from axle/axis Ox, and its strain in plane xOy let us designate $\eta(x, t)$; the abscissas of the ends of the body let us designate x_1 and x_2; the length of body $x_2 - x_1 = L_p$. Let us assume that the cross sections of body are formed by ellipses with the semimajor axis R = R(x), parallel axis Oz.

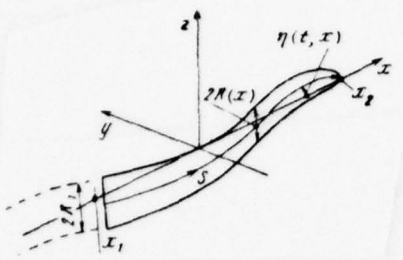

Fig. 1.

Page 12.

In connection with assumption about the fineness of body, we assume that at the entire length dR/dx there is a value small. Let us assume that, passing through certain "penetrable layer" motionless relative to the quiescent liquid, body in this layer gives rise to the transverse almost plane flow, close to the flow of ideal fluid. On trailing edge (on the tail of fish) with $x = x_1$ is fulfilled Joukowski's condition about the finiteness of velocity, and after body remains the trace, equivalent to the film of eddy/vortices with elliptical circulation distribution according to spread/scope $z = \pm B_1(x_1)$. This model of flow in essence represents the development of Jones' known diagram in connection with the low-aspect-ratio wing being deformed.

2. On element of length of body ds, acts normal force dF_n and suction force dP, which is caused by so-called circular pressure dQ. As is known, the apparent additional mass, which is necessary for unit of the length of ellipse, is $m^*(x) = \rho\pi R^2(x)$, normal to axle/axis s the velocity of layer $-v_n = \frac{\partial \eta}{\partial t} - V\frac{\partial \eta}{\partial x}$,

$$dF_n = -\frac{d}{dt}(m^* v_n)\,ds. \qquad (2.1)$$

Circular pressure we find as a result cf contour integration of the cross section of body s* cf overpressure $p - p_0 = \frac{\rho v_n^2}{2} f(s^*)$, determined only by velocity head. Specific suction force is equal to

$$\frac{dP}{ds} = -\int (p - p_0)\cos(n, x)\,ds^*. \qquad (2.2)$$

Thus, for instance, for a cylinder with circular cross section overpressure on its surface at points R, θ is determined by expression $p - p_0 = \frac{\rho v_n^2}{2}(1 - 4\sin^2\theta) + \frac{\rho\cos\theta}{R}\frac{d}{dt}(R^2 v_n)$. Normal to longitudinal axis force (2.1) gives the integral

$$\frac{dF_n}{ds} = -\int_0^{2\pi} (p - p_0)\cos\theta\, d(R\theta) = -\frac{d}{dt}(\rho\pi R^2 v_n),$$

circular pressure -

$$\frac{dQ}{ds} = \int_0^{2\pi} (p - p_0)\, d(R\theta) = -2\pi R\frac{\rho v_n^2}{2}.$$

This circular pressure is negative, i.e., it attempts to expand

cross section. If body is pointed from the front, then slope/inclination toward axle/axis Ox of generatrix dR/ds $\approx$ dR/dx is also negative and on each unit of length acts the directed forward (along axle/axis Os) force

$$\frac{dP}{ds} = -2\pi R \frac{\rho v_n^2}{2} \frac{dR}{ds} = -\frac{v_n^2}{2} \frac{dm^*(s)}{ds}. \qquad (2.3)$$

Page 13.

It is usually considered that suction force appears as a result of the action of infinite negative pressures on infinitesimal leading wing edge; here it is formed on entire length of body as a result of acting the stagnation pressures. Let us note that in service record for overpressure $p-p_0$, used to the expanded opening/aperture in layer, is reject/thrown the term (formally infinite), caused by the symmetrical expansion of cylinder. It is possible to show that this is admissible during the use of a hypothesis of flat/plane sections for calculating the forces, which act on slender bodies [1].

For determining the force in the case of elliptical cross section, we will use second-order of Lagrange equation in connection with kinetic energy in layer $T = m^*(R)\frac{v_n^2}{2}$, and as generalized coordinates and velocities, let us accept for determination of suction force the semimajor axis of cross section R, while for the determination of lateral force, - velocity v_n. As a result for

elliptical cross section, will be obtained the same expressions of force gradients, as for circular: $-\frac{\partial T}{\partial R}=-\frac{\partial m^*}{\partial R}\frac{v_n^2}{2}=-2\pi R\frac{\rho v_n^2}{2}=\frac{dQ}{ds}$;

$$\frac{d}{dt}\frac{\partial T}{\partial v_n}=\frac{d}{dt}(m^*v_n)=\frac{d}{dt}(\rho\pi R^2 v_n)=-\frac{dF_n}{ds}.$$

Apparent additional mass m* in our case is a function only x (or s). Formula (2.3) is valid for any elliptical cross section, and in particular for the case when minor axis vanishes and ellipse degenerates in the segment of line $\pm R$ (on tail).

Projections on the axis of the coordinates of the elementary forces, applied to body, will be

$$\left.\begin{aligned} dF_x &= -dF_n\frac{\partial\eta}{\partial x}+dP;\\ dF_y &= dF_n+dP\frac{\partial\eta}{\partial x}. \end{aligned}\right\} \qquad (2.4)$$

Integrals $F_x=\int dF_x$ and $F_y=\int dF_y$ the undertaken along the length bodies, will give resulting forces. During integration is to consider conditions $R(x_2)=0$ and $R(x_1)=R_1$. Condition $R(x_1)=R_1$ realizes the disruption/separation of the vortex sheet from the tail of body (Zhukovskiy condition). Since the forces are determined for the elementary pierced layer which rests relative to motionless liquid, let us note that $\frac{d}{dt}=\frac{\partial}{\partial t}-V\frac{\partial}{\partial x}$.

3. During periodic motion average during period resulting pull force, caused by "flowing" from tail momentum/impulse/pulses, it is possible to calculate without integration (2.4). Actually, liquid on

unit of the length of trace contains mcmentum/impulse/pulse $m^*(x_1)v_{n1}$. directed along the normal velocity of tail. Projection on axle/axis Ox of the momentum/impulse/pulse, "which flcws" from tail the second, undertaken with opposite sign, gives the instantaneous force, which acts cn body. Therefore pull force, obliged by its origin to the momentum/impulse/pulses, left in trace, will be

$$I = + m^*(x_1) V \left(\frac{\partial \eta}{\partial t} - V \frac{\partial \eta}{\partial x} \right) \frac{\partial \eta}{\partial x} \text{ (1) при } x = x_1. \qquad (3.1)$$

Key: (1). with.

Page 14.

For the explanation of the aforesaid, let us give following reasonings. Let the body be is enveloped by sufficiently distant ccntrol surface Σ_1 which moves together with body. Another control surface Σ_2 of the same configuration, as Σ_1 is connected with stationary liquid. At certain moment of time t, both control surfaces coincide. During period τ, control surface Σ_1 will move along axle/axis Ox to cut $V\tau$.

Since the flow of liquid inside Σ_1 at torque/moments t and t + τ is identical, all the increase in the kinetic energy and momentum/impulse/pulse cf liquid will be caused only by track segment, which remained between the rear walls of control surfaces

Σ_1 and Σ_2. According to the prerequisite/premises accepted, after "runoff" from the tail of fish each element of length of trace, being deformed, retains momentum/impulse/pulse and energy; therefore for calculating the composite force, it is possible for these values to take the values of specific impulse m^*v_{n1}, which relate to the torque/moment of descent from tail.

Thus, the average value of pull force, caused by the left in trace momentum/impulse/pulses, it will be $\{I\} = \frac{1}{\tau}\int_0^{\tau} I\,dt$. Value I under integral is calculated for point x_1, i.e., for a tail.

Another portion of pull force is realized in the form of suction force, which appears as a result of the lateral flow around body,

$$P = -\int_{x_1}^{x_2} \frac{dm^*(x)}{dx}\,\frac{1}{2}\left(\frac{\partial \eta_1}{\partial t} - V\frac{\partial \eta_1}{\partial x}\right)^2 dx. \qquad (3.2)$$

Let us note that the appearance of suction force P leads to the fact that momentum vector in the trace is turned on certain angle so that average total pull force is equal to { I } + { P }, where $\{P\} = \frac{1}{\tau}\int_0^{\tau} P\,dt$.

Average active power of pull forces is equal to ({ I } + { P }) V = { A }.

From tail into trace on unit of path "flows" the kinetic energy

$$\frac{1}{2}\,m^*(x_1)\left(\frac{\partial \eta_1}{\partial t} - V\frac{\partial \eta_1}{\partial x}\right)^2_{x=x_1} = E. \qquad (3.3)$$

The power, spent on the excitation of pull force, will be { N } = ({ I } + { P } + { E }) V, and efficiency $\{\eta_p\} = \frac{\{A\}}{\{N\}}$.

The given above formulas, used, for example, to delta low-aspect-ratio wing with spread/scope $2R_1$, give the known results of linear theory. It is real/actual, at constant angle of attack α, velocity $v_n = -V\alpha$ and from (2.1) is obtained $F_n = m_1^* V^2 \alpha = \rho\pi R^2{}_1 V^2 \alpha$, but from (2.3) after integration from x_1 to x_2 we have $P = 1/2\ m^*{}_1 V^2 \alpha^2$.

Page 15.

The integrals of expressions (2.4) from x_1 to x_2 give induced drag

$$F_x = -m_1^* V^2 \alpha^2 + \frac{1}{2} m_1^* V^2 \alpha^2 = -\frac{1}{2} \rho\pi R_1^2 V^2 \alpha^2$$

and lift

$$F_y = F_n + P\alpha = \rho\pi R_1^2 V^2 \alpha \left(1 + \frac{1}{2}\alpha^2 + \ldots\right).$$

Analogously under the same assumptions can be examined the general case of the unsteady fluctuation of low-aspect-ratio wing.

4. Undulations of body will be obtained, if law of strain is

assigned in the form $\eta_1 = \eta_{10} \sin\left(\frac{Ct}{L} - \frac{x_2 - x}{L}\right)$, assuming that length of body $x_2 - x_1 = L_p = 2\pi Ln$ (n number of waves, which are placed at length of body); C - phase wave velccity, progressive back/ago.

The amplitude of the strain of the axle/axis of body in the general case can be represented together

$$\eta_{10} = a_0 + a_1 (x_2 - x) + a_2 (x_2 - x)^2 + \ldots .$$

Let us examine below the simplest case, after accepting $\eta_{10} = \text{const.}$ Normal velocity will be

$$v_n = \frac{\eta_{10}}{L} (C - V) \cos\left(\frac{Ct}{L} - \frac{x_2 - x}{L}\right),$$

the period of oscillaticns $\tau = 2\pi(L/C)$

Generally speaking, the law of the distribution of apparent additional masses m* (x) is essential during the calculation of force of P. The average value of suction force is calculated from the formula

$$\{P\} = -\frac{1}{\tau} \int_0^{\tau} dt \int_{x_1}^{x_2} \frac{1}{2} v_n^2 (x, t) \frac{dm^*}{dx} dx = -\frac{1}{2} \int_{m_1^*}^{m_2^*} \{v_n^2\} dm^*.$$

In our case average value $\{v_n^2\} = \frac{1}{\tau} \int_0^{\tau} v_n^2 dt = \frac{1}{2} \left(\frac{\eta_{10}}{L}\right)^2 \times$ (C-V)^2 is constant in range from x_1 to x_2; therefore { P } = { E } = $\frac{1}{2} \{v_n^2\} m_1^*$ the law of the distributicn of apparent additional masses along the length L_p proves to be unessential.

Page 16.

Substituting these expressions in the preceding/previous formulas, let us find the average values

$$\left.\begin{aligned}
\{I\} &= \frac{1}{2} m_1^* \left(\frac{\eta_1}{L}\right)^3 V^2 \left(\frac{C}{V} - 1\right), \\
\{P\} &= \frac{1}{4} m_1^* \left(\frac{\eta_1}{L}\right)^2 V^2 \left(\frac{C}{V} - 1\right)^2 = \{E\}, \\
\{A\} &= \frac{1}{4} m_1^* \left(\frac{\eta_1}{L}\right)^3 V^3 \left[\left(\frac{C}{V}\right)^2 - 1\right], \\
\{N\} &= \frac{1}{2} m_1^* \left(\frac{\eta_1}{L}\right)^2 V^3 \left[\frac{C}{V}\left(\frac{C}{V} - 1\right)\right], \\
\{\eta_p\} &= \frac{1}{2}\left(1 + \frac{V}{C}\right).
\end{aligned}\right| \qquad (4.1)$$

Fig. 2, gives relative average values $\{\overline{I}\}$ and $\{\overline{P}\}$ of those comprise of impulsive and suction force, obtained from (4.1) by division on $\frac{1}{2} m_1^* \left(\frac{\eta_0}{L}\right)^2 V^2$. In the conditions/mode of floating with high efficiency, when $\{\eta_p\} > 0{,}9$, the portion of suction force does not exceed 20o/o of impulsive force. Fig. 3, gives the kinogram of the floating of mackerel, borrowed from S. G. Aleyeva's work [5]. On this, photographs it is possible to conclude that $C/V \approx 2$ and the efficiency is close to 0.75; wavelength somewhat lesser than the length of body and $\frac{\eta_0}{L} \approx 0{,}4$.

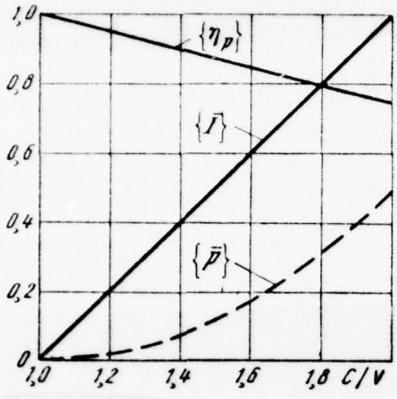

Fig. 2.

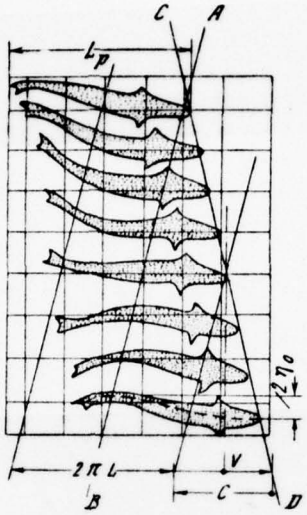

Fig. 3.

Page 17.

If we consider that the active thrust 1/V { A } overcomes resistance of friction $W = C_f S \frac{\rho V^2}{2}$, then the coefficient cf friction drag will be located from equality W = 1/V { A }. For C/V = 2 and $\frac{\eta_0}{L} = 0{,}4$ is obtained the following estimation of drag coefficient: $C_f \approx 0{,}24 \frac{\pi R_1^2}{S}$, where S - the moistened body surface.

According to experiments of V. Ye. Pyatetskiy [6] for bluefish 42 cm long with the spread/scope of tail of approximately 8 cm at velocity V = 0.55 m/s were obtained values C/V = 1.47 and $\frac{\eta_0}{V} =$

0.19-0.25. Average efficiency $\eta_p \approx 0{,}84$. In this case πR^2_1 = 50 cm² and S ≈ 640 cm²; therefore the coefficient of friction drag was obtained by close to $1.7\text{-}3.0 \cdot 10^{-3}$.

Calculations according to formulas (4.1) show that at values C/V = 1.5, $\frac{\eta_0}{L} = 0{,}2$ the "wave motor" with spread/scope 1 m at velocity v = of 10 m/s develops thrust/rod of approximately 90 kg, spending power of approximately 11.8 kW.

The methods of the evaluations of the effectiveness of "wave motors presented" can be developed for the configurations of body and laws of strains, closer to those observed at high-speed fishes. It is possible by the same way to consider the effect of back and ventral fins, variable along the length of amplitude and series of other observed in nature factors. Integral estimations according to the trace, left by body, are interesting by their generality. It is important to note that the used method was checked in the cases of gliding and motion within the liquid of solid bodies where the results of theory and experiment proved to be very close. It is possible to expect that and this estimation of the propulsive properties of fishes is close to reality. This to a certain extent is confirmed by the satisfactory convergence of the calculated values of pull force and frictional resistance for the fishes, inspected by V. Ye. Pyatetsky.

REFERENCES.

1. G. V. Logvinovich. Hydrodynamics of flows with free boundaries. Transactions of TsAGI, iss. 935, 1965.

2. J Siekmann. Zur Theorie der Vewegung schwimmender Tiere. Forschung im Ingenieurwesen, 1965, Nr. 6.

3. V. A. Yeroshin. Emergence of pulling force during the motion of the airfoil/profile being deformed. Izv. of the AS USSR, the mechanics of fluid and gas, 1969, No. 6.

4. L. I. Sedov. Two-dimensional problems of hydrodynamics and aerodynamics. Gostekhteorizdat, 1950.

5. Yu. G. Alеyev. Functional bases of the external structure of fish. Publishing house of the AS USSR, 1963.

6. V. Ye. Pyatetskiy. Hydrodynamic characteristics of the floating of some high-speed sea fishes. Kiev, "Scientific Thought", 1969.

The manuscript entered 10/VII 1969.

Page 18.

THEORY OF UNSTEADY CURVILINEAR MOTION OF LIFTING SURFACE IN GAS.

V. E. Baskin.

Is examined the general case of the unsteady curvilinear motion of lifting surface in gas (on the basis of linear theory).

For this surface are given the formulas, which express gas velocity through the density of distribution of eddy/vortices. These formulas generalize Biot-Savart's usual law in such a way that it becomes suitable for arbitrary transient vortices in gas (in linear approach/approximation). Generalization lies in the fact that Biot-Savart's usual formula is applied to vortex elements taking into account delay in the formation/education of velocity to the transit time of sound signal, and appear some supplementary "wave" component of induced velocities.

The numerous methods of solution of direct and reverse/inverse

problems of the flow around lifting surface of gas [1] - [3] they are related to rectilinear motion. The stationary helical motion of carrying filament in gas is investigated by Frankl [4], and lifting surface - by Maykapar.

Gas velocities during the curvilinear motion of carrying filament are examined in [5].

1. Let infinite gas to the torque/moment of time t = 0 be rested, and then it was agitated by the motion in it of lifting surface. Of perturbation rates we set/assume much the lower speed of the motion of the points of lifting surface. During the calculation of velocity fields, we consider permissible the transfer of the points of application of force to gas from lifting surface to certain the closely spaced to it, permeable for gas surface. The vector of the surface density of the applied forces we set/assume normal to the permeable surface indicated, continuous at each moment of time within certain that driving/moving along the surface of region and the equal to zero out of this region. Under these conditions is placed the problem - to determine the rates of flow of gas, if the motion of lifting surface and force on it are known.

2. Disturbed velocities $\vec{v}$ and pressure p cf infinite gas, set to motion by arbitrary field of external volume forces $\rho_0 \vec{F}$, in linear approach/approximation it is determined by system of equations

$$\rho_0 \frac{\partial \vec{v}}{\partial t} + \operatorname{grad} p = \rho_0 \vec{F}, \quad \frac{\partial p}{\partial t} + c^2 \rho_0 \operatorname{div} \vec{v} = 0 \tag{2.1}$$

and by initial conditions

$$\vec{v}\big|_{t=0} = 0, \quad p\big|_{t=0} = 0 \tag{2.2}$$

(ρ_0 - density of undisturbed air, c - speed of sound).

If we present the velocity and pressure in the form

$$\vec{v} = \vec{D} + \operatorname{grad} \varphi, \quad p = -\rho_0 \frac{\partial \varphi}{\partial t},$$

the system (2.1) it is reduced to nonhomogeneous wave equation for the potential φ:

$$\nabla^2 \varphi - \frac{1}{c^2} \frac{\partial^2 \varphi}{\partial t^2} = -\operatorname{div} \vec{D},$$

where $\vec{D} = \int_0^t \vec{F} dt$ - the referred to ρ_0 vector of the momentum density of external forces.

Potential φ is conveniently searched for in the form $\varphi = \operatorname{div} \vec{E}$, which reduces to following equation for vector $\vec{E}$:

$$\nabla^2 \vec{E} - \frac{1}{c^2} \frac{\partial^2 \vec{E}}{\partial t^2} = -\vec{D}. \tag{2.3}$$

Solution of equation (2.3) under the zero initial conditions, which correspond (2.2), is given by Kirchhoff's formula

$$\vec{E}(\vec{r}_0,\ t_0) = \iiint \frac{1}{4\pi l}\vec{D}\left(\vec{r},\ t_0 - \frac{l}{c}\right)dk, \quad l = |\vec{r}_0 - \vec{r}| \qquad (2.4)$$

(integral it is common on the part of the space where integrand is not equal to zero).

Vector $\vec{E}$, accordingly (2.4), is constructed as delaying potential of flows the vector equal in momentum density to. Therefore let us name this vector momentum/impulse/pulse-potential. Passage to the limit to the surface field of forces is converted (2.4) to the form

$$\vec{E}(\vec{r}_0,\ t_0) = \iint_W \frac{1}{4\pi l}\vec{\Gamma}\left(\vec{r},\ t_0 - \frac{l}{c}\right)dS, \qquad (2.5)$$

where $\vec{\Gamma}(\vec{r}, t)$ - the referred to ρ_0 vector of the surface momentum density of the external forces, which affected up to torque/moment t the gas at the points of surface W.

3. Let us examine infinite quiescent gas in which with certain moment of time begins to move lifting surface. As has already been spoken, let us consider that the points of lifting surface little are distant from certain staticrary permeable surface of W. Designating through $W_0(t)$ region on surface of W for which is design/projected (along standards) at torque/moment t the lifting surface, let us

identify this region with quite lifting surface, transferring to it the points of application/appendix to gas of external forces.

Page 20.

The part of the boundary of the lifting surface whose points have different from zero normal toward boundary composing the rates of motion, directed from region W_0, let us designate through $L_1(t)$, and inside region - $L_2(t)$ let us respectively call these curves leading and trailing edges. Region W_0 can be limited to the pieces of curves, not having the normal to them comprising rate of motion (by flank edges).

Let us describe the motion of lifting surface by the parametric equation $\vec{r} = \vec{r}(u, v)$ of surface W by the position of the curves L_1 and L_2 at different moment of time. For convenience we consider L_1 and L_2 at the initial moment coinciding, but in order not to exclude the case of the instantaneous emergence (or disappearance) of the section of lifting surface, let us allow/assume the motion of these lines with infinite velocities. $W_1(t)$ and $W_2(t)$ - region on surface of W, described by the curves L_1 and L_2 up to the torque/moment of time t, but $\tau_1(\vec{r})$, $\tau_2(\vec{r})$ - the torque/moments of the time when the curves L_1 and L_2 pass above the point $(\vec{r})$ on surface of W.

Let us realize that the points of regions W_1 and W_2 at the moment of the passage above them of lines L_1 and L_2 continuously emit the acoustic waves, which spherically diverge at a rate of c. Let us fix certain point of space $(\vec{r}_0)$, not locating on surface of W, and the torque/moment of time t_0. The parts of regions W_1 of andes W_2, from which had time to reach point $(\vec{r}_0)$ up to torque/moment t_0 acoustic waves, let us call the audible forms of these regions and designate respectively W_1^* and W_2^*.

The condition of the determination of point $(\vec{r})$ in region W_1^* (or W_2^*) will be $\Psi_1(\vec{r}_0, \vec{r}, t_0)<0$ (or $\Psi_2(\vec{r}_0, \vec{r}, t_0)<0$), where $\Psi(\vec{r}_0, \vec{r}, t_0)=|\vec{r}_0-\vec{r}|-c[t_0-\tau(\vec{r})]$ and $\Psi=\Psi_i$ when $\tau=\tau_i$ $(i=1, 2)$. The region, which supplements W_2^* to W_1^*, let us designate W_0^*. Region W_2^* can be named in an audible manner of the film of eddy/vortices, while region W_0^* - audibly of lifting surface. We will be restricted to the regular case when in the composition of boundaries of the region W_1^* and W_2^* enter the lines, determined by equalities [1]

$$\Psi_1(\vec{r}_0, \vec{r}, t_0)=0, \quad \Psi_2(\vec{r}_0, \vec{r}, t_0)=0. \tag{3.1}$$

FOOTNOTE [1]. In the special cases, further not examine/considered, equalities (3.1) can occur for the totality of the points, which form region. ENDFOOTNOTE.

Let us designate the lines indicated respectively L_1^*, L_2^* and will call them the audible forms of leading and trailing edges. Region W_1^* can be also limited by the section of boundary of the region W which let us designate through L_1^* (Fig. 1). Since the line L_1 has different from zero normal rates of motion its intersection with curved L_1^* for points $(\vec{r}_0)$, which do not lie on W, it is impossible. Region W_0^* besides lines L_1^* and L_2^* can be limited to the sections of boundary of the region W whose totality let us designate L_0^* (see Fig. 1).

Page 21.

4. $\vec{\sigma}(\vec{r}, t)$ - referred to ρ_0 vector of density of surface forces, which act on gas from the side of points of region W_0, in direction of standard $\vec{N}$ to surface of W. Regarding the vector of the surface momentum density of the forces

$$\vec{\Gamma}(\vec{r}, t) = \int_0^t \vec{\sigma}(\vec{r}, t)\, dt,$$

and the vector of momentum/impulse/pulse-potential of the flow, caused by these forces, accordingly (2.5) will be

$$\vec{E}(\vec{r}_0, t_0) = \iint_{W_1^*} \frac{dS}{4\pi l} \vec{\Gamma}\left(\vec{r}, t_0 - \frac{l}{c}\right).$$

For the determination of velocity potential Φ, it is necessary to know derivatives of vector $\vec{E}$ on the coordinates of point $(\vec{r}_0)$.

Let us examine the differential $\delta\vec{E}$ of vector $\vec{E}$, calculated when point $(\vec{r}_0)$ is displaced in the direction of arbitrary unit vector $\vec{\nu}$ in distance δh, and time t_0 grow/rises by δt. Since region W_1^* will obtain during this variation certain increase δW_1^*, then introducing derivatives under integral sign, let us find

$$\delta\vec{E} = \delta h \iint\limits_{W_1^*} \frac{dS}{4\pi} \frac{\partial}{\partial \nu_0}\left(\frac{1}{l}\right)\vec{\Gamma}\left(\vec{r},\ t_0 - \frac{l}{c}\right) + \\ + \iint\limits_{W_1^*} \frac{dS}{4\pi l}\vec{\Gamma}'_t\left(\vec{r},\ t_0 - \frac{l}{c}\right)\left(\delta t - \frac{\delta h}{c}\frac{\partial l}{\partial \nu_0}\right) + \iint\limits_{\delta W_1^*} \frac{dS}{4\pi l}\vec{\Gamma}\left(\vec{r},\ t_0 - \frac{l}{c}\right). \quad (4.1)$$

Through $\Gamma'_t(\vec{r},\ t)$ is designated the time derivative, a $\frac{\partial}{\partial \nu_0}$ indicates differentiation in the sense of the vector $\vec{\nu}$ with respect to the coordinates of point $(\vec{r}_0)$.

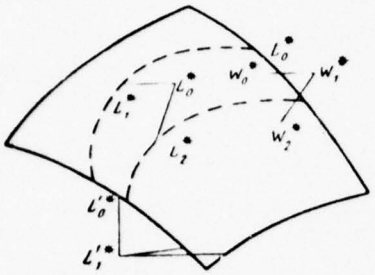

Fig. 1.

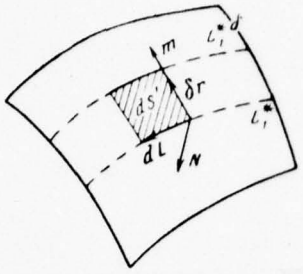

Fig. 2.

Page 22.

$L_1^{*\delta}$ — displaced during variation position of line L_1^*, a $\vec{r}+\delta\vec{r}$ and $\vec{r}$ — radius-vectors of the arbitrary infinitely close points of these lines (Fig. 2). Regarding lines L_1^* and $L_1^{*\delta}$ we have the equalities

$$\Psi_1(\vec{r}_0,\ \vec{r},\ t_0)=0, \qquad \Psi_1(\vec{r}_0+\vec{v}\delta h,\ \vec{r}+\delta\vec{r},\ t_0+\delta t)=0,$$

difference in which within limit when $\delta\vec{r}\to 0,\ \delta t\to 0$ gives the following condition, superimposed on $\delta\vec{r}$:

$$\vec{v}\delta h\nabla_0\Psi_1+\delta\vec{r}\,\nabla\Psi_1+\frac{\partial\Psi_1}{\partial t_0}\delta t=0,$$

where ∇_0 and ∇ - Hamilton's operators on alternating/variable $\vec{r}_0$ and $\vec{r}$.

Since

$$\vec{\nabla}_0 \Psi_1 = (\vec{r}_0 - \vec{r})/|\vec{r}_0 - \vec{r}|, \quad \nabla \Psi_1 = (\vec{r}_0 - \vec{r})/|\vec{r}_0 - \vec{r}| + c \operatorname{Grad} \tau,$$

this condition can be written in the form

$$(\vec{e} + \vec{\mu}) \delta\vec{r} - (\vec{e} \cdot \vec{v}) \delta h - c\delta t = 0, \tag{4.2}$$

suitable both for a curve L_1^*, and for L_2^*, moreover $\vec{e} = (\vec{r} - \vec{r}_0)/|\vec{r} - \vec{r}_0|$, $\vec{\mu} = c \operatorname{Grad} \tau$. In the particular case $\delta h = \delta t = 0$ equality (4.2) gives the following condition, superimposed on vector $d\vec{L}$ of the cell/element of curves L_1^* or L_2^*:

$$d\vec{L}(\vec{e} + \vec{\mu}) = 0. \tag{4.3}$$

Let us introduce in curves L_1^* and L_2^* the families of the alternating/variable vectors $\vec{m}$, which lie at tangent to surface of W cf plane, but clear these curves. Assuming that the tangent toward surface of W component of vector $\delta\vec{r}$ is directed along the appropriate vector $\vec{m}$, we will obtain from (4.2) with an accuracy to infinitesimal first order

$$\delta\vec{r} = \frac{(\vec{e} \cdot \vec{v}) \delta h + c\delta t}{\vec{m}(\vec{e} + \vec{\mu})} \vec{m}. \tag{4.4}$$

The element of area dS', constructed on vectors $\delta\vec{r}$ and $d\vec{L}$, we consider positive, if $\delta\vec{r}$ it is directed from region W_i^* $(i = 1, 2)$, and $d\vec{L}$ with view along standard $\vec{N}$ has region W_i^* to the left of its direction. Then $dS = -|\vec{N}\delta\vec{r}d\vec{L}|$ and on (4.4) we find

$$dS' = \frac{-[\vec{N}\,\vec{m}d\vec{L}]}{\vec{m}(\vec{e}+\vec{\mu})}\,[(\vec{e}\cdot\vec{\nu})\,\delta h + c\delta t].$$

During replacement curved L_1^* by broken line from cell/elements $d\vec{L}$ the corresponding areas dS' form the region $\delta' W_1^*$, which differs from δW_1^* to the small second-order quantity relative to δh and δt.

Page 23.

Producing in (4.1) the replacement of region δW_1^* on $\delta' W_1^*$ (that it will not influence the differential $\delta\vec{E}$), we will obtain

$$\delta\vec{E} = \delta h \iint\limits_{W_1^*} \frac{dS}{4\pi}\,\frac{\partial}{\partial\nu_0}\left(\frac{1}{l}\right)\vec{\Gamma}\left(\vec{r},\ t_0-\frac{l}{c}\right)+$$

$$+\iint\limits_{W_0^*}\frac{dS}{4\pi l}\,\vec{\sigma}\left(\vec{r},\ t_0-\frac{l}{c}\right)\left(\delta t-\frac{\delta h}{c}\,\frac{\partial l}{\partial\nu_0}\right)-$$

$$-\int\limits_{L_1^*}\frac{[\vec{N}\vec{m}d\vec{L}]}{4\pi l\vec{m}(\vec{e}+\vec{\mu})}\,\vec{\Gamma}\left(\vec{r},\ t_0-\frac{l}{c}\right)[(\vec{e}\cdot\vec{\nu})\,\delta h + c\delta t].$$

The coefficient of δh in this expression gives derivative of vector $\vec{E}$ on the position of point $(\vec{r}_0)$ in direction $\vec{\nu}$, i.e.,

$$\frac{\partial \vec{E}}{\partial \nu} = \iint\limits_{W_1^*} \frac{dS}{4\pi} \frac{\partial}{\partial \nu_0}\left(\frac{1}{l}\right)\vec{\Gamma}\left(\vec{r},\ t_0 - \frac{l}{c}\right) - \iint\limits_{W_0^*} \frac{dS}{4\pi l}\vec{\sigma}\left(\vec{r},\ t_0 - \frac{l}{c}\right)\frac{1}{c}\frac{\partial l}{\partial \nu_0} -$$

$$- \int\limits_{L_1^*} \frac{[\vec{N}m d\vec{L}](\vec{e}\cdot\vec{\nu})}{4\pi l m\,(\vec{e}+\vec{\mu})}\vec{\Gamma}\left(\vec{r},\ t_0 - \frac{l}{c}\right). \qquad (4.5)$$

Since $\vec{\sigma}(\vec{r},\ t) = 0$ with $t < r_1(\vec{r})$, value $\vec{\Gamma}\left(\vec{r}, t_0 - \frac{l}{c}\right)$ to curve L_1^* is equal to zero and the third integral in (4.5) is absent. Calculating with the aid of (4.5) derivatives along coordinate axes and determining div $\vec{E}$, we will obtain velocity potential

$$\varphi(r_0,\ t_0) = \iint\limits_{W_1^*} \frac{dS}{4\pi} \frac{\partial}{\partial N_0}\left(\frac{1}{l}\right)\Gamma\left(\vec{r},\ t_0 - \frac{l}{c}\right) +$$

$$+ \iint\limits_{W_0^*} \frac{dS}{4\pi c} \frac{\partial}{\partial N_0}\left(\frac{1}{l}\right) l\,\sigma\left(\vec{r},\ t_0 - \frac{l}{c}\right); \qquad (4.6)$$

here Γ and σ - projection of vectors $\vec{\Gamma}$ and $\vec{\sigma}$ on the going along them standard $\vec{N}$, a $\frac{\partial}{\partial N_0}$ indicates differentiation with respect to the position of point $(\vec{r}_0)$ in direction $\vec{N}$.

According to (4.6) in all points of space, beyond exception/elimination which are located on surface W_1^*, potential φ exists and it is continuous, and gradient φ determines the rates of flow of gas.

Potential jump Φ with approach from the different sides of surface W to the located on it point $(\vec{r})$ on the basis of the maximum properties of the potential of dual layer is equal to $\Gamma(\vec{r}, t)$; that means $\Gamma(\vec{r}, t)$-circulation on duct/ccntour G, which pierces surface of W at this point (positive Γ correspond to the intersection of surface of W in the circuit/bypass of duct/contour G in the direction of standard $\vec{N}$). In the case of $c \to \infty$ equality (4.6) transfer/converts intc known expression for the velocity potential of lifting surface in the incompressible fluid.

5. Assuming that function $\sigma(\vec{r}, t)$ is differentiated in all points of lifting surface and it is final on its boundaries, let us determine derivatives of potential Φ with respect to coordinates and time. For this, preliminarily let us find differential $\delta\varphi$ when point $(\vec{r}_0)$ is displaced by vector $\vec{\delta h}$, and time increases on δt. Designating through δW_1^* and δW_2^* the increases of regions W_1^* and W_2^* during this variation, we can write

$$\delta\varphi = \delta h \frac{\partial}{\partial \nu_0} \iint\limits_{W_1^* = \text{const}} \frac{dS}{4\pi} \frac{\partial}{\partial N_0}\left(\frac{1}{l}\right)\left[\Gamma\left(\vec{r},\ t_0 - \frac{l}{c}\right) + \frac{l}{c}\sigma\left(\vec{r},\ t_0 - \frac{l}{c}\right)\right]\Big|_{r_0 = \text{const}} +$$

$$+ \iint\limits_{W_0^*} \frac{dS}{4\pi} \frac{\partial}{\partial N_0}\left(\frac{1}{l}\right)\Gamma_t'\left(\vec{r},\ t_0 - \frac{l}{c}\right)\left(\delta t - \frac{\delta h}{c}\frac{\partial l}{\partial \nu_0}\right) +$$

$$+ \iint\limits_{\delta W_1^*} \frac{dS}{4\pi} \frac{\partial}{\partial N_0}\left(\frac{1}{l}\right)\Gamma\left(\vec{r},\ t_0 - \frac{l}{c}\right) +$$

$$+ \iint\limits_{W_0^*} \frac{dS}{4\pi c} \frac{\partial}{\partial N_0}\left(\frac{1}{l}\right)\left[\frac{\partial l}{\partial \nu_0}\sigma\left(\vec{r},\ t_0 - \frac{l}{c}\right)\delta h + l\sigma_t'\left(\vec{r},\ t_0 - \frac{l}{c}\right)\left(\delta t - \frac{\delta h}{c}\frac{\partial l}{\partial \nu_0}\right)\right] +$$

$$+ \iint\limits_{\delta W_1^*} \frac{dS}{4\pi c} \frac{\partial}{\partial N_0}\left(\frac{1}{l}\right) l\sigma\left(\vec{r},\ t_0 - \frac{l}{c}\right) - \iint\limits_{\delta W_2^*} \frac{dS}{4\pi c} \frac{\partial}{\partial N_0}\left(\frac{1}{l}\right) l\sigma\left(\vec{r},\ t_0 - \frac{l}{c}\right).$$

The entering here integrals on regions δW_1^* and δW_2^* are converted into integrals on lines L_1^* and L_2^* analogous with that, as this was made during calculation δE. Fulfilling this conversion and taking into account that to curve L_1^* value $\Gamma\left(\vec{r},\ t_0 - \frac{l}{c}\right)$ turns into zero, we obtain

$$\delta\varphi = \delta h \frac{\partial}{\partial \nu_0} \iint\limits_{W_1^* = \text{const}} \frac{dS}{4\pi} \frac{\partial}{\partial N_0}\left(\frac{1}{l}\right)\left[\Gamma\left(\vec{r},\ t_0 - \frac{l}{c}\right) + \frac{l}{c}\sigma\left(\vec{r},\ t_0 - \frac{l}{c}\right)\right]\Big|_{\vec{r}_0 = \text{const}} +$$

$$+ \iint\limits_{W_0^*} \frac{dS}{4\pi} \frac{\partial}{\partial N_0}\left(\frac{1}{l}\right)\left[\frac{l}{c}\sigma_t'\left(\vec{r},\ t_0 - \frac{l}{c}\right)\left(\delta t - \frac{1}{c}\frac{\partial l}{\partial \nu_0}\delta h\right) +\right.$$

$$\left. + \sigma\left(\vec{r},\ t_0 - \frac{l}{c}\right)\delta t\right] - \int\limits_{L_0^*} \frac{1}{4\pi c} \frac{\partial}{\partial N_0}\left(\frac{1}{l}\right)\frac{|\vec{N}\vec{m}d\vec{L}|}{\vec{m}(\vec{e}+\vec{\alpha})} l\sigma\left(\vec{r},\ t_0 - \frac{l}{c}\right)|(\vec{e}\vec{\nu})\delta h + c\delta t|, \quad (5.1)$$

where L_0^* - the part of the boundary of the region W_0^*, which goes along lines L_1^* and L_2^*, moreover positive circuit/bypass L_0^* with

view along $\vec{N}$ must leave region W_0^* to the left.

Page 25.

Coefficients of δh and δt in (5.1) essence derivatives $\frac{\partial \varphi}{\partial \nu_0}$ and $\frac{\partial \varphi}{\partial t}$ respectively. Calculating with the aid of (5.1) gas velocity $\vec{v}$ pressure p, we will obtain

$$\vec{v}(\vec{r}_0, t_0) = \operatorname{grad}_0 \iint\limits_{W_1^*=\text{const}} \frac{1}{4\pi} \frac{\partial}{\partial N_0}\left(\frac{1}{l}\right)\left[\Gamma\left(\vec{r}, t_0 - \frac{l}{c}\right) + \frac{l}{c}\sigma\left(\vec{r}, t_0 - \frac{l}{c}\right)\right]_{\vec{r}_0=\text{const}} +$$

$$+ \iint\limits_{W_0^*} \frac{\vec{e}(\vec{e}\vec{N})}{4\pi c^2 l}\sigma_t'\left(\vec{r}, t_0 - \frac{l}{c}\right)dS - \int\limits_{L_0^*} \frac{\vec{e}(\vec{e}\vec{N})[\vec{N}\vec{m}d\vec{L}]}{4\pi c l m(\vec{e}+\vec{\mu})}\sigma\left(\vec{r}, t_0 - \frac{l}{c}\right); \quad (5.2)$$

$$p(\vec{r}_0, t_0) = -\rho_0 \iint\limits_{W_0^*} \frac{dS}{4\pi} \frac{\partial}{\partial N_0}\left(\frac{1}{l}\right)\left[\sigma\left(\vec{r}, t_0 - \frac{l}{c}\right) + \frac{l}{c}\sigma_t'\left(\vec{r}, t_0 - \frac{l}{c}\right)\right] +$$

$$+ \rho_0 \int\limits_{L_0^*} \frac{(\vec{e}\vec{N})[\vec{N}\vec{m}d\vec{L}]}{4\pi l m(\vec{e}+\vec{\mu})}\sigma\left(\vec{r}, t_0 - \frac{l}{c}\right). \quad (5.3)$$

The first integral in formula (5.2) can be interpreted what velocity in point $(\vec{r}_0)$ of the flow of the incompressible fluid, caused by the dipoles, distributed over surface W_1^* with density $\Gamma^*(\vec{r}) = \Gamma\left(\vec{r}, t_0 - \frac{l}{c}\right) + \frac{l}{c}\sigma\left(\vec{r}, t_0 - \frac{l}{c}\right)$ and oriented along the normal. Such dipoles produce the same velocities, as covering this surface eddy/vortices with circulation $\Gamma^*(\vec{r})$ [function $\Gamma^*(\vec{r})$ depends besides $\vec{r}$ on the torque/moment of time t_0 and of the position of point $(\vec{r}_0)$]. Let us further call Γ^* audible circulation. The corresponding to audible circulation vortex system consists of layer on surface W_1^*

with the vector of surface intensity $\vec{\gamma}^* = -\vec{N} \times \operatorname{Grad} \Gamma^*$ and the going along lines $L_1^{\Gamma^*}$ and L_0^* discrete eddy/vortices, intensity ΔG^* of which is equal to $-\Gamma^*$ on $L_1^{\Gamma^*}$ and $-\sigma\left(\vec{r}, t_0 - \frac{l}{c}\right) c^{-1}$ on L_0^*. Utilizing for calculating first term (5.2) Biot-Savart's formula, we will obtain the following resultant expression for a gas velocity through the intensities of the eddy/vortices:

$$\vec{v} = \iint\limits_{W_1^*} \frac{1}{4\pi l^3} \vec{e} \times \vec{\gamma}^* \, dS + \int\limits_{L_0^* + L_1^{\Gamma^*}} \frac{\vec{e} \times d\vec{L}}{4\pi l^2} \Delta\Gamma^* + \\ + \iint\limits_{W_0^*} \frac{\vec{e}\,(\vec{N}\vec{e})}{4\pi l c^2} \sigma_t'\left(\vec{r}, t_0 - \frac{l}{c}\right) dS - \int\limits_{L_0^*} \frac{\vec{e}\,(\vec{N}\vec{e})\,[\vec{N} m d\vec{L}]}{4\pi l c m\,(\vec{e} + \vec{\mu})} \sigma\left(\vec{r}, t_0 - \frac{l}{c}\right). \quad (5.4)$$

Page 26.

Expressing element of area dS, standard $\vec{N}$ and surface gradient from Γ^* by means of curvilinear coordinates u, v

$$dS = \varkappa du dv, \quad \vec{N} = [\vec{r}_u \times \vec{r}_v]\,\varkappa^{-1} \quad (\varkappa = |\vec{r}_u \times \vec{r}_v|),$$
$$\operatorname{Grad} \Gamma^* = \varkappa^{-1}\left([\vec{r}_u \times \vec{N}]\,\Gamma_u^* - [\vec{r}_v \times \vec{N}]\,\Gamma_v^*\right),$$

we can present the obtained expression for velocity also in the following form:

$$\vec{v} = \iint\limits_{W_1^*} \frac{1}{4\pi l^2} \vec{e} \times \frac{\partial(\vec{r}, \Gamma^*)}{\partial(u, v)} du dv + \int\limits_{L_0^* + L_1^{\Gamma^*}} \frac{\vec{e} \times d\vec{L}}{4\pi l^2} \Delta\Gamma^* + \\ + \iint\limits_{W_0^*} \frac{\vec{e}\,(\vec{N}\vec{e})}{4\pi l c^2} \sigma_t'\left(\vec{r}, t_0 - \frac{l}{c}\right) dS - \int\limits_{L_0^*} \frac{\vec{e}\,(\vec{N}\vec{e})\,\varkappa\,[a dv - b du]}{4\pi l c\,(Aa + Bb)} \sigma\left(\vec{r}, t_0 - \frac{l}{c}\right); \quad (5.5)$$

here $A = \vec{r}_u \vec{e} + c\tau_u$, $B = \vec{r}_v \vec{e} + c\tau_v$, but value a and b essence the coefficients of vector $\vec{m}$ on basis $\vec{r}_u$, $\vec{r}_v$. As a result of (4.3) to curve occurs equality Adu + Bdv = 0, that ensures the independence of the determined by formula (5.5) velocities from the selection of coefficients a and b. That entering in (5.5) jacobian from vector $\vec{r}(u, v)$ and scalar $\Gamma^*(u, v)$ is easily determined by direct differentiation of the function $\Gamma^*(u, v)$:

$$\frac{\partial(\vec{r}, \Gamma^*)}{\partial(u, v)} = \frac{\partial(\vec{r}, \Gamma(\vec{r}, t))}{\partial(u, v)}\Bigg|_{t=t_0-\frac{l}{c}} + \frac{l}{c}\frac{\partial(\vec{r}, \sigma(\vec{r}, t))}{\partial(u, v)}\Bigg|_{t=t_0-\frac{l}{c}} + \\ + \frac{lx}{c^2}[\vec{e}\times\vec{N}]\times\sigma_t'\left(\vec{r}, t_0-\frac{l}{c}\right).$$

In expressions (5.4) and (5.5) it is possible to transfer/convert to limit, fixing point $(\vec{r}_0)$ to surface of W. The "direct/straight" value of velocity, equal to the half-sum of the limiting values with approach to point $(\vec{r}_0)$ from the different sides W, will be determined by these expressions (improper integrals are taken in the sense of principal values). In the most important for practice case when W there is a plane and point $(\vec{r}_0)$ it lie/rests on it, the third and fourth integrals in (5.4) disappear.

Formula (5.4) solves stated problem of the rates of flow of gas, caused by the arbitrarily driving/moving in it lifting surface with the assigned/prescribed final surface load. It expresses Biot-Savart's law, generalized in the case of the compressed medium.

According to this law during the unsteady motion of lifting surface in gas Biot-Savart's formula it is required to apply only to that vortex elements from which had time to reach the point of application/appendix sound signals. Besides in addition to this appear the supplementary "wave" which comprise of velocities, which decrease as first degree of distance of eddy/vortices.

6. Example 1. To the quiescent gas from the torque/moment of time $\tau = 0$ at the points of plane $z = 0$, comes into action the field of the directed along axle/axis Oz forces with constant surface density $\sigma = p$. Let us find the gas velocity in torque/moment t_0 in the point of axle/axis Oz with coordinate z_0.

Page 27.

Auditory sensation area W_1^* will be determined by inequality $\Psi = t - ct_0 \leqslant 0$ and will represent by itself circle with a radius of $R = \sqrt{c^2 t_0^2 - z_0^2}$ with center in the beginning of coordinates. The vector of momentum density is directed along axle/axis Oz and along value is equal to $\Gamma(t) = pt$. Hence

$$\Gamma^* = \Gamma\left(t_0 - \frac{l}{c}\right) + \frac{l}{c}\sigma\left(t_0 - \frac{l}{c}\right) = pt_0.$$

To this circulation corresponds circular eddy/vortex with a radius of R with intensity - pt_0. It will excite at point (z_0) the

directed along axis Oz velocity $v_z' = \frac{\Gamma^* R}{2\beta}$. Furthermore, in the expression of gas velocity accordingly (5.4) will enter component

$$v_z^* = \int \frac{\vec{e}\,(\vec{N}\vec{e})\,[\vec{N}\vec{m}d\vec{L}]}{4\pi l c m\,(\vec{e}+\mu)}, \tag{6.1}$$

where integration it is conducted in circle with radius of with a of R, which limits auditory sensation area. Introducing vectorial angle θ between the radius-vector of the points of this circumference and the axle/axis Ox and assuming that vectors $\vec{n}$ are directed radially, we will obtain

$$[\vec{N}\vec{m}d\vec{L}] = Rd\theta, \quad \vec{N}\vec{e} = -\cos\alpha, \quad \vec{m}\vec{e} = \sin\alpha, \tag{6.2}$$

where α - a half-apex angle of the cone with circle W_1^* as basis/base and apex/vertex in point (z_0). Taking into account (6.2) integral (6.1) elementary is integrated and gives $v_z'' = \frac{pz_0^2}{c^2 t_0^2}$, whence

$$v_z = v_z' + v_z'' = \begin{cases} \frac{p}{2c} & \text{при } t_0 > \frac{|z_0|}{c}, \\ 0 & \text{(1) при } t_0 < \frac{|z_0|}{c}. \end{cases}$$

Key: (1). with.

This result can be obtained by another way, for example by the solution of one-dimensional problem.

Example of 2. On the plane z = 0 Cartesian coordinate system, evenly moves from infinity the carrying band of final width. From the side of band to gas, acts the field of those directed conversely of

axle/axis Oz of the forces, which have constant surface density $\rho_0 p$. It is required to determine the gas velocity at certain moment of time t_0 in point Q, which is located on band. It is arranged axle/axis in such a way that up to the torque/moment t_0 the forward edge of band would coincide with axle/axis Cy, and the positive part of axle/axis Ox traversed point Q. The functions τ_1 and τ_2, which show the transit time of the leading and trailing edges of the band above the point of plane z = 0 with coordinate x > 0, will be

$$\tau_1 = t_0 - \frac{x}{V} \text{ and } \tau_2 = t_0 - \frac{(x-b)}{V},$$

where b - width of band, v - a rate of its motion.

The vector of momentum density for this flow will be $\vec{\Gamma} = k(t'-\tau_1)p$ ($t'=t$ with $\tau_1 < t < \tau_2$, $t' = \tau_2$ with $t > \tau_2$). Areas W_1 and W_2 are half-plane z = 0, x > 0 and z = 0, x > b. Lines L_1^* and L_2^* are determined by equalities $\Psi_1 = t - \frac{cx}{V} = 0$ and $\Psi_2 = t - \frac{c(x-b)}{V} = 0$; i.e. represent by itself conic sections with focus at point Q, eccentricity $\mu = c/V$ and directrices x = 0 and x = b.

Page 28.

Let us examine the case of supersonic speed of motion, when $\mu >$ 1, line L_1^* - ellipse, and line L_2^* it is absent. Areas W_1^* and W_0^*

ccincide and represent by themselves the interior of ellipse (Fig. 3). Audible within ellipse circulation $\Gamma^* = \frac{px}{V}$. The corresponding to this circulation vortex system consists of the layer of those cover the interior of ellipse of parallel to axle/axis Oy eddy/vortices with a density of p/V and the concentrated eddy/vortex with an intensity of px/V, that goes over ellipse. Since $(\vec{e}\ \vec{N}) = 0$ for point Q, the rate of flow of gas accordingly (5.4) are wholly determined by Biot-Savart's formula, used to the vortex system pointed out above. Introducing the vectorial angle between a focal radius and the axle/axis Ox for the directed along axle/axis Oz velocities from the rectilinear and elliptical eddy/vortex, we will obtain

$$v_z' = \int_{\theta=\pi}^{\theta=0} \frac{p \sin\theta\, dx}{2\pi V (x - x_0)};$$

$$v_z^* = \int_{\theta=\pi}^{\theta=0} \frac{px}{2\pi V l^2} (\cos\theta\, dy - \sin\theta\, dx), \qquad (6.3)$$

where x_0 - coordinate of point Q.

The first of the integrals is undertaken in the sense of principal value. Coordinates x and y of the points of ellipse and the lengths of a focal radius l are connected with θ relationship/ratios $x = Ml$, $y = l\sin\theta$, $l = \frac{x_0}{(M - \cos\theta)}$, where M = V/c. Calculation of integrals (6.3) gives $v_z' = \frac{p(M - \sqrt{M^2 - 1})}{2V}$, $v_z^* = -\frac{pM}{2V}$, whence $v_z = -\frac{p\sqrt{M^2 - 1}}{2V}$. This result is well known from the theory of fine/thin airfoil/profile in the

supersonic flow.

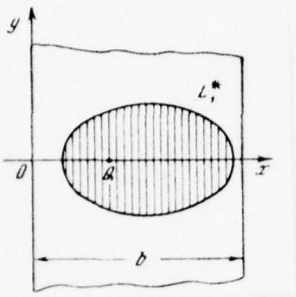

Fig. 3.

REFERENCES

1. S. M. Belotserkovskiy. Fine/thin surface in the subsonic flow of gas, M., "science", 1965.

2. Ye. A. Krasil'shchikova. Finite-span wing in compressible flow. State Technical Press, 1952.

3. G N Ward. Linearized theory of steady high-speed flow. Cambride University Press, 1955.

4. F. I. Frankl. Theory of screw/propeller with the finite number of blade/vanes at high forward/progressive and peripheral speed. Transactions of TsAGI, iss. 540, 1942.

5. V. E. Baskin. To the linear theory of the unsteady motion of gas under the action of nonpotential external forces. Izv. of the AS USSR, MZhG, 1969, No 4.

The manuscript entered 26/VI 1969.

FLOW AROUND DELTA WING BY HYPERSONIC FLOW.

V. P. Kolgan

Work examines the problem of the flow around delta wing of hypersonic flow of gas at low angle of attack. Is used the method of the "sources" of the pressure, with the aid of which the problem came to singular equation. There is carried out regularization of this equation, because of which obtained integral equation with continuous nucleus. The results of the work are illustrated by examples of the calculations for pressures for the disturbed zone of flow.

This problem has already been examined by a number of the authors [1], [2], who applied for the determination of solution the method of expansion/decomposition in series, reflect/representing physical flow plane to certain fictiticus plane. In this article is proposed another approach to this problem, which ensures obtaining solution immediately in physical plane. Method can render/show useful for the solution of a series of other problems.

1. Formulation of problem. Let us examine the lower surface of

the delta flat/plane wing, arrange/located at low angle of attack α << 1 in the supersonic flow of perfect gas with large mach number ($M_\infty > 1$). $2\gamma_1$ - angle, formed by leading wing edges. Let us assume also that the parameters M_∞, α and γ_1 satisfy the following relationship/ratios:

$$M_\infty \alpha \sim 1; \quad M_\infty \gamma_1 \gg 1. \tag{1.1}$$

let us search for asymptotic solution for a flow around of the wing under the made assumptions. It began the systems of coordinates xyz was arranged in the spout of wing so that the plane xz would coincide with wing plane, and X-axis coincided with the axis of the symmetry of wing. Let us introduce the dimensionless unknown velocity functions, pressure and density

$$\vec{V} = U_\infty (u^*, v^*, w^*); \quad p = \rho_\infty U_\infty^2 p^*; \quad \rho = \rho_\infty \rho^*, \tag{1.2}$$

where U_∞ and ρ_∞ - velocity and the density of flow in the undisturbed flow. By virtue of assumption (1.1) leading wing edge will be supersonic, shock wave - plane and the parameters of flow after it by constants up to the disturbance cone, proceeding from spout wing. This zone of flow with the constant parameters is designated by index 1 (Fig. 1) and it will be further called exterior. The zone of flow, which lies within Mach cone, which emerges from the spout of wing, let us call/name internal area (area 2, Fig. 1).

Page 30.

Let us write out the sclution for an exterior. By virtue of the made assumptions solution can be presented in the form

$$\left.\begin{aligned} u^* &= 1 + \alpha^2 u_0 + O(\alpha^4); & p^* &= \alpha^2 p_0 + O(\alpha^4); \\ v^* &= O(\alpha^3); & \rho^* &= \rho_0 + O(\alpha^2); \\ w^* &= \alpha^2 w_0 + O(\alpha^4); & Y^*(x, z) &= \alpha Y_0(x, z) + O(\alpha^3), \end{aligned}\right\} \quad (1.3)$$

where y = Y* (x, z) - a surface of shock wave, and values with zero indices remain the order of one with tendency α toward zero.

Utilizing relationship/ratios on oblique shock wave, it is possible to obtain the following sclutiон fcr the exterior:

$$\left.\begin{aligned} Y_0 &= A_0 x + B_0 z; \quad p_0 = A_0 + 1 + \frac{1}{\gamma M_\infty^2 \alpha^2}; \\ u_0 &= -\frac{1}{2} - A_0; \quad \rho_0 = \frac{1 + A_0}{A_0}; \quad w_0 = \frac{A_0}{\lambda}, \end{aligned}\right\} \quad (1.4)$$

where $A_0 = \frac{\gamma + 1}{4} - 1 + \left[\left(\frac{\gamma + 1}{4}\right)^2 + \frac{1}{M_\infty^2 \alpha^2}\right]^{1/2}$;

$B_0 = -\frac{A_0}{\lambda}$;

$\lambda = \operatorname{tg} \gamma_1$;

γ — adabatic index

Let us examine interior. Let us introduce the new unknown functions and new variables with the aid of the relationship/ratios

$$\left.\begin{aligned} u^* &= 1 + \alpha^2 u_0 + \alpha^3 U_1 + O(\alpha^4); & \rho^* &= \rho_0 + \alpha R_1 + O(\alpha^2); \\ v^* &= \alpha^2 V_1 + O(\alpha^3); & Y^* &= \alpha A_0 x + \alpha^2 Y_1(x, z^*) + O(\alpha^3); \\ w^* &= \alpha^2 w_1 + O(\alpha^3); & z^* &= z/\alpha; \\ p^* &= \alpha^2 p_0 + \alpha^3 p_1 + O(\alpha^4); & y^* &= y\ \alpha. \end{aligned}\right\} \quad (1.5)$$

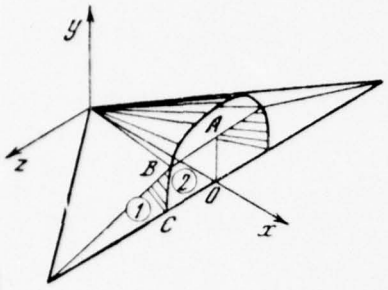

Fig. 1.

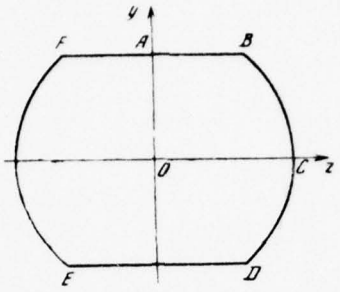

Fig. 2.

Page 31.

Then for interior of the equation of gas dynamics in this approach/approximation they seem in the form

$$\left.\begin{aligned} &\frac{\partial U_1}{\partial x}+\frac{\partial}{\partial x}\left(\frac{p_1}{\rho_0}\right)=0; \quad \frac{\partial}{\partial x}\left(p_1-a_0^2R_1\right)=0;\\ &\frac{\partial V_1}{\partial x}+\frac{\partial}{\partial y^*}\left(\frac{p_1}{\rho_0}\right)=0; \quad \frac{\partial}{\partial x}\left(\frac{p_1}{\rho_0}\right)+a_0^2\left(\frac{\partial V_1}{\partial y^*}+\frac{\partial w_1}{\partial z^*}\right)=0;\\ &\frac{\partial w_1}{\partial x}+\frac{\partial}{\partial z^*}\left(\frac{p_1}{\rho_0}\right)=0; \quad a_0^2=\gamma\frac{p_0}{\rho_0}. \end{aligned}\right\} \quad (1.6)$$

Boundary conditions on shock wave for this problem when $y^*=A_0x$ take the form

$$\left.\begin{aligned} &U_1 + A_0 V_1 = -Y_{1x}; \quad p_1 = \frac{4}{\gamma+1}(1+A_0) Y_{1x}; \\ &w_1 = -\frac{\partial Y_1}{\partial z^*}; \quad R_1 = \frac{4\rho_0^2}{(\gamma+1) M_\infty^2 \alpha^2 (1+A_0)^3} Y_{1x}; \\ &V_1 = \frac{2}{\gamma+1}\left[1 + \frac{1}{M_\infty^2 \alpha^2 (1+A_0)^2}\right] Y_{1x}. \end{aligned}\right\} \quad (1.7)$$

If we introduce conical variables $Y = \frac{y^*}{a_0 x}$ and $Z = \frac{z^*}{a_0 x}$ and to exclude from equations (1.6) U_1, V_1, ω_1, then problem it is reduced tc cne equation relative to p_1

$$\Delta p_1 - \left(Y\frac{\partial}{\partial Y} + Z\frac{\partial}{\partial Z} + 1\right)\left(Y\frac{\partial p_1}{\partial Y} + Z\frac{\partial p_1}{\partial Z}\right) = 0 \quad (1.8)$$

under following boundary conditions (Fig. 2):

on the shock wave AB

$$\left.\begin{aligned} &Y = M = \frac{A_0}{a_0}; \quad 0 \leqslant Z \leqslant k \quad (k = \sqrt{1-M^2}); \\ &\frac{p_{1Y}}{p_{1Z}} = \frac{1}{k^2 a_0 Z}\left[a_0^2\left(\frac{A_0}{a_0^2} + \frac{4A_0+3-\gamma}{4A_0(A_0+1)}\right)Z^2 - \frac{\gamma+1}{4}\right] - A_1 Z - \frac{B_1}{Z}; \end{aligned}\right\} \quad (1.9)$$

on the arc of unit circle BC

$$Y = \sqrt{1-Z^2}; \quad k \leqslant Z \leqslant 1; \quad p_1 = 0; \quad (1.10)$$

on the surface of wing CO

$$Y = 0; \quad 0 \leqslant Y \leqslant 1; \quad p_{1Y} = 0; \quad (1.11)$$

on the plane of symmetry AO

$$Z=0;\quad 0\leqslant Y\leqslant M;\quad p_{1\,z}=0. \tag{1.12}$$

Function p_1 can be analytically continued to entire polygon BDEF symmetrically, and, if we search for the analytical solution p_1 (Y, Z) in the form of the function, even relative to its arguments, then conditions (1.11) and (1.12) will be satisfied automatically. Condition (1.9) is spread to AF and ED by symmetrical form, and on the arcs of the unit circle, is retained as before condition $p_1 = 0$.

Page 32.

2. Information of boundary-value problem to integral equation. Let us search for p_1 in the form of the contour integral

$$p_1=\int g(\eta,\ \zeta)\,\varphi(Y,\ Z,\ \eta,\ \zeta)\,ds, \tag{2.1}$$

where

$$\varphi(Y,\ Z,\ \eta,\ \zeta)=\frac{1}{\sqrt{1-\eta^2-\zeta^2}}\ln\frac{[(1-Y\eta-Z\zeta)^2-(1-Y^2-Z^2)(1-\eta^2-\zeta^2)]^{1/2}}{1-Y\eta-Z\zeta-\sqrt{(1-Y^2-Z^2)(1-\eta^2-\zeta^2)}};$$

$g(\eta,\ \zeta)$ - the intensity of the "sources" of pressure, arrange/located in a symmetrical manner on EF and ED;

s - arc length.

The solution of form (2.1) satisfies equation (1.8), elliptical within unit circle, and bourdary tc conditicns (1.10)-(1.12). For this, in order to satisfy condition (1.9), let us find the limiting values of derivatives p_{1Y} and p_{1Z} with apprcach to shock wave of from within area BDEF:

$$\left.\begin{aligned} p_{1Y}(M-0,\ Z) &= \int g(\eta,\ \zeta)\,\varphi_Y(M,\ Z,\ \eta,\ \zeta)\,ds + \frac{\pi g(M,\ Z)}{k^2}\ ; \\ p_{1Z}(M-0,\ Z) &= \int g(\eta,\ \zeta)\,\varphi_Z(M,\ Z,\ \eta,\ \zeta)\,ds. \end{aligned}\right\} \quad (2.2)$$

Substituting expressicn (2.2) under ccndition on shock wave (1.9), we will obtain fcllowing singular furction g(Z):

$$\left.\begin{aligned} &\frac{\pi Z\sqrt{k^2-Z^2}}{k^2}\,g(Z) + (B_1 - A_2 Z^2)\int_{-k}^{k}\frac{g(\zeta)\,d\zeta}{\zeta - Z} + \int_{-k}^{k}\Phi(Z,\ \zeta)\,g(\zeta)\,d\zeta = 0; \\ &A_2 = A_1 - M k^{-2}, \\ &\Phi(Z,\ \zeta) = \frac{M Z|Z(Z+\zeta)-2| - |Z(1+M^2) - \zeta k^2|(B_1 - A_1 Z^2)}{(Z^2+\zeta^2)k^2 + 4M^2 - 2Z\zeta(1+M^2)}\ . \end{aligned}\right\} \quad (2.3)$$

Equation (2.3) is related to the class of homogeneous complete special integral equations for open circuits.

Let us search for function g(Z) in the class of bounded functions. Then pressure p_1, calculated acccrding to formula (2.1), will be bounded function.

Let us write characteristic equation fcr equation (2.3):

$$\frac{\pi Z\sqrt{k^2-Z^2}}{k^2}\,f(Z) + (B_1 - A_2 Z^2)\int_{-k}^{k}\frac{f(\zeta)\,d\zeta}{\zeta - Z} = 0. \quad (2.4)$$

The index of equation (2.4) in the class of bounded functions x = 1, and the limited solution of equation (2.4) is record/written with an accuracy to constant factor in the form

$$\left.\begin{aligned} f(Z) &= \sqrt{k^2 - Z^2}\, b(Z) \exp \Gamma(Z); \\ b(Z) &= \frac{k^2 (B_1 - A_2 Z^2)}{[Z^2 (k^2 - Z^2) + k^4 (B_1 - A_2 Z^2)^2]^{1/4}}; \\ \Gamma(Z) &= -\frac{k^2}{\pi} \int_0^k \frac{\ln |Z^2 - x^2|}{\sqrt{k^2 - x^2}} \frac{2A_2 x^2 (k^2 - x^2) + (B_1 - A_2 x^2)(k^2 - 2x^2)}{x^2 (k^2 - x^2) + k^4 (B_1 - A_2 x^2)^2}\, dx. \end{aligned}\right\} \quad (2.5)$$

Page 33.

Let us conduct now for equation (2.3) the usual procedure of regularization by the solution of characteristic equation. As a result we will obtain the regularized equation

$$g(Z) + \int_0^k K(Z, \zeta)\, g(\zeta)\, d\zeta = f(Z), \quad (2.6)$$

where

$$\begin{aligned} K(Z, \zeta) &= a(Z)\, c(Z)\, \Phi_1(Z, \zeta) - \\ &- \frac{2\, b(Z) \sqrt{k^2 - Z^2} \exp \Gamma(Z)}{\pi} \int_0^k \frac{\tau c(\tau) \Phi_1(\tau, \zeta)\, d\tau}{\sqrt{k^2 - \tau^2} (\tau^2 - Z^2) \exp \Gamma(\tau)}; \\ a(Z) &= \frac{Z \sqrt{k^2 - Z^2}}{[Z^2 (k^2 - Z^2) + k^4 (B_1 - A_2 Z^2)^2]^{1/4}}; \\ c(Z) &= \frac{k^2}{\pi [Z^2 (k^2 - Z^2) + k^4 (B_1 - A_2 Z^2)^2]^{1/4}}; \\ \Phi_1(Z, \zeta) &= \Phi(Z, \zeta) + \Phi(Z, -\zeta). \end{aligned}$$

When deriving the equation (2.6) there was used the parity of function g(Z). From the theory of special integral equations [3] it

follows that equation (2.6) represents by itself the integral second-order of Fredholm equation with the continuous nucleus which already can be solved by the approximate numerical methods.

Let us note that the procedure of regularization becomes inaccurate when $M, a \to \infty$, because is changed the index of equation (2.4), and coefficient c(Z) and, consequently, also nucleus K(Z,ζ) become disruptive.

3. Obtaining solution and its standardization. The problem of finding the distribution of source strength g(Z) came to second-order of the integral equation of Fredholm solution with continuous nucleus (2.6). For finding the solution, let us use the following approximate diagram. The cut of the integration [0, k] let us divide into n equal parts Δs = k/n and on each section Δs_i approximately let us count the function g_i of constant. Then, replacing in (2.6) integral by the sum and varying n times variable Z, we obtain for g_i the system of the linear algebraic equations

$$A\vec{g} = \vec{f}, \qquad (3.1)$$

where the matrix element A takes the form

$$a_{ij} = K(Z_i, \zeta_j)\Delta s + \delta_{ij};$$

column element $f_i = f(Z_i)$; Z_i - the coordinate of the middle of the i

cut.

For providing the necessary accuracy/precision during calculation $K(Z_i, \zeta_j)$ the integral, entering the expression for K(Z, ζ), was calculated from the formula of rectangles with the number of separations n^2.

Solution g(Z), obtained from equation (2.6), is determined with an accuracy to constant factor due to the arbitrary selection of the solution of the characteristic equation f(Z). Let us note that from conditions on shock wave (1.7) it follows that along shock wave is correct the relationship/ratio between w_1 and p_1:

$$\frac{\partial p_1}{\partial Z} = \frac{4}{\gamma+1} A_0 \rho_0 a_0 Z \frac{\partial w_1}{\partial Z}. \tag{3.2}$$

Page 34.

Since during motion along the shock wave AB function w_1 with continuous form changes from zero to $w_0 = \frac{A_0}{\lambda}$, the with the aid of relationship/ratio (3.2) condition of the standardization of function p_1, can be presented in the form

$$\int_0^k \frac{1}{Z} \frac{\partial}{\partial Z} p_1(M, Z)\, dZ = \frac{4}{\gamma+1} \frac{A_0^2 \rho_0 a_0}{\lambda}. \tag{3.3}$$

Substituting in (3.3) expression (2.1), we will obtain

standardization condition for function g(Z):

$$2(1+M^2)\int_0^k \frac{dZ}{\sqrt{k^2-Z^2}}\int_0^k \frac{|k^2(\zeta^2-Z^2)-4M^2|\,g(\zeta)\,d\zeta}{[k^2(Z^2+\zeta^2)+4M^2]^2-4Z^2\zeta^2(1+M^2)^2}+$$
$$+\frac{1}{2}\int_{-k}^{k}\frac{dZ}{Z\sqrt{k^2-Z^2}}\int_{-k}^{k}\frac{g(\zeta)\,d\zeta}{\zeta-Z}=\frac{4}{\gamma+1}\frac{A_0^2\rho_0 a_0}{k}. \qquad (3.4)$$

The second integral in equation (3.4) is located with the aid of the known formula of the exchange of the order of integration in the dual integrals:

$$\frac{1}{2}\int_{-k}^{k}\frac{dZ}{Z}\int_{-k}^{k}\frac{g(\zeta)\,d\zeta}{\sqrt{k^2-Z^2}(\zeta-Z)}=-\frac{\pi^2 g(0)}{2k}+$$
$$+\frac{1}{2}\int_{-k}^{k}g(\zeta)\,d\zeta\int_{-k}^{k}\frac{dZ}{Z\sqrt{k^2-Z^2}(\zeta-Z)}. \qquad (3.5)$$

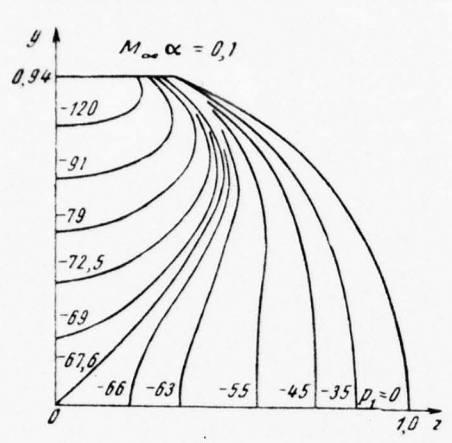

Fig. 3.

Page 35.

Last/latter integral in equation (3.5) is equal to zero, since internal integral on Z turns into zero. Finally the condition of the standardization of functicn g(Z) takes the form

$$2(1+M^2)\int_0^k g(\zeta)\,d\zeta \int_0^k \sqrt{k^2-Z^2}\,\frac{|k^2(\zeta^2-Z^2)-4M^2|\,dZ}{|[k^2(Z^2+\zeta^2)+4M^2]^2-4Z^2\zeta^2(1+M^2)^2|} - \frac{\pi g(0)}{2k} = \frac{4}{\gamma+1}\frac{A_0^2\rho_0 a_0}{\lambda}. \qquad (3.6)$$

4. Examples of calculations. Employing the given above procedure was comprised the program of calculatien fcr ccmputers. During calculations was set/assumed $\gamma = 1.4$ and $\lambda = 1$. It turned out that with an increase in the number of separaticns (n = 5; 10; 20; 40) the

difference between the consecutively obtained sclutions is rapidly reduced; for example, at the value of the parameter M_∞ $\alpha = 1$ the difference in the values of pressure p_1 during calculations for n = 20 and 40 is exhibited only in the fifth sign. By this is confirmed the effectiveness of the selection cf the calculation method. In Fig. 3-5, are constructed the isobars p_1 in the disturbed area respectively for the values of the parameter M_∞ $\alpha = 0{,}1;\ 1;\ 5$. In these cases the calculations were performed with n = 20. Given data of calculations are confirmed by the results cf [2], in which the solution is found in the form cf a series.

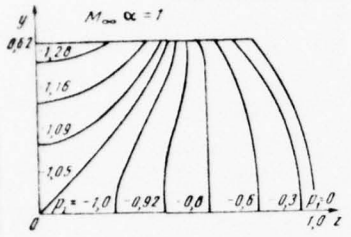

Fig. 4.

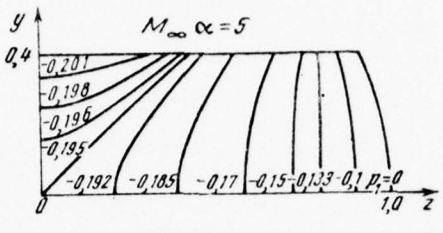

Fig. 5.

REFERENCES

1. S. M. Ter-Minasyants. Problem of the supersonic flow around the lower surface of delta wing. Izv. of the AS USSR, MZhG, 1966, No 6.

2. N D Malmuth. Linear, rotational flow over the windward side of a hypersonic delta wing. Los Angeles, North American (interim report), NA-66-495.

3. F. D. Gakhov. Boundary-value problems. Fizmatgiz, 1958.

The manuscript entered 12/IV 1969.

Page 36.

AERODYNAMIC INVESTIGATION OF ELEVONS ON LOW-ASPECT-RATIO WINGS.

V. G. Mikeladze.

Are examined the aerodynamic characteristics of elevons as organ/controls of longitudinal and lateral control on low-aspect-ratio wings. Is presented the method of calculation of the aerodynamic characteristics of elevons at subsonic and supersonic speeds. Are given the results of systematic studies in the effect of the separate parameters of elevons on their aerodynamic characteristics. Is given the flow pattern of low-aspect-ratio wing with the deflected to large angles elevons at subsonic, transonic and supersonic speeds.

METHOD OF CALCULATION OF THE EFFECTIVENESS OF ELEVONS AT SUBSONIC SPEEDS.

The method of calculation of the effectiveness of elevons on the wings of arbitrary planform at subsonic speeds is instituted on the

use of a reciprocity theorem[1]. which establishes communication/connection between aerodynamic wing characteristics in direct/straight and return flow when the direction of velocity of incident flow V_0 is replaced by reverse/inverse.

FOOTNOTE [1]. The use of a reciprocity theorem for the evaluation of the control effectiveness was suggested by A. I. Golubinskiy. ENDFOOTNOTE.

The derivatives of the lift coefficient $c_y^{\delta_{эв}}$, of the coefficient of pitching moment $m_z^{\delta_{эв}}$ and of the rolling-moment coefficient $m_x^{\delta_{эв}}$ in the angle of deflection of elevon $\delta_{эв}$ can be presented as follows:

$$c_y^{\delta_{эв}} = \frac{1}{S}\int\limits_{S_{эв}}\int \bar{p}_{\alpha=} dS; \quad (1)$$

$$m_{z_1}^{\delta_{эв}} = \frac{1}{S}\int\limits_{S_{эв}}\int \bar{p}_{\omega_z=} dS; \quad (2)$$

$$m_{x_1}^{\delta_{эв}} = \frac{1}{S}\int\limits_{S_{эв}}\int \bar{p}_{\omega_x=} dS; \quad (3)$$

here S - an area of wing;

Page 37.

$p = \frac{\Delta p_\alpha}{q}$ pressure-drop coefficient between lower and suction sides of wing, driving/moving at angle of attack without rotation, in the turned flow;

$p_{\omega_z} = \frac{\Delta p_{\omega_z}}{q}$ – pressure-drop coefficient during the rotation of wing relative to axle/axis Oz in the turned flow;

$p_{\omega_x} = \frac{\Delta p_{\omega_x}}{q}$ – pressure-drop coefficient during the rotation of wing relative to axle/axis Ox in the turned flow;

$q = \frac{\rho V_0^2}{2}$ – velocity head.

For $m_{z_1}^{\delta_{эв}}$ and $m_{x_1}^{\delta_{эв}}$ as characteristic linear dimension is accepted root wing chord b_0.

The problem of flow around of the wing in the turned flow is solved by the approximation method in which the wing is replaced by vortex/eddy surface[1].

FOOTNOTE [1]. S. M. Belotserkovskiy. Fine/thin lifting surface in the subsonic flow of gas. M., "science", 1965. ENDFOOTNOTE.

Carrying vortex/eddy surface is simulated by connected Vikhrev's series cords. Each cord is replaced by several oblique horseshoe vortices, which consist of the bound vortex with constant intensity/strength along spread/scope Γ_i and free vortices.

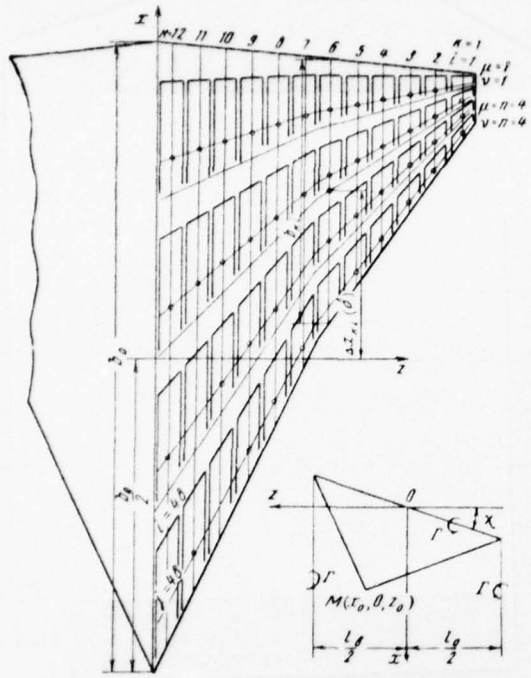

Fig. 1.

Page 38.

Design diagram is represented in Fig. 1. Wing with the fracture of leading edge in the examined case of determining the effectiveness of elevons was replaced by four Vikhrev by the cords from chord, each of which was, in turn, was replaced by twelve oblique horseshoe vortices along the semirange of wing.

Thus, on each half of the wing it is arrange/located of 48 bound vortices. In each cell of the formed grid, the bound vortex coincides

with the line of 1/4 chords of cell, and the distance between free Vikhrev by cords is equal to the spread/scope of this cell. The boundary conditions of nonpassage are satisfied for each cell at the point, arrange/located cn the middle of the line of 3/4 chords.

During the calculation of the effectiveness of elevons, it is necessary to have values of the dimensionless circulation of eddy/vortex during the motion of wing at angle of attack without rotation γ_{α_i}, dimensionless circulation $\gamma_{\omega z_i}$ during the rotation of wing of relatively axle/axis Oz and dimensionless circulation $\gamma_{\omega_{x_i}}$ for the wing, which rotates around axle/axis Ox.

Satisfaction to boundary conditions gives three independent systems of equations which make it possible to determine three the dimensionless circulations indicated above

$$\left.\begin{aligned}
&\sum_{i=1}^{m}(W_{y_{ij}}+\Delta W_{y_{ij}})\gamma_{\alpha_i}=-2\pi;\\
&\sum_{i=1}^{m}(W_{y_{ij}}+\Delta W_{y_{ij}})\gamma_{\omega z_i}=2\pi\frac{x_{0_j}}{b_0};\\
&\sum_{i=1}^{m}(W_{y_{ij}}-\Delta W_{y_{ij}})\gamma_{\omega x_i}=-2\pi\frac{z_{0_j}}{b_0}
\end{aligned}\right\} \qquad (4)$$

$$(j=1,\ 2,\ \ldots\ m;\quad m=Nn),$$

where $W_{y_{ij}}$ - dimensionless velocities, caused by the oblique horseshoe vortex i at point j,

$$W_{y_{ij}}=W_y(\xi_{0_{ij}},\ \zeta_{0_{ij}},\ \gamma);$$

x_{0_j}, z_{0_j} - coordinate of the junction/unit calculation point j; $\gamma=\dfrac{\Gamma}{V_0 l_в}$

- dimensionless circulation of eddy/vortex; $l_в$ - distance between free vortices (see Fig. 1); $\xi_0 = \frac{x_0}{l_в/2}$ and $\zeta_0 = \frac{z_0}{l_в/2}$ - dimensionless coordinates of point M; χ - sweep angle of the bound vortex; $\Delta W_{y_{ij}}$ - additional dimensionless velocities which appear at point j from the eddy/vortex, which is located on left half wing and symmetrical to eddy/vortex i,

$$\Delta W_{y_{ij}} = W_y(\xi_{0_{ij}}, \Delta\zeta_{0_{ij}}, \chi).$$

Page 39.

The calculation of all dimensionless velocities was conducted on the formulas

$$W_y = \frac{V_0\gamma}{2\pi} W_y(\xi_0, \zeta_0, \chi), \tag{5}$$

where

$$W_y(\xi_0, \zeta_0, \chi) = U_y(\xi_0, \zeta_0, \chi) + V_y(\xi_0, \zeta_0, \chi), \tag{6}$$

$U_y(\xi_0, \zeta_0, \chi)$- the velocity, caused by the bound vortex at the arbitrary point:

$$U_y(\xi_0, \zeta_0, \chi) = \frac{1}{\xi_0\cos\chi + \zeta_0\sin\chi}\left[\frac{\xi_0\sin\chi - \zeta_0\cos\chi + \frac{1}{\cos\chi}}{\sqrt{(\xi_0 + \operatorname{tg}\chi)^2 + (1-\zeta_0)^2}} + \right.$$
$$\left. + \frac{\frac{1}{\cos\chi} - \xi_0\sin\chi + \zeta_0\cos\chi}{\sqrt{(\xi_0 - \operatorname{tg}\chi)^2 + (1+\zeta_0)^2}}\right]; \tag{7}$$

$V_y(\xi_0, \zeta_0, \chi)$- the velocity, caused by free vortices at the arbitrary point:

$$V_y(\xi_0, \zeta_0, \chi) = -\frac{1}{1-\zeta_0}\left[1 + \frac{\xi_0 + \operatorname{tg}\chi}{\sqrt{(\xi_0 + \operatorname{tg}\chi)^2 + (1-\zeta_0)^2}}\right] -$$
$$-\frac{1}{1-\zeta_0}\left[1 + \frac{\xi_0 - \operatorname{tg}\chi}{\sqrt{(\xi_0 - \operatorname{tg}\chi)^2 + (1+\zeta_0)^2}}\right]. \tag{8}$$

After solving system of equations (4) and after calculating values $\bar{p}_{\alpha-}$, $\bar{p}_{\omega_z-}$ and $\bar{p}_{\omega_x-}$, we determine total wing characteristics with the deflected elevons on the formulas

$$C_y^{\delta_{эв}} = \lambda \int_{\bar{z}_1}^{\bar{z}_2} \psi_{\Gamma\alpha}\, d\bar{z}; \tag{9}$$

$$m_{z_1}^{\delta_{эв}} = \lambda \int_{\bar{z}_1}^{\bar{z}_2} \psi_{\Gamma\omega_z}\, d\bar{z}; \tag{10}$$

$$m_{x_1}^{\delta_{эв}} = \lambda \int_{\bar{z}_1}^{\bar{z}_2} \psi_{\Gamma\omega_x}\, d\bar{z}, \tag{11}$$

where $\lambda = \frac{l^2}{S}$ - wing aspect ratio;

$$\psi_{\Gamma\alpha} = \frac{1}{2 \cdot 57{,}3} \int_{\bar{x}^*-b_{эв}}^{\bar{x}^*} \bar{p}_{\alpha-}\, d\bar{x}; \tag{12}$$

$$\psi_{\Gamma\omega_z} = \frac{1}{2 \cdot 57{,}3} \int_{\bar{x}^*-b_{эв}}^{\bar{x}^*} \bar{p}_{\omega_z-}\, d\bar{x}; \tag{13}$$

$$\psi_{\Gamma\omega_x} = \frac{1}{2 \cdot 57{,}3} \int_{\bar{x}^*-b_{эв}}^{\bar{x}^*} \bar{p}_{\omega_x-}\, d\bar{x}; \tag{14}$$

here $\bar{x}^*$ - coordinate of the leading edge of wing section in the turned flow; $\bar{b}_{эв}$ - relative chord of elevon.

Page 40.

For an example Fig. 2, gives the results of calculations with the aid of the computers of the effectiveness of elevons on wing with the fracture of leading edge. The comparison of calculated and

experimental data shows that computed values of coefficients $c_y^{\delta_э}$, $m_z^{\delta_э}$ and $m_x^{\delta_э}$ are higher experimental. One of the reasons for this disagreement is the not considered by theory presence of the slots which are formed between the staticnary part of the wing and the deflected elevon. The effect of slot on the effectiveness of elevons is shown on Fig. 3. The introductien of the empirical coefficients of $k \approx 0.85$ into computed values of derivatives $c_y^{\delta_э}$, $m_z^{\delta_э}$ and $m_x^{\delta_э}$ makes it possible to obtain the values of these derivatives with an accuracy tc $\pm$5o/o.

AD-A065 783 FOREIGN TECHNOLOGY DIV WRIGHT-PATTERSON AFB OHIO F/G 20/4
SCIENTIFIC NOTES FROM THE CENTRAL AEROHYDRODYNAMIC INSTITUTE.(U)
JUL 78
UNCLASSIFIED FTD-ID(RS)T-0680-78 NL

2 OF 3
AD
A065783

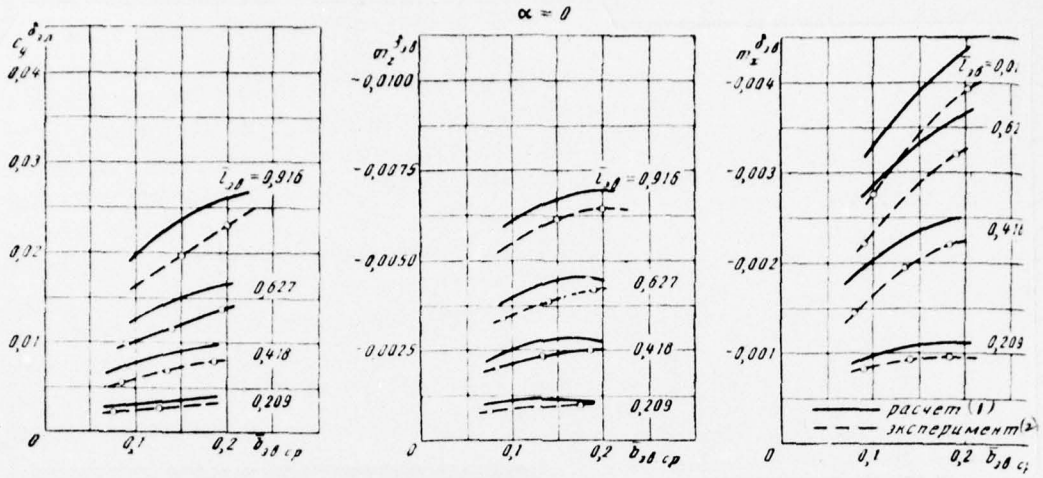

Fig. 2.

Key: 1) Calculation; 2) Experiment.

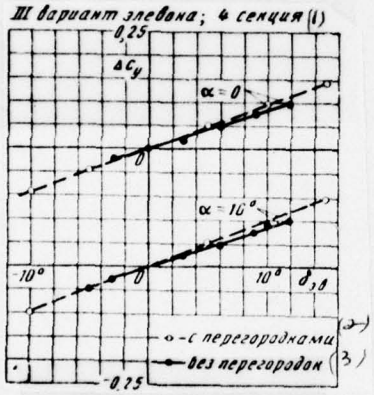

Fig. 3.

Key: (1). III Version of elevon; 4 sections. (2) with partition/baffles. (3) without partition/baffles.

METHOD OF CALCULATION OF EFFECTIVENESS AND HINGE MOMENTS OF ELEVONS AT SUPERSONIC SPEEDS.

Effectiveness of elevons. The method of calculation of the effectiveness of elevons on low-aspect-ratic wings at supersonic speeds is instituted on the linear theory of supersonic flows. During the calculation of the effectiveness of elevons, it is assumed that the rotational axis of elevon is supersonic, Mach lines do not intersect the wing chord and elevon.

Elevon with the adjacent sections of wing is divide/marked off into zones (Fig. 4): zone I is limited by the Mach lines, which proceed from the point of intersection of rotational axis with the root chord of elevon, and the trailing edge of elevon; zone II is limited by the Mach lines, which proceed from the point of intersection of rotational axis with the root and end chords of elevon, rotational axis and the trailing edge of elevons; zone III is limited by the Mach lines, which proceed from the point of intersection of rotational axis with the end chord of elevon, and the trailing edge of elevon.

The pressure-drop coefficients in these zones are equal to

$$\bar{p}_{\text{I}}^{\delta_{\text{эл}}} = \frac{4}{\pi \sqrt{\beta^2 - \text{tg}^2 \chi_{\text{эл}}}} \arccos \frac{a - \beta \frac{y}{x}}{1 - \alpha\beta \frac{y}{x}}; \tag{15}$$

$$\bar{p}_{\text{II}}^{\delta_{\text{эл}}} = \frac{4}{\sqrt{\beta^2 - \text{tg}^2 \chi_{\text{эл}}}}; \tag{16}$$

$$\bar{p}_{\text{III}}^{\delta_{\text{эл}}} = \frac{4}{\pi \sqrt{\beta^2 - \text{tg}^2 \chi_{\text{эл}}}} \arccos \frac{\beta \frac{y}{x} - a}{1 - a\beta \frac{y}{x}}; \tag{17}$$

here $\bar{p}_i^{\delta_{\text{эл}}}$ - jump/drop in the pressure coefficient between the lower and upper surfaces of elevon in the i zone during the deviation of elevon of 1 rad; $a = \frac{\text{tg}\,\chi_{\text{эл}}}{\beta}$ (where tg $\chi_{\text{эл}}$ - sweep angle along the axis of the rotation of elevon); $\beta = \sqrt{M^2 - 1}$; $\delta_{\text{эл}}$ - angle of deflection of elevon, determined in section throughout flow.

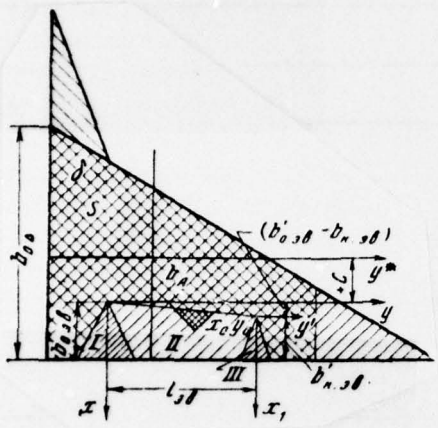

Fig. 4.

Page 42.

For a low-aspect-ratio wing, including for wings with alternating/variable sweepback on leading edge and the trailing edge, perpendicular to the axle/axis of syssetry, expression for derivatives $c_y^{\delta_{эв}}$, $m_x^{\delta_{эв}}$ and $m_z^{\delta_{эв}}$ they take the form

$$c_y^{\delta_{эв}} = \frac{4 S_\Delta \operatorname{tg}\varepsilon}{57{,}3\, S \sqrt{\beta^2 - \operatorname{tg}^2 \chi_{эв}}} \left[\frac{(\bar{b}_{0\,эв}'^2 - \bar{b}_{к.\,эв}'^2)(\sqrt{1-a^2}-1)}{\operatorname{tg}\chi_{эв}} + (\bar{b}_{0\,эв}' + \bar{b}_{к.\,эв}')\bar{l}_{эв}) \right]; \quad (18)$$

$$m_x^{\delta_{эв}} = -\frac{2 S_\Delta l_\Delta \operatorname{tg}\varepsilon}{57{,}3\, S l \sqrt{\beta^2 - \operatorname{tg}^2 \chi_{эв}}} \left\{ \frac{\sqrt{1-a^2}-1}{\operatorname{tg}\varepsilon} \left[(\bar{b}_{0\,эв}'^2 - \bar{b}_{к.\,эв}'^2)\bar{z}_{0\,эв} - \bar{b}_{к.\,эв}'^2 \bar{l}_{эв} + \frac{(\bar{b}_{0\,эв}'^3 - \bar{b}_{к.\,эв}'^3)}{3 \operatorname{tg}\chi_{эв}} \right] + (\bar{b}_{0\,эв}' + \bar{b}_{к.\,эв}')\bar{l}_{эв}\bar{z}_{0\,эв} + \frac{1}{3}(\bar{b}_{0\,эв}' + 2\bar{b}_{к.\,эв}')\bar{l}_{эв}^2 \right\}; \quad (19)$$

$$m_z^{\delta_{эв}} = -\frac{1}{57{,}3} \left[m_{z\,I}^{\delta_{эв}} + m_{z\,II}^{\delta_{эв}} + m_{z\,III}^{\delta_{эв}} + c_{y\,III}^{\delta_{эв}} (\bar{b}_{0\,эв}' - \bar{b}_{к.\,эв}') \frac{l_\Delta/2}{b_A} \right], \quad (20)$$

where

$$m_{z\,I}^{\delta_{эв}} = \frac{2}{3}\,\frac{b_{0\Delta}\,S_\Delta\,\mathrm{tg}^2\varepsilon\,(a-1+\sqrt{1-a^2})\,\bar{b}_{0\,эв}^{\prime 3}}{b_A\,S\,\mathrm{tg}\,\chi_{эв}\sqrt{\beta^2-\mathrm{tg}^2\chi_{эв}}}, \tag{21}$$

$$m_{z\,II}^{\delta_{эв}} = \frac{4}{3}\,\frac{b_{0\Delta}\,S_\Delta\,\mathrm{tg}^2\varepsilon}{b_A\,S\beta\sqrt{\beta^2-\mathrm{tg}^2\chi_{эв}}}\,[3\bar{l}_{эв}\,b_{0\,эв}^{\prime 2}-(\bar{b}_{0\,эв}^{\prime}-\bar{b}_{к.\,эв}^{\prime})^2\,\beta\bar{l}_{эв}-$$
$$-(\bar{b}_{0\,эв}^{\prime}-\bar{b}_{к.\,эв}^{\prime})^3-\bar{b}_{0\,эв}^{\prime 2}\,(b_{0\,эв}^{\prime}+3\bar{b}_{к.\,эв}^{\prime 3})]; \tag{22}$$

$$m_{z\,III}^{\delta_{эв}} = \frac{8}{3}\,\frac{b_{0\Delta}\,S_\Delta\,\mathrm{tg}^2\varepsilon\,(a-1+\sqrt{1-a^2}\,\bar{b}_{к.\,эв}^{\prime 3}}{b_A\,S\,\mathrm{tg}\,\chi_{эв}\sqrt{\beta^2-\mathrm{tg}^2\chi_{эв}}}; \tag{23}$$

$$c_{y\,III}^{\delta_{эв}} = \frac{4S_\Delta\,\bar{b}_{к.\,эв}^{\prime 2}\,\mathrm{tg}\,\varepsilon}{S\,\mathrm{tg}\,\chi_{эв}\sqrt{\beta^2-\mathrm{tg}^2\chi_{эв}}}\,(1+a-\sqrt{1-a^2}). \tag{24}$$

In these formulas: $c_y^{\delta_{эв}}$ - lift coefficient of wing from the deviation of elevons on both halves of wing to one side on 1°; $m_x^{\delta_{эв}}$ - rolling-moment coefficient during the deviation of elevons on both halves of wing to opposite sides on ±1°; $m_z^{\delta_{эв}}$ - coefficient of longitudinal moment with respect to z axis, passing through the point of intersection of the root chord of elevon with its rotational axis (Fig. 4) during the deviation of elevons on both halves of wing to one side on 1°;.

Page 43.

S_Δ, $b_{0\Delta}$, l_Δ, ε - area, root chord, span and semiapex angle of base delta wing (Fig. 4);

$\bar{b}_{0\,эв}^{\prime}=\frac{b_{0\,эв}^{\prime}}{l_\Delta/2}$, $\bar{b}_{к.\,эв}^{\prime}=\frac{b_{к.\,эв}^{\prime}}{l_\Delta/2}$, $\bar{z}_{0\,эв}=\frac{z_{0\,эв}}{l_\Delta/2}$ — relative chord, the span and the position of the

beginning of elevon, in reference to the semirange of base delta wing.

In the case when elevon has the constant absolute chord ($\chi_{эв} = 0$) of expression for derivatives c_y^{δ}, m_x^{δ} and m_z^{δ} substantially they are simplified:

$$c_y^{\delta_{эв}} = \frac{8 S_{\Delta} \bar{b}'_{эв} \bar{l}_{эв} \operatorname{tg} \varepsilon}{57{,}3\, S\beta}; \tag{25}$$

$$m_x^{\delta_{эв}} = -\frac{2 S_{\Delta} l_{\Delta} \bar{b}'_{эв} \bar{l}_{эв} \operatorname{tg} \varepsilon}{57{,}3\, Sl\beta} (2\bar{z}_{0\,эв} + \bar{l}_{эв}); \tag{26}$$

$$m_z^{\delta_{эв}} = \frac{4 S_{\Delta} b_{0\,\Delta} \operatorname{tg}^2 \varepsilon \bar{l}_{эв} \bar{b}'^2_{эв}}{57{,}3\, Sb_A \beta}. \tag{27}$$

Those obtained by the calculation of the characteristic of the effectiveness of elevons are more experimental values. Processing the results of experimental data and their comparison with the results of calculations shows that for the evaluation of the effectiveness of elevons at the moderate supersonic velocities of the value of derivatives $c_y^{\delta_{эв}}$, $m_x^{\delta_{эв}}$, $m_z^{\delta_{эв}}$, determined according to formulas (18)-(20) it is necessary to multiply by the empirical coefficient of k = 0.85-0.9.

Hinge moments of elevons. The calculation of the hinge moments of elevons at supersonic speeds is done with the same limitations, which were accepted for the calculation of the effectiveness of elevons. The hinge-moment coefficient relative to the rotational axis of elevon during its deviation on 1° is equal to

$$m_{ш}^{\delta_{эв}} = -\frac{1}{57,3}\left(m_{ш\,I}^{\delta_{эв}} + m_{ш\,II}^{\delta_{эв}} + m_{ш\,III}^{\delta_{эв}}\right), \tag{28}$$

$$m_{ш\,I}^{\delta_{эв}} = \frac{8\bar{b}'^{3}_{эв}\operatorname{tg}\varepsilon}{3\bar{S}_{эв}\bar{b}'_{A\,эв}\operatorname{tg}\chi_{эв}\sqrt{\beta^2-\operatorname{tg}^2\chi_{эв}}}\left[a-1+\frac{\sqrt{1-a^2}}{2}\left(\frac{1}{2}-\frac{a}{\pi}\right)+\right.$$
$$\left.+\frac{\arccos a}{2\pi}+\frac{1-a^2}{2}\right]; \tag{29}$$

$$m_{ш\,II}^{\delta_{эв}} = \frac{4\operatorname{tg}\varepsilon}{\bar{S}'_{эв}\bar{b}'_{A\,эв}\beta\sqrt{\beta^2-\operatorname{tg}^2\chi_{эв}}}\left[\frac{1}{3}\left\{\bar{b}'^{2}_{0\,эв}\left[3\bar{l}_{эв}\beta-4\bar{b}'_{0\,эв}+3\left(\bar{b}'_{0\,эв}-\bar{b}'_{к.\,эв}\right)\right]-\right.\right.$$
$$-\left(\bar{b}'_{0\,эв}-\bar{b}'_{к.\,эв}\right)^2\left[\bar{l}_{эв}\beta+\left(\bar{b}'_{0\,эв}-\bar{b}'_{к.\,эв}\right)\right]\Big\}-\operatorname{tg}\chi_{эв}\left\{\bar{l}_{эв}\bar{b}'_{0\,эв}\left[\bar{l}_{эв}\beta-\right.\right.$$
$$-\bar{b}'_{0\,эв}+2\left(\bar{b}'_{0\,эв}-\bar{b}'_{к.\,эв}\right)\Big]-\bar{l}_{эв}\left(\bar{b}'_{0\,эв}-\bar{b}'_{к.\,эв}\right)\left[\frac{2}{3}\bar{l}_{эв}\beta+\left(\bar{b}'_{0\,эв}-\bar{b}'_{к.\,эв}\right)\right]-$$
$$\left.\left.-\frac{\bar{b}'_{0\,эв}\bar{b}'_{к.\,эв}\left(\bar{b}'_{0\,эв}-\bar{b}'_{к.\,эв}\right)}{\beta}-\frac{\left(\bar{b}'_{0\,эв}-\bar{b}'_{к.\,эв}\right)^2}{3\beta}\right\}\right]; \tag{30}$$

$$m_{ш\,III}^{\delta_{эв}} = \frac{8\bar{b}'^{3}_{к.\,эв}\operatorname{tg}\varepsilon}{3\bar{S}'_{эв}\bar{b}'_{A\,эв}\operatorname{tg}\chi_{эв}\sqrt{\beta^2-\operatorname{tg}^2\chi_{эв}}}\left[a+\frac{\sqrt{1-a^2}}{2}\left(\frac{1}{2}-\frac{a}{\pi}\right)+\right.$$
$$\left.+\frac{\arccos a}{2\pi}-\frac{1-a^2}{2}\right]; \tag{31}$$

here $\bar{S}'_{эв}=\frac{S'_{эв}}{S_{\Delta}}$, $\bar{b}'_{A\,эв}=\frac{b'_{A\,эв}}{l_{\Delta}/2}$ - relative area and the mean aerodynamic chord of elevon to rotational axis.

Page 44.

In the case of the constant absolute chord of elevon, the hinge-moment coefficient is equal to

$$m_{ш}^{\delta_{эв}} = -\frac{1}{57,3}\,\frac{4\operatorname{tg}\varepsilon\,b'^{2}_{эв}}{\bar{S}'_{эв}\bar{b}'_{A\,эв}\beta}\left(\bar{l}_{эв}-\frac{4\bar{b}'_{эв}}{3\pi\beta}\right). \tag{32}$$

As showed the comparisen of the calculated and experimental values of hinge-moment characteristics, calculated hinge-moment coefficients prove to be somewhat overstated. Therefore during the

estimation of the hinge moments of elevons at the moderate supersonic velocities computed value cf coefficient $m_{III}^{\delta_B}$, determined in formula (28), must be multiplied by the empirical ccefficient of $k \approx 0.85$.

Physical flow pattern of wirg with the deflected elevons, obtained by the method of pressure distribution.

The studies of the physical flow pattern of wing with the deflected elevons were conducted on the model of low-aspect-ratio wing with alternating/variable sweepback on leading edge (Fig. 5). The analysis of the effect cf mach number of the incident flow on flow around of the wing with the deflected elevcn is carried out based cn the example of the examination of the air-load distribution in wing section, arrange/located approximately in the middle the spread/scope of elevon.

Fig. 6, depicts the diagram/curve of pressure distribution along wing chord in the presence of the deflected elevon with Mach number = 0.6.

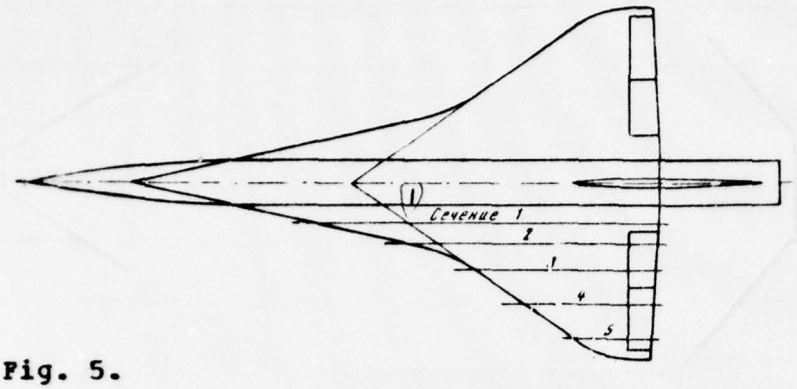

Fig. 5.

Key: (1). Section.

Page 45.

It is evident that the deviation of elevon causes the redistribution of pressure along an entire wing chord both on upper and on lower surface. With Mach number = 0.83, deviation of elevon of negative angles is no longer caused the redistribution of pressure along an entire wing chord on lower surface[1].

FOOTNOTE [1]. Analogous results on airfoil/profile with control at transonic speeds were obtained by G. P. Svishchev into 1948. ENDFOOTNOTE.

During transition to small supersonic velocities (M = 1.05, Fig.

7) the deviation of elevon of negative angles causes the redistribution of pressure on lower surface only along the chord of elevon. On suction side of wing, the zone of the effect of the deviation of elevon of pressure distribution is spread forward, the further, the greater the angle of deflection of elevon.

The analogous phenomenon is observed with large mach numbers of the incident flow. The greater the mach number, up to smaller distance elevon is forward from spread its effect on the side, turned to flow (Fig. 8). During transition from the subsonic to supersonic speeds, changes the form of the diagram/curve of pressure on elevon itself. If at subsonic speeds the form of diagram/curve is close to triangular, then at supersonic speeds it is close to rectangular.

The enumerated above special feature/peculiarities of a change in the character of flow around of the wing with the deflected elevons explain the reasons for an incidence/drop in the effectiveness of elevons and an increase in their hinge moments during transition from the subsonic to supersonic speeds.

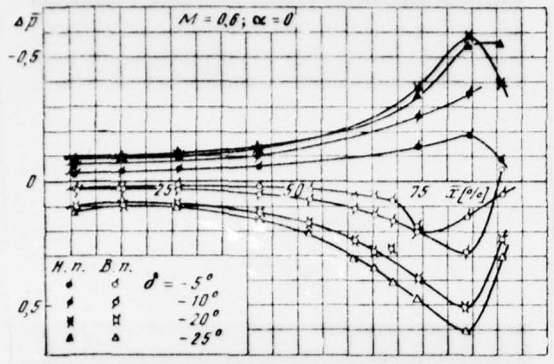

Fig. 6.

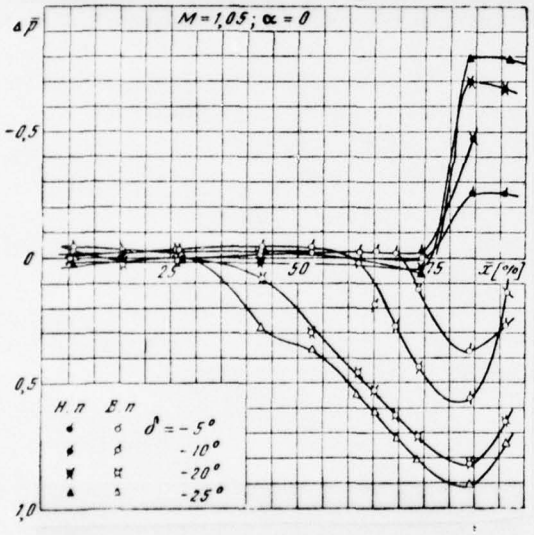

Fig. 7.

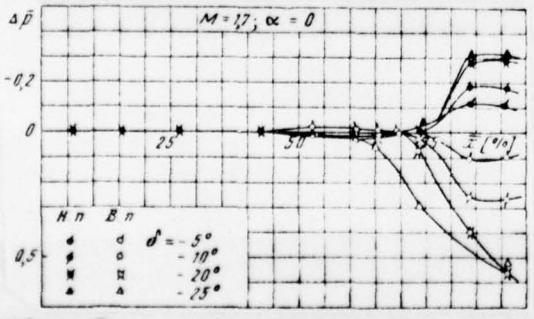

Fig. 8.

Key: (1). L.p., H.p.

Received 20 April 1969.

104

THE EFFECT OF REAL PROPERTIES OF AIR ON PARAMETERS OF FLOW NEAR AN ELLIPTIC CONE. AERODYNAMIC CHARACTERISTICS OF ELLIPTIC CONES AT LARGE ANGLES OF ATTACK

A. P. Bazzhin, O. N. Trusova, and
I. F. Chelysheva

The calculation results of a flow around a family of elliptic cones by a flow of ideal gas at large angles of attack were presented in works [1, 2]. Subsequently, several variants of flow were calculated taking into account the real properties of air, which are in a state of thermodynamic equilibrium. These calculation results permit one to evaluate the effect of real gas properties, which proves to be insignificant for the variants of flow, examined in works [1] and [2]. The first part of this paper is devoted to this problem.

Calculated aerodynamic characteristics of elliptic cones over the angle of attack range from 30° to 50° in the case of an ideal gas are presented in the second part of this paper. The comparison of these results with the calculated and experimental results of other authors [3, 4] has confirmed the validity of the results obtained by the calculation method with large angles of attack.

THE EFFECT OF REAL PROPERTIES OF AIR ON PARAMETERS OF FLOW NEAR AN ELLIPTIC CONE

A calculation was made of the flow around an elliptic cone having a cross-section axes ratio of $\delta = 2$, half-angle aperture of the cone in a horizontal plane $\theta_к = 15°$, with the angle of attack $\alpha = 30°$. The air was examined as a three-component gas consisting of 78.08% nitrogen, 20.95% oxygen, and 0.97% argon, and its thermodynamic functions were calculated according to the standardized program.

The incident flow velocities were equal to 2350, 3356, and 6713 m/s, which corresponded to the M_∞ numbers equaling 7, 10, and 20 (with the speed of sound $a_\infty = 335.6$ m/s). The main bulk of calculation data in works [1] and [2] was obtained at $M_\infty = 7$.

Figure 1 shows the position of shock waves near the cone in the perfect and imperfect gases at velocities $V_\infty = 2350$ and 6713 m/s. The difference in distance from the body to the shock wave in the symmetry plane of the flow, in the case where $M_\infty = 7$ ($V_\infty = 2350$ m/s), comprises about 10%. The absolute shock wave displacement arising when considering the real properties of air has a negligible change through out their duration. The same thing applies also to the case of the flow with $V_\infty = 6713$ m/s. Transition lines II near the lower surface change together with the change in the position of shock waves; however, the points of transition on the body surface are displaced very little. Change in the relative distance from the body to the shock wave $\varepsilon/\varepsilon_0$ (ε_0 - distance from the body to the wave in the symmetry plane) are plotted in Fig. 2 as a function of central angle ω (see Fig. 1). The range of angles ω corresponds to the lower surface of the cone. In the range $\omega < 80°$ all values of quantity $\varepsilon/\varepsilon_0$ fall on the line having a width of not more than

0.04. In other words, in the examined area, dependence $\varepsilon/\varepsilon_0 = f_1(\omega)$ can be represented by a curve pertaining to the perfect gas, with an accuracy to within 4%.

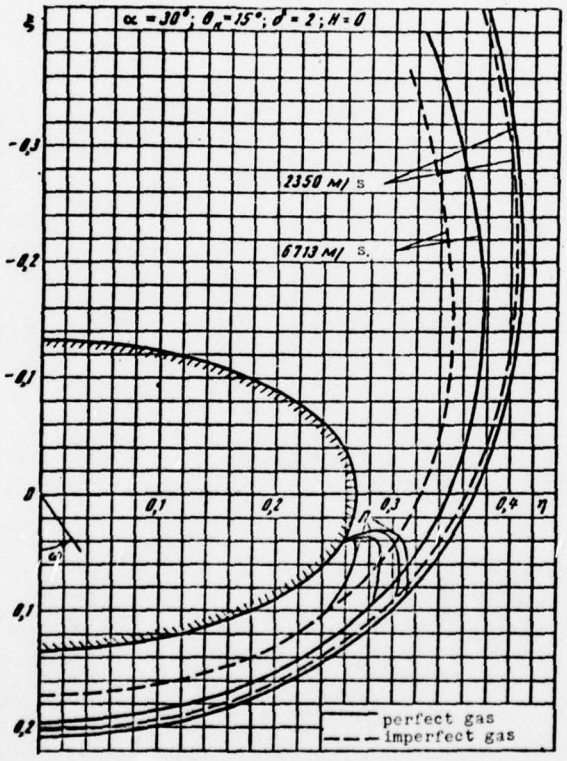

Fig. 1.

Functions $\frac{p}{p_0} = f_2(\omega)$ and $\frac{\rho}{\rho_0} = f_3(\omega)$ have a similar nature (Fig. 3). Values p_0 and ρ_0 (pressure and density) in the symmetry plane of the flow (on the wave and body) are referred to $\rho_\infty V^2_{max}$ and ρ_∞, respectively (see Table 1). First of all we should note the extremely slight effect of the real properties of air on the magnitude of relative pressure when V_∞ = 2350 m/s (M_∞ = 7). The

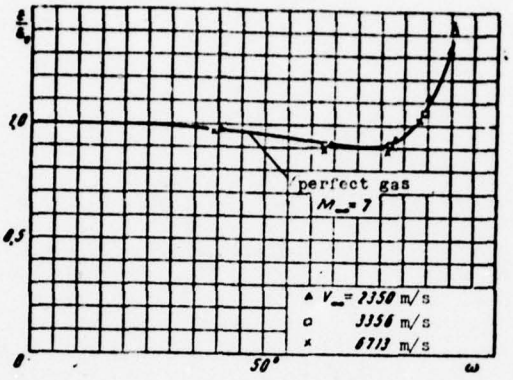

Fig. 2.

relative pressure on the body surface and shock wave, when $0 \leq \leq \omega \leq 100°$, is virtually independent of the real properties of air. Changes in the p_0 value of the body, to which the pressure on the body is referred, are also negligibly small. This means that the values of aerodynamic coefficients, calculated at $M_\infty = 7$ in the case of a perfect gas, will also be valid with high accuracy in the case of an imperfect gas as well.

The effect of the real properties of air on the relative density when V_∞ 2350 m/s ($M_\infty = 7$) is also slight; however, the change in values of these parameters in the symmetry plane, with the consideration of the real properties of air, comprises about 8% (see Table 1).

Change in the relative pressure and relative density on the body surface remains slight when considering the real properties of air, even at velocity $V_\infty = 6713$ m/s ($M_\infty = 20$). This variation does not exceed several percent. On the shock wave, especially on the upper section, the change in the relative values is more noticeable.

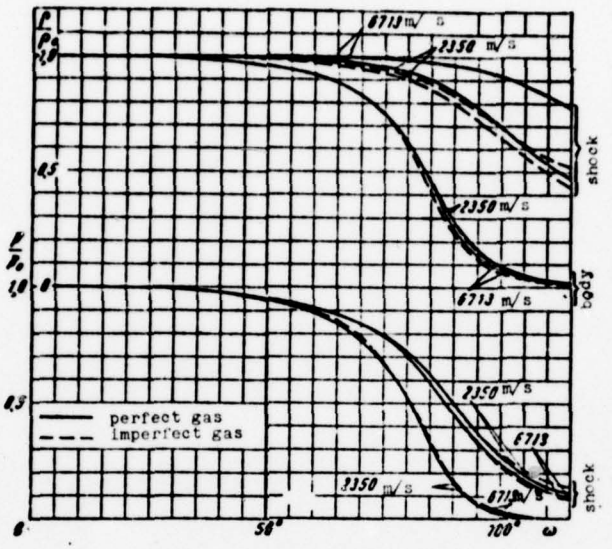

Fig. 3.

Table 1.

$V_\infty \left[\frac{M}{s}\right]$	p_{0T}	ρ_{0T}	p_{0B}	ρ_{0B}
2350	0,3591 0.3598	5,584 5,134	0,3362 0,3339	5,307 4,868
3356	0,3692 0,3698	6,672 5,633	0,3497 0,3458	6,392 5,369
6713	0,3759 0,3778	9,482 6,075	0,3627 0,3551	9,210 5,813

Note: The lower numbers pertain to perfect gas.

Table 2.

V_∞ (m/s)	2350	3356	6713
$\frac{\rho_0 \text{ perf. gas}}{\rho_0}$	0,918	0,840	0,630
$\frac{\varepsilon}{\varepsilon_0 \text{ perf. gas}}$	0,915	0,835	0,623

If we assume that the indicated nature of change in relative values is valid not only for the examined variants of flow, but also in the case of other variants close to those examined, then it is possible to propose the following method of approximate calculation of the effect of properties of an imperfect gas.

Parameters on the shock wave and body surface in the symmetry plane, when calculating the real properties of air, vary with an accuracy to within several percent (see Table 1). This variation is easily obtained when the slope of the shock wave is known. Then, using the distribution of relative parameters obtained for perfect gas, it is possible to obtain the real distribution of gas-dynamic parameters along the surface.

With regard to the determination of the shock wave inclination or the distance from the shock wave to the body in the flow of an imperfect gas, as a result of the calculations it was revealed that the ratio of distances to the shock wave in the plane symmetry in the case of an imperfect gas, to the corresponding distance in the case of a perfect gas, is equal, with high accuracy, to the inverse ratio of densities on the shock wave, as this can be seen from Table 2. Consequently, if the calculation data are available for a perfect gas, then it is possible to approximately determine value $\varepsilon_0 \approx \varepsilon_{0 \text{ perf. gas}}$ on the shock wave in the symmetry plane in an imperfect gas; then to find value $\frac{\rho_{0 \text{ perf. gas}}}{\rho_0}$, refine the inclination of the shock wave in an imperfect gas, and find a

more precise value for ρ_0 on the shock wave in an imperfect gas and the new value for c_0. Then, using the available dependence $\frac{\rho}{\rho_0} = f(M_\infty)$ for perfect gas, it is possible to determine the location of the shock wave near the lower surface of the cone in an imperfect gas.

AERODYNAMIC CHARACTERISTICS OF ELLIPTIC CONES AT LARGE ANGLES OF ATTACK

Aerodynamic characteristics of elliptic cones were calculated for a perfect gas with $M_\infty = 7$ over the angle of attack range of 30 to 50°. The error in determining the flow parameters on the cone surface, in particular the distribution of pressure according to the carried out estimations, comprises the value on the orier of 1%. The error in calculating the aerodynamic coefficients should be on the magnitude of the same order. The forces acting on that part of the upper body surface where the flow was not calculated were not considered, when calculating the forces and moment. However, it is entirely obvious that if the streamlining occurs without a break in the flow over the upper surface of the body the forces are very slight.

Aerodynamic coefficients were calculated using the formulas:

normal force coefficient

$$c_N = \frac{N}{q_\infty S} = \frac{2V_{\infty 1}^2}{\operatorname{tg}\theta_k V_\infty^2} \int_0^{\eta^*} p\, d\eta; \qquad (1)$$

axial force coefficient

$$c_T = \frac{T}{q_\infty S} = \frac{2V_{\infty 1}^2}{\operatorname{tg}\theta_k V_\infty^2} \int_0^{\eta^*} p\eta^2 \frac{d\eta}{f(\eta)}; \qquad (2)$$

coefficient of longitudinal momentum

$$c_m = \frac{M}{q_\infty S \cdot l} = -\frac{2}{3}(1 + a^2) c_N, \qquad (3)$$

where $q_\infty = \frac{1}{2} \rho_\infty V_\infty^2$; S - cone area in the plan.

Limits of integration correspond to the bypass of the cross-section contour from the symmetry plane to the last point at which the solution is known, i.e., the change in the variable is first from zero to b and then from b to η^*. In range (2) $\xi(b) = 0$. In the vicinity of this point the integration was carried out by means of variable ξ, for which the following substitution was made $a^2 \frac{d\gamma_1}{\xi(\gamma_1)} = -b^2 \frac{d\xi}{\eta(\xi)}$ [$\gamma_1 = \eta(\xi)$ or $\xi = \xi(\gamma_1)$ – equations of transverse elliptic section; ξ and η conical variables].

The coefficients of the lift and resistance forces were determined using the c_N and c_T:

$$c_y = c_N \cos\alpha - c_T \sin\alpha, \quad c_x = c_N \sin\alpha + c_T \cos\alpha.$$

Figure 4 shows the aerodynamic coefficients c_x, c_y, c_m and aerodynamic quality K as a function of the angle of attack of cones with opening semiangles $\theta_н = 10°$, 15° and 20° and the ratio of axes of the cross section $\delta = 1$; 2 and 3. Values c_x, c_y, c_m and $K(\delta = 1)$ are given over the entire range of the angles of attack from zero to 50°. The solid lines indicate the calculation data from work [3] at small angles of attack. Solid lines in the angle of attack range from 30° to 50° indicate the results obtained in this work. The experimental data from work [4] are plotted by different points pertaining to air. The axes indicate the experimental data obtained by authors earlier at $M_\infty = 6$. Such a

comparison of the various data had one purpose in mind - to arrive at a concept concerning the nature of change of the aerodynamic characteristics of elliptic cones over the entire range of the angles of attack and to determine the validity of the calculation data obtained by us over the angle of attack of attack range from 30° to 50°. As can be seen, as a whole, there is good qualitative and quantitative agreement between all the results presented. The dashed lines in the intermediate angle of attack range can be considered as a possible interpolation of the aerodynamic coefficient values in this area. The remaining curves in Fig. 4 represent the aerodynamic characteristics of elliptic cones in the range of large angles of attack at different values of δ.

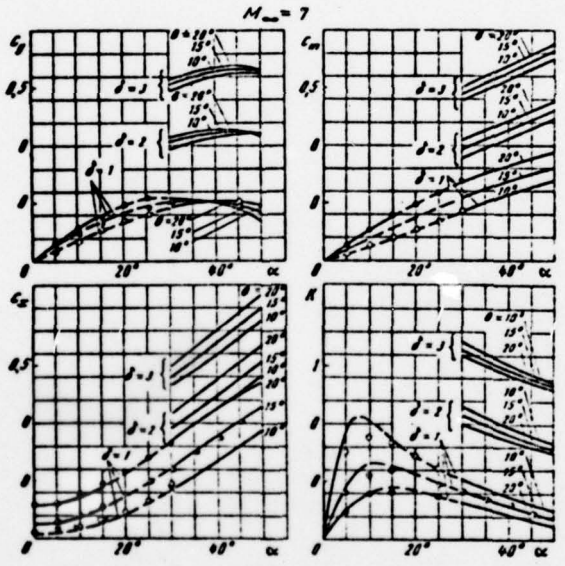

Fig. 4.

The effect of δ with different constant parameters is shown in Fig. 5. We will note that the aerodynamic quality of cones

always increases when passing to greater ellipticity of the cone cross section. The coefficient of longitudinal momentum over the range of large angles of attack changes almost linearly with the angle of attack. According to formula (3), the position of the pressure center of an elliptic cone is determined by value (1 + + a^2), i.e., only by the opening semiangle of the cone in the symmetry plane of the flow.

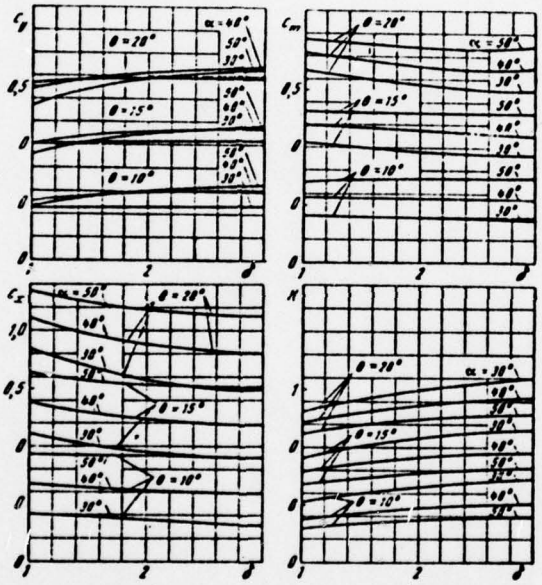

Fig. 5.

BIBLIOGRAPHY

1. Баэжин А. П., Трусова О. Н., Челышева И. Ф. Расчет течений совершенного газа около эллиптических конусов при больших углах атаки. Труды ЦАГИ, вып. 1114, 1969.

2. Баэжин А. П., Трусова О. Н., Челышева И. Ф. Расчет течений совершенного газа около эллиптических конусов при больших углах атаки. Изв. АН СССР, МЖГ, 1968, № 4.

3. Бабенко К. И. и др. Пространственное обтекание гладких тел идеальным газом. М., «Наука», 1964.

4. Maddalon D. V. Aerodynamic characteristics of the sharp right circular cone at M=20,3 and angles of attack to 110° im helium NASA TN D-3201.

Received
10 November 1969

Page 53.

STUDY OF THE FLOW OF GAS IN A CYLINDRICAL CHANNEL DURING THE SUDDEN EXPANSION OF SONIC FLOW.

G. F. Glotov, E. K. Moroz.

Is carried out the study of flow during the sudden expansion of sonic airflow in axisymmetric cylindrical channel. Changed relative length and the area of channel in ranges = 1.5-4.5; F = 1.5-3.0. Are investigated the special feature/peculiarities of flow in the area of the connection of flow to the wall of channel and is establish/installed the existence of the single condition of connection.

The problem of the connection of turbulent supersonic flow - one of the basic with solution of which we encounter in a series of the gas-dynamic equipment/devices: air intakes, ejector nozzles, the camera/chamber of Eiffel, etc. One Of the problems in this case consists of the determination of pressure of stagnation zone. The experimental investigation of pressure in stagnation zone at the large lengths of axisymmetric cylindrical channel (in connection with ejectors with the zero coefficient of ejection) was for the first

time carried out by G. L. Grodzovskiy et al. into 1953 [1]. Subsequently similar data were obtained in a series of the works (for example, see [2] and [3]). The effect of the length of channel on pressure in stagnation zone was for the first time establish/installed in the experiments of G. L. Grodzovskiy and V. T. Zhdanov whose results were presented in work [3].

The beginning of theoretical studies of the problem of the connection of the turbulent flow was placed in work [4] and it is continued in [5], [6].

In this article are investigated the basic physical phenomena, which appear during the connection of turbulent supersonic flow to wall, and the condition of the connection of separating flow line.

For this purpose, was carried out the experimental study of the flow of turbulent supersonic flow in cylindrical channel with sudden expansion. The schematic of the model of channel with designations and the geometric parameters of the investigated versions are given to Fig. 1.

In experiments discretely changed the relative length of channel. The range of the lengths of channel, in reference to the height/altitude of step, the equal to the half-difference of

diameters camera/chambers and nozzle throats h = (D - d)/2, comprised $\bar{l}$ = 1.5-4.5, but the area of channel, in reference to the area of critical nozzle, changed in the range F = 1.5-3.

Page 54.

Boundary layer thickness in nozzle throat, referred to the height/altitude of step, it was equal to δ = tc 0.10-0.25. Reynolds number, calculated according to critical throat diameter, comprised Re = (2-7.2) x 10^6. Testings were conducted at the pressure air flow in precombustion chamber, equal to 3-8 atm (abs.), and to temperature T_0 = ~ 290°K.

During testings, besides the total pressure in precombustion chamber, were measured the pressure in stagnation zone p_1 and the distribution of pressure according to the wall of channel p with the aid of static-pressure probes 0.8 mm in diameter, arrange/located with space 1.5 mm. The accuracy/precision of the determination of relative pressure was ± 1o/o.

The picture of flow at output/yield from channel was photographed by Toepler's instrument. With the aid of oil film (mixture of oil and carbon black) was visualized the picture of flow on the wall of channel and in the meridian plane of stagnation zone.

Fig. 2, gives the typical dependence of relative pressure in stagnation zone p_1 ($p_1 = p_1/p_0$, where p_0 - averaged according to expenditure/consumption total pressure flow in the section/shear of sonic nozzle) on relative nozzle pressure p_0 ($p_0 = p_0/p_2$, where p_2 - ambient pressure). Are isolated three characteristic conditions/modes: 1 - conditions/mode of the connected flow, which is characterized by constant quantity of relative pressure in stagnation zone, 2 - transient conditions/mode, 3 - separating conditions/mode. Further analysis of the obtained experimental data is conducted for conditions/mode 1.

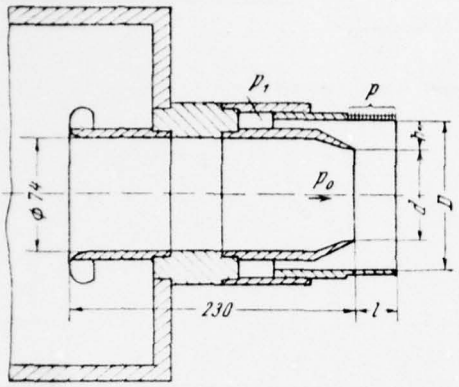

(1) Вариант	d [мм]	D [мм]	h [мм]	F
I	63	77	7,0	1,5
II	70	99,4	14,7	2.0
III	63	99,4	18,2	2,5
IV	57,4	99,4	21	3,0

Fig. 1. Key: 1) Variant

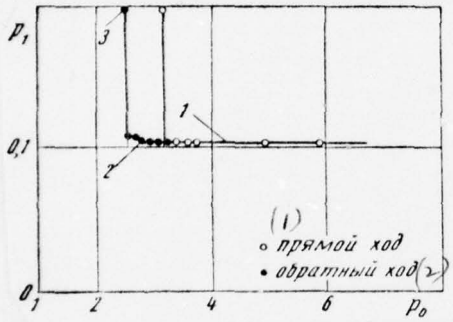

Fig. 2.

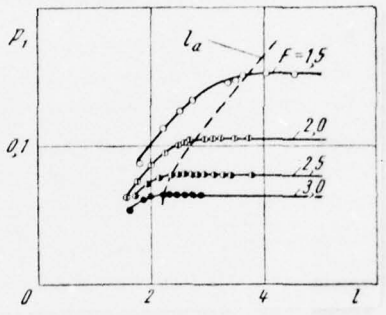

Fig. 3.

Key: (1) foreward stroke. (2) back strcke.

Page 55.

The generalized dependences $p_1 = f(l)$ at the different values of the relative areas of channels F are given to Fig. 3. As can be seen frcm this curve/graph, the value of relative pressure in stagnation

zone p_1 remains constant/invariable for this value of F during the decrease of the relative length of channel l to certain value which let us designate l_a. We will call the area of the lengths of channel $l \geq l_a$ the region of self-similar flow along the length. During further decrease of the relative length of channel to $l < l_a$ value p_1 begins to decrease (region of non-self-simulating flow). Fig. 3, gives the boundary of the region of self-similar flow.

Comparison showed that our data on pressure in stagnation zone for the region of self-similar flow will agree well with other authors's data, obtained during the discharge of sonic flow into cylindrical channel.

Was also carried out the estimation of the known criteria of the connection of turbulent flow.

One of the most successful criteria is the examined in works [5], [6] condition for the angle of the connection of flow $\psi = \psi(M_0)$, where M_0 - mach number on the boundary of inviscid jet. At angle is understood the angle of incidence with the wall of the channel of the boundary of the inviscid jet, constructed by method of characteristics according to the measured in experiment sense of pressures p_0/p_1 (see schematic in Fig. 4). As is shown comparison, the values $\psi = \psi(M_0)$, calculated according to the results of this work,

in the region of self-similar flow virtually coincide with the values ψ given for the appropriate flow in work [5] (Fig. 4). However, in the region of non-self-simulating flow, angles ψ grow/rise and for each value of F is obtained its dependence $\psi' = \psi(M_0)$. Thus, in the examined case the criterion of the connection of turbulent flow in the form of single dependence $\psi = \psi(M_0)$ is valid only in the range of self-simulating flow and is not spread to the non-self-simulating region (this observation is related also to the correlation parameter χ introduced in work [5]). Therefore is necessary the search of other more common/general/total criteria of connection.

For purpose of the explanation of the physical picture of flow in the region of the connection of flow to the wall of cylindrical channel, was carried out the visualization of the picture of flow on the wall of channel and in the zone of mixing with the simultaneous measurement of static pressure distribution on wall and the photographing of flow at output/yield with the aid of Toepler's instrument.

The examination of the obtained photographs of oil film and their comparison with the diagram/curves of the distribution of pressure on wall made it possible to present the real picture of flow in the region of connection (Fig. 5a). In photographs are visible three zones. In zone I (we examine from nozzle edge) oil remained

intact. The comparison of this zone with the air-load distribution on wall which in this zone it is constant, shows that the flow here either entirely is absent or so weak that it does not act on oil film. In zone II, are observed the longitudinal overflows of oil and an insignificant change in the pressure, which indicates the presence of weak current in the limited region towards nozzle. In zone III oil is washed off completely on an entire wall, except the narrow transverse band with a width approximately 1 mm (line of the connection P). Flow in this zone is accompanied by sharp pressure increase on wall to certain maximum value p_{max}/p_1.

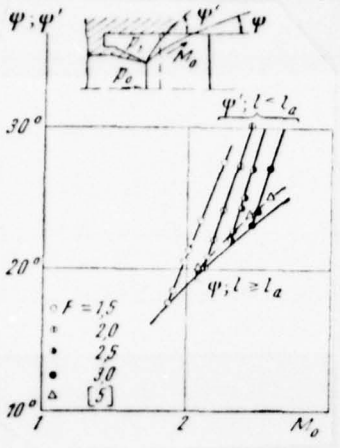

Fig. 4.

Page 56.

This testifies to the presence of powerful flow with interface (line II), to the left of which flow is directed toward nozzle, and to the right - toward the section/shear of channel. It is logical to assume that the interface represents by itself the pcint of rendezvous of separating flow line (line I) with the wall of channel.

Fig. 6, gives the photograph of oil film to longitudinal plate and the corresponding schematic of flow. On figure are noted: 1 - separating flow line, 2 - boundary of zero longitudinal velocities, 3 - boundary of flow, 4 - boundary of inviscid jet, 5 - point of the connection, by 6 - duct/contour of the plate. In photograph clearly

is outlined the rotation of flow line in viscous layer, arrange/located lower than separating line, into stagnation zone and the formation/education of the reverse/inverse flow near the wall. The mass of the reflux gas returns to the main flow, forming the local eddy/vortex between wall and boundary of flow. The longitudinal size/dimension of this eddy/vortex virtually coincides with the extent of zone II (Fig. 6).

The part of the viscous layer, arrange/located higher than separating flow line after meeting with wall turns to output/yield from channel. During this rotation in flow, appears the system of characteristics. Intersecting, they create the oblique shock wave, seen at output/yield from the channel (see Fig. 5).

Is of interest the comparison of calculated and determined in experiments in the positions of separating flow line. In work [5] as separating line is accepted the boundary of inviscid jet. For the region of self-similar flow, it is possible to note the satisfactory conformity of the calculated and experimental results (see Fig. 6).

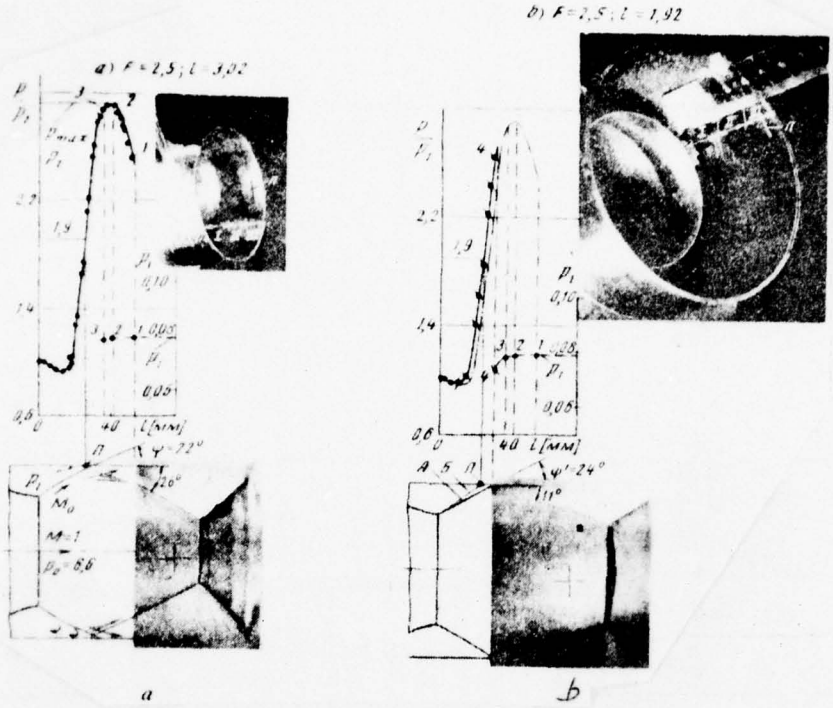

Fig. 5.

Page 57.

Only of wall itself begins their disagreement, as a result of which the calculated boundary of inviscid jet meets the wall of channel at the point, which lies approximately tc 7-10c/o further from nozzle, than the real line of connection.

In the case of small length of channel (non-self-simulating zone of flow) the calculated boundary of the inviscid jet A (Fig. 5b) can

even exceed the limits of channel, although in actuality the flow is that connected. For such channels, as shows the visualization of flow in meridian plane, separating flow line B ccnsiderably differs from line of demarcation of inviscid jet and more steeply it turns to wall (Fig. 5b).

The specific in experiments positions cf the line of connection on the wall of channel made it possible by the measured diagram/curves of pressure to determine the pressure at attachment point, equal to the total pressure on separating flow line (Fig. 5). The comparison of this value of pressure with pressure in stagnation zone shows that their sense for all investigated values of relative areas and lengths of channels approximately is constant and is equal tc $p_н/p_1 \approx$ to 1.9 $\pm$ 0.05 (Fig. 7a).

The results of processing given works [6] - [9] show (Fig. 7b) that during the flow around flat/plane step is observed certain tendency toward an increase in value $p_н/p_1$ ($p_н/p_1$ = 1.7-2 with M_0 = 2.1-4.4). In the first approximation, this sense can be accepted equal to 1.9. A change of the relative maximum pressure on wall depending on number M_0 both for the flow in channel and during the flow around flat/plane step does not in practice affect value $p_н/p_1$ (Fig. 7).

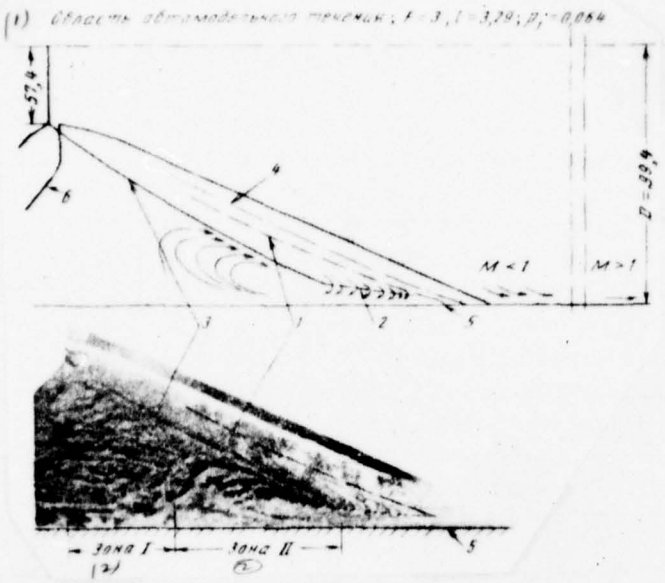

Fig. 6.

Key: (1). Region of self-similar flow. (2). Zone.

Page 58.

The relationship/ratio $p_{II}/p_I \approx 1,9$ obtained for flow in axisymmetric cylindrical channel and during the flow around flat/plane step, can be used in the analysis of the connection of supersonic turbulent flow on wall in the range of numbers $M_0 \approx 2$-3.5.

The conducted investigations made it possible to also explain the mechanism of the effect of the length of channel on relative

pressure in the stagnation zone (see Fig. 5). In accordance with a change of the basic flow parameters in the region of connection, it is possible to isolate three reference lengths of the channel: $l > l_a$, $l_{kp} < l < l_a$ and $l < l_{kp}$ (this to some degree of analogous the introduction critical points for the case of the flow around flat/plane step [5]). The specific above relative length of channel l_a (see Fig. 3) it corresponds to maximum pressure increase on wall in the region of self-similar flow. During the decrease of the length of channel to l_a (position of the section/shear of channel 1 and 2, Fig. 5a) relative pressure in stagnation zone remains constant. In this case, remain without change the position of the line of connection, maximum pressure on wall and the angle of the slope of the resulting shock wave, observed in output/yield from the channel (see Fig. 5a), it which indicates the invariability of flow disturbance in local region after the line of the connection (the value of slope angle very weakly depending on value of F). The observing when $l > l_a$ decreases of pressure on the wall (see Fig. 5a) testify to the presence on this section of the accelerated supersonic flow.

With the decrease of the length of channel into the region of non-self-simulating flow $l < l_a$ to certain value which let us call/name critical l_{kp}, the form of the distribution curve of pressure and the position of the line of connection remain without change. In

this case, maximum pressure on the wall of channel and the angle of the slope of the resulting jump at output/yield decrease. The decrease of flow disturbance after the line of connection leads to the decrease of relative pressure in stagnation zone. In this case, maximum by pressure on wall is greater than pressure environment ($p_{max}/p_2 > 1$)..

During the decrease of the length of channel $l \geq l_{sp}$ (position 4, Fig. 5b) occurs the shift/shear of the air-load distribution and line of connection to nozzle, as a result of which the length of stagnation zone it decreases.

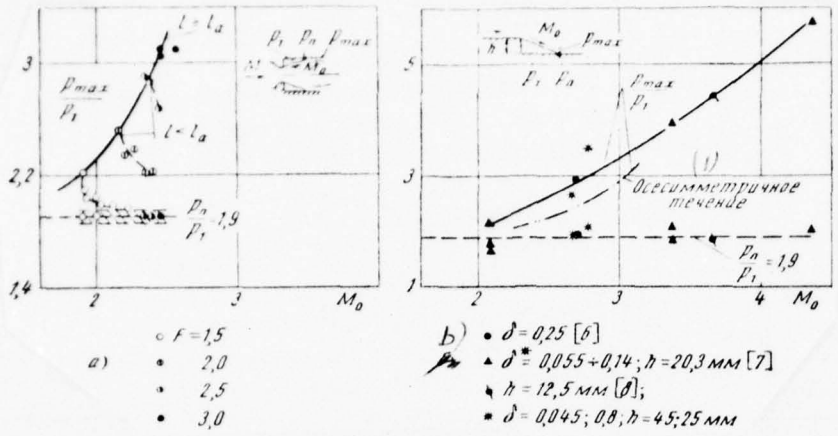

Fig. 7.

Key: (1). Axisymmetric flow.

Page 59.

On section from attachment point tc the point, which corresponds to critical length ($l_{\text{п}} < l \leq l_{\text{кр}}$), flow in wall viscous layer subsonic [9]. Therefore when $l = l_{\text{кр}}$ the picture of flow either must be bricken as a result of the report/communication of stagnatien zone with environment or, at the sufficiently large pressure flow, the line of connection must move from the section/shear of channel, that also is observed in experiment. In this case, maximum pressure on wall continues to decrease, remaining more than pressure environment, and with respect it decreases pressure in stagnatien zone.

Thus, for the investigated conditions/modes of the connected flow pressure environment does not affect value p_1. Pressure in stagnation zone depends on maximum pressure on the wall of channel after the line of connection, that it is necessary to consider during the development of the calculation method.

REFERENCES

1. G. L. Grodzovskiy. To the theory of the gas ejector of high compression ratio with the cylindrical mixing chamber. IZV. AS USSR, MZhG, 1968, No 3.

2. L. P. Volkova, M. Ya. Yudelovich. Losses by shock in stepped ducts in the supersonic ratios of pressure. Izv. of the AS USSR, OTN, 1958, No 4.

3. L. I. Sorkin, V. S. Baykov. Study of flow in the initial section of the sonic ejector with the short mixing chamber. in coll. "rctodynamic machines and jet apparatuses". Iss. 3. M., "machine-building", 1958.

4. H H Korst. A theory for base pressures in transsonic and

supersonic flow. J Appl. Mech., Vol. 28, No 4, 1956.

5. M Sirieix, J Mirande, J Delery et. Basic experiments on turbulent convergence of a supersonic jet. AGARD, Conference Proceedings, n°. 4, 1966.

6. M Sirieix. Bottom pressure and turbulent mixing processes in a plane supersonic flow. Space Research, 1960, n°, 78.

7. R Hastings. Turbulent flow past two-dimensional bases in supersonic streams. ARC RM, 1965, No 3401.

8. F G Bavagnoli. Reaction point of a supersonic turbulent boundary layer downstream of a step. Aerotecnica, VIII, Vol. 47, n 4, 1967.

9. R. K. Tagirov. Experimental study of detached flows after flat/plane step with M_1=1.97. IZV. AS USSR, MZhG, 1969.

Received 4 March 1969.

Page 69.

Flow of gas in a flat duct, caused longitudinal gradient of the temperature at Knudsen's arbitrary number.

M. N. Kogan, N. K. Makashev.

For the kinetic model equation of Boltzmann in linear setting, is solved the problem of temperature creep in flat duct for the arbitrary values of Knudsen's number.

Obtained approximate analytical solution. On the basis of this solution, are made evaluations of possible faults of measurement of pressure, for example, the heated gas with the aid of "cold" instrument.

As she was noted already by Maxwell [1], if along wall is a gradient of temperature, then the coming into contact with it gas moves relative to wall. This motion calls thermal slip or creep. The gas flow in this case depends on the number of Knudsen Kn, equal to

the ratio of mean free path λ to the width of channel or the diameter of tube d. If by the unevenly heated tube are connected two containers with different temperature, then the equilibrium (zero expenditure/consumption through the tube) stops at certain the pressure differential which also depends on Knudsen's number.

These phenomena can exert the essential influence, for example, during low-pressure measurement the heated gas by "cold" instrument; in the porous media they can cause flow or the pressure differentials.

Various cases of the flow of a gas, expressed by the temperature gradient at the walls, are examined in [2] - [7].

Different cases of the flow of gas, caused in flat/plane duct by the gradient of the temperature at the arbitrary values of Knudsen's number. Approximate solution of the model equation of Boltzman is obtained in analytical form.

1. Let us examine gas between two infinite parallel motionless plates. The temperature of walls T_w is changed on z. Let us consider that this change is small, so that

$$T_w = T_0[1 + \tau(z)]; \quad \tau(z) \ll 1; \quad T_0 = T_w(0), \tag{1.1}$$

and problem is linearized. Let us assume also that the walls reflect molecules according to Maxwellian law; the temperature of the molecules reflected is equal to the temperature of wall T_w.

Page 70.

For the solution of problem, we will use the model equation of Boltzmann (for example, see [8]):

$$\xi_x \frac{\partial f}{\partial x} + \xi_z \frac{\partial f}{\partial z} = An(f_0 - f); \quad f_0 = n\left(\frac{m}{2\pi k T}\right)^{\frac{3}{2}} \exp\left\{-\frac{m(\vec{\xi} - \vec{u})}{2kT}\right\}, \quad (1.2)$$

where f - distribution function; $n, m, \vec{\xi} = (\xi_x \xi_y \xi_z)$ - respectively numerical density, mass and the velocity of molecules; $\vec{u}$ and T - macroscopic velocity and temperature; k - Ecltzmann constant.

Condition on the wall:

$$f\left(\pm\frac{d}{2}, z, \xi_x \gtrless 0\right) = n_w\left(\frac{m}{2\pi k T_w}\right)^{\frac{3}{2}} \exp\left\{-\frac{m\vec{\xi}^2}{2kT_w}\right\}, \quad (1.3)$$

where n_w it is determined from the condition of nonpassage.

Solution let us search for in the form

$$\left.\begin{aligned} f &= f_{00}[1 + \varphi(x, \vec{\xi})]; \\ f_{00} &= n_0\left(\frac{m}{2\pi k T_0}\right)^{\frac{3}{2}} \exp\left\{-\frac{m\vec{\xi}^2}{2kT_0}\right\}, \end{aligned}\right| \quad (1.4)$$

where $n_0 = n(0, 0)$; φ - small addition squares of which we disregard.

Linearizing equation (1.2) and after making it dimensionless, we will obtain

$$\frac{v_x}{\alpha}\frac{\partial\varphi}{\partial x_1}+\frac{v_z}{\alpha}\frac{\partial\varphi}{\partial z_1}=\nu+2v_z u_1+\left(v^2-\frac{3}{2}\right)\tau-\varphi. \qquad (1.5)$$

Are here introduced designations:

$$x_1=\frac{x}{d};\quad z_1=\frac{z}{d};\quad h_0=\frac{m}{2kT_0};\quad \xi_{x,z}\sqrt{h_0}=v_{x,z};\quad \xi^2 h_0=v^2;$$

$$n=n_0(1+\nu);\quad T=T_0(1+\tau);\quad \alpha=\Lambda n_0 d\sqrt{h_0}\approx \mathrm{Kn}^{-1};$$

$$u_1=u_z\sqrt{h_0}=\frac{1}{\pi^{\frac{3}{2}}}\int e^{-v^2}\varphi v_z d\vec{v};\quad \nu=\frac{1}{\pi^{\frac{3}{2}}}\int e^{-v^2}\varphi\, d\vec{v};$$

$$\tau=\frac{2}{3}\frac{1}{\pi^{\frac{3}{2}}}\int e^{-v^2}v^2\varphi d\vec{v}-\nu.$$

Boundary condition (1.3) takes the form:

$$\varphi_w\left(\pm\frac{d}{2},\ z,\ v_x\gtrless 0\right)=\nu_w-\left(\frac{3}{2}-v^2\right)\tau_w. \qquad (1.6)$$

2. Let temperature of wall change linearly:

$$\tau_w=az. \qquad (2.1)$$

Page 71.

Then the solution of equation (1.6) it is possible to search for in the form

$$\varphi=az\,v^2+v_z\psi(x,\vec{v}), \qquad (2.2)$$

in this case

$$\left.\begin{aligned} v &= \frac{3}{2}\,az; \quad \tau = az; \\ p &= kn_0T_a\left(1+\frac{5}{2}\,az\right), \end{aligned}\right| \qquad (2.3)$$

and for ψ are obtained following equation and the boundary condition:

$$\left.\begin{aligned} &\frac{v_x}{\alpha}\,\frac{\partial\psi}{\partial x_1}+\frac{ad}{\alpha}\,v^2 = -\psi+2u_1; \\ &\psi\left(\pm\frac{d}{2},\ v_x \gtrless 0\right)=0. \end{aligned}\right| \qquad (2.4)$$

Set/assuming temporarily u_1 by known function and integrating (2.4), we obtain integral equation for ψ

$$\psi(x_1,\ v_x \gtrless 0) = \alpha \int_{\pm\frac{1}{2}}^{x_1} \left[2u_1(s) - \frac{ad\,v^2}{\alpha}\right] e^{-\alpha\frac{x_1-s}{v_x}}\,\frac{ds}{v_x}. \qquad (2.5)$$

Multiplying this equation on $v_z\exp(-v^2)$ and integrating by velocities $\vec{v}$, we will obtain integral equation for $u_1(x_1)$:

$$\left.\begin{aligned} u_1 &= \frac{\alpha}{\sqrt{\pi}} \int_{-\frac{1}{2}}^{+\frac{1}{2}} \left[u_1(s)-\frac{ad}{\alpha}\right] J_{-1}(\alpha|x_1-s|)\,ds - \frac{ad}{2\sqrt{\pi}} \int_{-\frac{1}{2}}^{\frac{1}{2}} J_1(\alpha|x_1-s|)\,ds; \\ J_n(x) &= \int_0^\infty v^n \exp\left\{-\left(v^2+\frac{x}{v}\right)\right\} dv, \\ J_n(x) &= -\frac{dJ_{n+1}(x)}{dx}. \end{aligned}\right| \qquad (2.6)$$

Function $J_{-1}(\alpha|x_1-s|)$ has logarithmic special feature/peculiarity with $s = x_1$/ Therefore approximately it is possible to assume $u_1(s) = u_1(x_1)$ and to remove $u_1(x_1)$ from under integral. In this approximation of solution of equation (2.6) is obtained in an explicit form:

$$u_1 = \frac{ad}{\alpha} \frac{(\Delta_0 - \sqrt{\pi}) + \frac{1}{2}\left(\Delta_2 - \frac{1}{2}\sqrt{\pi}\right)}{\Delta_0}, \qquad \Delta_n = J_n\left[\gamma\left(\frac{1}{2} + x_1\right)\right] + J_n\left[\gamma\left(\frac{1}{2} - x_1\right)\right]. \tag{2.7}$$

Analogous approach/approximation was used in [8] for the examination of Poiseuille flow in the same setting. Problem in [8] differs from that examine/ccnsidered cnly by the fact that in it τ_w it is set/assumed by constant and is assign/prescribed pressure gradient. In this case

$$u_{1p} = \frac{bd}{2\alpha} \frac{\Delta_0 - \sqrt{\pi}}{\Delta_0}; \qquad b = \frac{1}{p_0}\frac{dp}{dz}. \tag{2.8}$$

Page 72.

The comparison of the cbtained solutien with precise sclution of Cherchin'yani [9] showed its satisfactory accuracy/precision (Fig. 1). It is possible to expect the same accuracy/precision of approach/approximation, alsc, in the problem in question. Accordingly (2.1) and (2.3) solution (2.7) correspcnds to the gradient of temperature $a = (1/T_0)(dT/dz)$ and to pressure gradient $b = 5/2\ a$. Since in linear setting it is valid superposition, let us exclude with the

aid of (2.8) from solution (2.7) the part, caused by pressure gradient. Then with dr/dz = 0 we obtain

$$u_{1T} = \frac{ad}{2\eta}\left(\frac{\Delta_2}{\Delta_0} - \frac{1}{2}\right). \qquad (2.9)$$

3. Knowing distribution of velocities, it is easy to determine volumetric flow rate:

$$\left.\begin{aligned} Q_{T.p} &= d\int_{-\frac{1}{2}}^{\frac{1}{2}} u_{1T.p}(x_1)\,dx_1; \\ Q_p &= \frac{bd^2}{2}\,q_p(\alpha); \\ Q_T &= \frac{ad^2}{2}\,q_T(\alpha). \end{aligned}\right\} \qquad (3.1)$$

Results of its numerical calculation are represented in Fig. 1. These results were obtained with the aid of the tables of integrals J_n, given in [10]. At Poiseuille flow, as is known, has the minimum of expenditure/consumption (Knudsen's paradox). As can be seen from Fig. 1 of the flow, caused by temperature gradient, expenditure/consumption is changed monotonically, after grow/rising with the decrease of pressure. Zero expenditure/consumption is established with a specific ratio between the gradient of temperature and pressure gradient. Set/assuming $Q_p = Q_T$, accordingly (3.1) we have

$$\frac{\Delta p}{p} = K(\alpha)\frac{\Delta T}{T}; \quad K(\alpha) = \frac{q_T(\alpha)}{q_p(\alpha)}. \qquad (3.2)$$

To dependence K(α) it is represented in Fig. 2. During the

measurement of temperature on the value of the order of magnitude of temperature itself the pressure differential can comprise to 59o/o of its average value. This maximum value K(α) is reached in free molecular conditions/mode when Kn → ∞ and it was obtained from the sclution of the equation of Boltzmann for this case. Thus, for instance, if instrument and the measured volume are connected by the tube with a diameter of 1 mm and is measured pressure order 0.1 mm Hg with $\Delta T/T = 0.3$, then the error in readings will comprise approximately 8o/o.

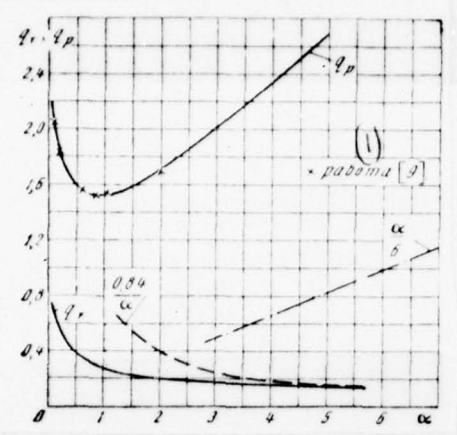

Fig. 1.

Key: (1). work.

Page 73.

For a comparison Fig. 1 and 2 by dotted line show results for Navier-Stokes equation with slip conditions on boundary.

With large α the accuracy/precision of obtained approximate solution falls and it gives inaccurate asymptotic behavior when α → ∞, i.e., when Kn → 0. With Knudsen's small numbers, it is possible to utilize Navier-Stokes equations with the conditions of temperature slip on wall.

According to the solution, obtained in [8], this slip

[1] is equal

$$u_{1w} = \frac{p}{n}\sqrt{\frac{2}{mkT}}\,0{,}42a = 0{,}42\frac{ad}{\alpha}, \qquad (3.3)$$

since for here the model equation in question the coefficient of ductility/toughness/viscosity $\mu = kT/A$.

FOOTNOTE [1]. in work [7] is obtained the value of coefficient, equal to 0.383. ENDFOOTNOTE.

Consequently, the rates of flow, caused by creep, are of the order μa, and the inertia and viscous terms of Navier-Stokes equations - an order $\mu^2\alpha^2$, i.e., the same order as some of the additive terms, entering the equations of Barnet. However, it is possible to show that for here a small linear gradient of temperatures ($\tau_w = az$ and $a \ll 1$) in question the solutions of the equations of Barnett and Navier-Stokes coincide (with $p = \text{const}$, i.e., with $b = 0$):

$$u_1(x, z) = \text{const} \cdot 0{,}42\frac{ad}{\alpha}; \qquad (3.4)$$

$$Q_T = 0{,}42\frac{ad^2}{\alpha} + 0\left(\frac{1}{\alpha^3}\right). \qquad (3.5)$$

Work [7] shows, that for the axisymmetric case solution in the approach/approximations of Navier-Stokes and Barnett they do not coincide and in the appropriate expansion/decomposition of type (3.5) enters term $0(\alpha^{-2})$. Thus, in here the flat/plane case in question

Navier-Stokes's asymptotic behavior (3.5) must be satisfactory already with not very large α (see Fig. 1).

Let us note that Navier-Stokes's asymptotic behavior for Poiseuille flow is much worse (see Fig. 1). It is real/actual, accepting for the rate of slip (see [8])

$$u_{1w} = -1{,}012\,\frac{1}{\alpha}\,\frac{du_1}{dx_1}\Big|_w,$$

we have

$$\frac{2Q_p}{bd^2} = \frac{\alpha}{6} + 1{,}012 + O\left(\frac{1}{\alpha}\right). \tag{3.6}$$

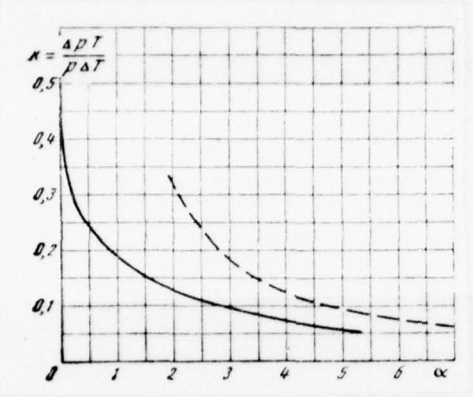

Fig. 2.

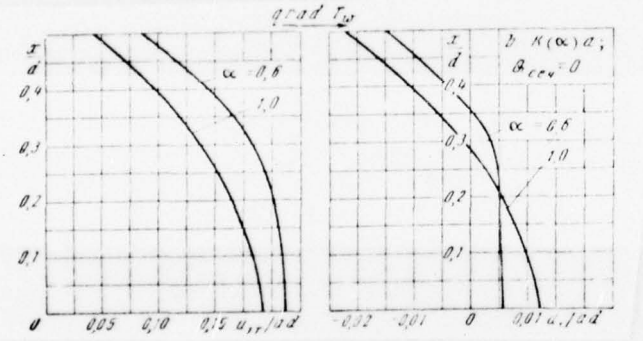

Fig. 3.

Page 74.

With zero flow rate the gas of wall flows to one side, and in center another (Fig. 3).

It is interesting to note that under the condition of the zero flow rate through the section and at the sufficiently high values of number Kn the velocity profile is such, that about wall gas flows in the direction, opposite to the gradient of the temperature of the walls (see Fig. 3). At the same time from solution this same of problem with the small numbers Kn, obtained from Navier-Stokes equation, it follows that the gas velocity of wall has another direction, i.e., during a change in the number of Knudsen, under the condition of the zero flow rate through the section, gas velocity of wall reverses the sign.

REFERENCES.

1. Clerk Maxwell, Jr. On stresses in raregied gases arising flow inequalities of temperature. Royal Society of London, Philosophical Transactions, vol. 170, 1879, pp. 231-256.

2. M Knudsen. Eine Revision der Gleichgewichtsbedingung der Gase. Thermische Molekularstroming. Annalen der Physik, vol. 31, 1910, pp. 205-229.

3. M Knudsen. Thermischer Molekulardrusk in Rohren. Annalen der Physik, vol. 83, 1927, pp. 797-821.

4. J L Potter, et. Rarefied gas dynamics (Edited by J H de Leeuw), vol. 2, Academic Press, New York, 1966, pp. 175-194.

5. F C Tompkins, D E Wheeler. The correction for thermo-molecular flow. Transactions of the Faraday Society, vol. 29, November 1933, pp. 1248-1254.

6. M Kinslow, G P Arney. Corrections for thermo-molecular pressures in tubes and at orifices. VI Symp. on Rerefied Gas Dynamics. 1968.

7. Y Sone, K Yamamoto. Flow of rarefied gas through a circular pipe. Phys Fluids, No. 9, 1968.

8. M. N. Kogan. Dynamics of the rarefied gas. M., "science". 1967.

9. C Cerciqnani. Rarefied gas dynamics. Third Symp., Acad Press, 1963.

10. M T Chahine, R Narasimha. The integral $\int_0^\infty v^n \exp$ x [-(v-u)^2-x/v)dv. J of Math. and Phys. vol. 43, No. 2, 1964.

The manuscript entered 12/VI 1969.

OPTIMIZATION OF THE FLYING RANGE OF VEHICLE IN THE ATMOSPHERE TAKING INTO ACCOUNT LIMITATION TO COMPLETE OVERLOAD.

V. V. Dikusar, A. A. Shilov.

Is examined the problem of the determination of maneuverability capabilities of the space vehicle, which possesses lift, during reduction in the atmosphere taking into account limitation to phase coordinates. Problem is solved with the use of classical principle of L. S. Pontriagin's maximum. Are given numerical examples.

Great practical interest represents the application/use of methods of the optimization of trajectories in the presence of limitations during the function of phase coordinates. To theoretical questions of these problems are dedicated works [1] - [5]. In works [1], [2], [4], [5] the principle of maximum is demonstrated for the case when in the optimum trajectory in question everywhere is retained the local effectiveness of control. This case is called regular [3].

The basic difficulty of applying the principle of maximum is

connected with the need for the solution of the boundary-value problem which is complicated upon consideration of limitations. In the present work are examined the systematic special feature/peculiarities of the solution of placed problem which make it possible to overcome the difficulty indicated.

1. Setting and the analysis of problem.

Let us examine the problem of the selection of the angle of attack control of the vehicle, which is braked in the atmosphere, in flight to minimum and maximum distance taking into account limitation to the value of the complete overload whose solutions make it possible to determine the maneuverability capabilities of vehicle (Fig. 1).

Expression for a complete overload takes the following form:

$$n_2 = V\sqrt{c_x^2 + c_y^2}\, q \frac{S}{G} \leq N, \qquad (1.1)$$

where $q = \rho V^2/2$ - velocity head [kgf/m^2]; ρ - atmospheric density [kgf$\cdot$s^2/m^4]; V - velocity [m/s]; c_x - drag coefficient; c_y - lift coefficient S - characteristic area of vehicle [m^2]; G - weight of vehicle [kg].

From (1.1) it is evident that n_z clearly depends on steering function c_{y_1} and the limitation in question belongs to class $\Phi_1(x, u) \leq 0$ (see [4]).

Let us assume that the aerodynamic forces, which act on vehicle, are characterized by the polar of the form

$$c_x = c_{x0} + \chi c_{y_1}^2$$

where c_{x0} - a drag coefficient of zero angle of attack; χ - parameter of polar.

The use of the dependence indicated makes it possible to sufficient simply explain the physical sense of optimum solution.

To value c_y (i.e. to the value of angle of attack) are superimposed the limitations:

$$c_{y\min} \leq c_y \leq c_{y\max}.$$

For the development/detection of a broader class of solutions and role of the superimposed for value c_y limitations the parameters of polar and value $c_{y\min,\max}$ let us select so that $c_y(K_{\max}) = \sqrt{\frac{c_{x0}}{\chi}}$ would be inside of cut $[c_{y\min} c_{y\max}]$. Here K - lift-drag ratio;

$K = \frac{c_y}{c_x}$. The equations of the plane motion of vehicle in the atmosphere take the form

$$\left.\begin{aligned} V &= -c_x q \frac{S}{m} - g \sin\theta; \\ \theta &= c_y q \frac{S}{mV} + \left(\frac{V}{R+h} - \frac{g}{V}\right)\cos\theta; \\ H &= V \sin\theta; \\ L &= \frac{RV\cos\theta}{R+h}, \end{aligned}\right| \qquad (1.2)$$

where $g = g_0 R^2/(R + h)^2$ - acceleration of gravity [m/s^2]; R - radius of planet [m]; h - height/altitude of vehicle [m]; g_0 - surface gravity of planet [m/s^2]; θ - local flight path angle [rad]; L - flying range [km]; t - time [s]; m - mass of vehicle [$kg \cdot s^2/m$].

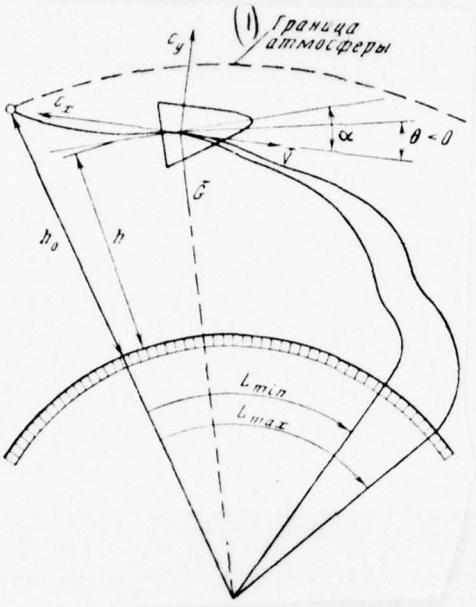

Fig. 1. Key: (1). Boundary of the atmosphere.

Page 77.

Point designates differentiation with respect to t.

Let us count the atmosphere of isothermal $\rho = \rho_0 e^{-\beta h}$, where ρ_0 - atmospheric density on the surface of planet [kgf•s^2/m^4); β - index of the exponential in formula for density [1/m].

Let the descent vehicle come from initial state into final optimally in the sense of maximum or minimum of distance. Let us

assume that in optimum trajectory when $n_2 = N$ (N - limitation to the total overload) is satisfied the condition of regularity $\frac{\partial n_2}{\partial c_y} \neq 0$ (see [3]). In this case for the solution of stated problem, it is possible to use the mathematical vehicle, developed in works [1] - [5].

Designating those conjugate/combined to θ, h, V and L alternating/variable of variational problem for system 81.2) through p_1, p_2, p_3, p_4, let us write the expression of the Hamiltonian of the expanded system

$$H = p_1\left[\frac{c_y \rho V S}{2m} + \left(\frac{V}{R+h} - \frac{g}{V}\right)\cos\theta\right] + p_2 V \sin\theta - p_3\left(\frac{c_x \rho V^2 S}{2m} + g\sin\theta\right) + \frac{p_4 R V \cos\theta}{R+h}. \quad (1.3)$$

Since system (1.2) is autonomous during the period of the descent no limitations are imposed, the H = C in all interval of action.

In accordance with [1] and [4] the system the adjoint from 81.2) equations must take the form

$$p_i = -\frac{\partial H}{\partial x_i} + \lambda(t)\frac{\partial n_2}{\partial x_i}.$$

Then

$$\left.\begin{aligned}
\dot{p}_1 &= p_1\left(\frac{V}{R+h}-\frac{g}{V}\right)\sin\theta - p_2 V\cos\theta + \\
&\quad + p_3 g\cos\theta + p_4\frac{RV\sin\theta}{R+h};\\
\dot{p}_2 &= p_1\left|\frac{\beta c_y \rho V S}{2m}+\frac{V\cos\theta}{(R+h)^2}-\frac{2g\cos\theta}{V^2}\right| - \\
&\quad - p_3\left(\frac{\beta c_x \rho V^2 S}{2m}+\frac{2g\sin\theta}{R+h}\right)+p_4\frac{RV\cos\theta}{(R+h)^2} - \\
&\quad - \lambda(t)\frac{\beta\rho V^2 S}{2m g_0}\sqrt{c_x^2+c_y^2};\\
\dot{p}_3 &= -p_1\left(\frac{c_y\rho S}{2m}+\frac{\cos\theta}{R+h}-\frac{g\cos\theta}{V^2}\right)-p_2\sin\theta + \\
&\quad + p_3\frac{c_x\rho V S}{m}-p_4\frac{R\cos\theta}{R+h}+2\lambda(t)\frac{\rho V S}{2m g_0}\sqrt{c_x^2+c_y^2};\\
\dot{p}_4 &= 0,
\end{aligned}\right\} \qquad (1.4)$$

where λ(t) - Lagrange's factor, moreover $\lambda(t)(n_2 - N) = 0,$

$$\lambda(t) = \frac{g_0}{V}\frac{\left(\frac{p_1}{2}-\varkappa p_3 c_y V\right)}{c_y(1+2\varkappa c_x)}\sqrt{c_x^2+c_y^2}.$$

For system (1.2) are assign/prescribed the initial conditions $v(t_0) = V^0$, $\theta(t_0) = \theta^0$, $L(t_0) = 0$, $t_0 = 0$, $h(t_0) = h^0$. It is required at the specific fixed/recorded height/altitude h^1, is sufficient small, so that the distance flight it would be possible to consider finished, the provision for maximum or minimum of flying range. Inasmuch as θ and V at the end of the flight are not fix/recorded, then at the end point

$$p_1^{(1)} = p_4^{(1)} = 0. \qquad (1.5)$$

Conditions (1.5) are boundary for system 81.4). From condition $p_4 = 0$ and $p_4(1) = -1$, it follows that $p_4 \equiv -1$ in an entire trajectory. Thus, stated problem is reduced to two-point boundary-value problem

for the system of ordinary differential equations.

If we assign $p_1^{(0)}$ and $p_3^{(0)}$, then of the condition H = 0 it is possible to determine $p_2^{(0)}$, and the number of those controlled at the end of the trajectory of functions $p_1^{(1)}$ and $p_3^{(1)}$ it coincides with the number of parameters, assigned at initial point. With this program of control it is determined from the conditions

$$H_{c_y} \to \min_{c_y} \text{ при } L^{(1)} \to \max \text{ или } H_{c_y} \to \max_{c_y} \text{ при } L^{(1)} \to \min. \quad (1.6)$$

The constancy of overload is provided by a change in absolute value $c_y(t)$ in accordance with the condition of communication/connection $n_\Sigma = N$, and the sign of function $c_y(t)$ is determined by sign p_1 accordingly (1.6). If in the process of motion along limitation $n_\Sigma = N$ in some point $c_y = 0$ and $q \neq 0$, then in this trajectory at the subsequent torque/moment is possible the disturbance of the assigned/prescribed limitation. This is connected with the fact that the local effect of control on the amount of g-force is already exhausted $\left(\frac{\partial n_\Sigma}{\partial c_y} = 0\right)$. During the solution of boundary-value problem by iterative methods the fact indicated is important first of all because in some test trajectories can occur the disturbance of limitation. Simultaneously with this appear computational difficulties in the construction of the iterative calculation methods, since of (1.4) it follows that $\lambda(t) \to \infty$ when $|c_y| \to 0$.

So that the iterative process would not have the special feature/peculiarity indicated, but the trajectory of the expanded system of equations with the disturbance of limitation they continuously transfer/converted in trajectory without the disturbance of limitation, let us artificially restrict the decrease of value $|c_y|$ from below by value ε. Then upon reaching of value $|c_y| \leq \varepsilon$ the value $\lambda(t)$ is limitedly on top by value $O\left(\frac{1}{\varepsilon}\right)$. Inasmuch as by hypothesis on unknown optimum trajectory $\frac{\partial n_\Sigma}{\partial c_y} \neq 0$, then with sufficiently small ε and $|c_y^{opt}(t)|_{min} > \varepsilon$ it is possible to satisfy boundary conditions (1.5). This makes it possible to carry out the regular iterative process of the sclution of boundary-value problem, without exceeding calculation grid ETsVM [digital computer].

Page 79.

Let us examine the systematic special feature/peculiarities of the solution of problem taking intc account limitation $n_\Sigma \leq N$. During motion in open domain $n_\Sigma < N$ accordingly [1] - [4] $\lambda(t) = 0$; in this case value n_Σ corresponds to value c_y, determined according to the principle of maximum (maximum):

$$c_y = c_{y\min}, c_{y\max} \overset{(1)}{\text{ИЛИ}} c_y^*, \overset{(2)}{\text{ГДЕ}} c_y^* = \frac{p_1}{2c p_3 V}.$$

Key: (1). or. (2). where.

At certain torque/moment function n_Σ will become more than N, and by this "intersection" will be determined output/yield to limitation. During motion along limitation $c_y = c_y\ (n_\Sigma = N)$. In order to determine the torque/moment of descent from limitation, simultaneously with $c_y(N)$ we compute $c_y(p_i)$ without the account of limitation in terms of the instantaneous values of pulses p_i [see (1.4)] from condition (1.6). Then the torque/moment of descent is determined by their intersection : $c_y(p_i) = c_y(N)$.

let us examine the trajectory phase, which adjoins the end point, determined by boundary conditions (1.5). On this trajectory phase when $L^{(1)}$ - max. carried out condition $n_\Sigma < N$, then it is possible to determine the character of optimum control in the vicinity of the end of the trajectory. For this, let us examine $c_y^* = \frac{p_1}{2\varkappa p_3 V}$. With $h \to h^{(1)}$ functions $p_1^{(1)}$ and $p_3^{(1)}$ decrease to zero. According to l'Hopital's rule $\lim\limits_{t \to (t_1)} c_y^* = \frac{p_1^{(1)}}{2\varkappa p_3^{(1)} V^{(1)}}$. From condition $H \equiv 0$ and system (1.4) we obtain the following relationship/ratios:

$$p_1^{(1)} = \frac{R V^{(1)}}{(R + h^{(1)}) \sin \theta^{(1)}}; \tag{1.7}$$

$$\dot{p}_3^{(1)} = -p_1^{(1)} \frac{g \cos \theta^{(1)}}{V^{(1)2}} - p_3^{(1)} \frac{g \sin \theta^{(1)}}{V^{(1)}}. \tag{1.8}$$

With sufficiently small $h^{(1)}$ usually $\sin \theta^{(1)} < 0$, since the vehicle

loses altitude; then $p_1(t) > 0$. Hence it follows that $p_1 < 0$ with $t = t - \Delta$ ($\Delta > 0$).

Value $p_3(t_1)$, as $p_3(t_1)$, is equal to zero. Then from conditions $p_1(t_1-\Delta) < 0$ and $0 > \theta - \pi/2$ follow $p_3(t_1-\Delta) < 0$, i.e., $c_y^*(t-t_1) \to +\infty$ and $c_{y\,opt}(t_1) = c_{y\,max}$, but when $-\pi < \theta < \pi/2$ follows $c_y^*(t - t_1) \to -\infty$ and $c_{y\,opt}(t_1) = c_{y\,min}$ in accordance with (1.6). In the case of flight to maximum of distance $L(t_1) > 0$ and $\cos\theta > 0$; therefore during the solution of problem on $I^{(1)} \to \max$. the last/latter case drops off. However, in problem on $I^{(1)} \to \min$ both the case ($-\pi/2 < \theta < 0$ and $-\pi < \theta < -\pi/2$) are possible.

In the initial stage of motion in the presence of communication/connection c_x and c_y it is a priori unclear, that it is better in the sense of the maximization of gliding distance $c_y = c_y^{max}$ or $c_y = c_y(K_{max})$. With increase c_y increases c_x, increases and distance with some initial $V^{(0)}$, $\theta^{(0)}$ can decrease as a result of premature speed loss. The selection of control is clearer at the end of the trajectory when the effect of the instantaneous value of velocity is small (momentum/impulse/pulse p_3 - this the influence coefficient of a variation in the velocity on distance) and distance can be increased because of an increase in the positive lift, i.e., $c_y = c_{y\,max}$. For the last/latter phase of trajectory $I^1 \to \min$ with $\sin\theta < 0$ and $\cos\theta > 0$; according to to H - max. follows $c_{y\,opt} = c_{y\,min}$ and

$c_{y\,opt} = c_{y\,max}$ with sin θ < 0 and cos θ < 0.

Page 80.

In the case of the trajectory of minimum range, control $c_y(t) < 0$ with - $\pi/2 < \theta < 0$ contributes to the decrease of flying range. But if $-\pi < \theta < \pi/2$, then flight is accomplished in the direction, opposite initial, and for the minimization of distance $L(t_1)$ it is necessary to increase the duration of the last/latter trajectory phase. This occurs when $c_y = c_{y\,min}$ which corresponds to the fact that the lift is directed against weight.

The made analysis makes it possible tc solve two-point boundary-value problem taking into account limitation $n_\Sigma < N$, if in optimum trajectory $\frac{\partial n_\Sigma}{\partial c_y} \neq 0$. Case $\frac{\partial n_\Sigma}{\partial c_y} = 0$ is examined in separate work.

2. Procedure and the results of the numerical determination of optimum trajectories.

For practical determination of optimum trajectories the presence of limitation to the value of complete overload, it is necessary to numerically solve system of equations (1.2), (1.4) under boundary conditions (1.5). The boundary-value problem of the selection of

initial momentum/impulse/pulses $p_i^{(0)}$ for satisfaction of conditions (1.5) was solved by Newton's method. It was reveal/detected that the sensitivity of solution tc changes $p_i^{(0)}$ is very great, and surfaces $p_{1,3}^{(1)}(p_{1,3}^{(0)})$ have very complex structure. For the search of the first approximation, was suggested the procedure, based on with the aid of the principle of maximum the functional $L^{(1)}$ in QUESTION can be expressed as function of parameters $p_1^{(0)}$, $p_3^{(0)}$.

In optimum trajectory are fulfilled ccnditions $p_1^{(1)} = p_3^{(1)} =$ by 0 and $L^{(1)} =$ max. $L^{(1)}$ (min $L^{(1)}$) with appropriate $p_{1,3}^{(0)}$, but at other values $p_{1,3}^{(0)}$ and $L^{(1)} < L_{\max}^{(1)}$ $(L^{(1)} > L_{\min}^{(1)})$.

In stated problem only d^2L/dt^2 contains clearly control c_y, surface $L^{(1)}(p_{1,3}^{(0)})$ must be smooth or, at least, have simpler structure, than $p_{1,3}^{(1)}(p_{1,3}^{(0)})$. During search by the method cf the gradient of sequence $\{p_{1,3}^{(0)}\}$, which ensures $L^{(1)} \to$ max. ($L^{(1)} \to$ min) will automatically decrease values $p_{1,3}^{(1)}$, and when as a result of the flatness of surface $L^{(1)}(p_{1,3}^{(0)})$ the convergence of the methcd of gradient in the region of extremum it will deteriorate, it is possible to refine values $p_{1,3}^{(0)}$ by Newton's method. This approach can be used also with the larger number of unknown parameters.

During limitation $n_\Sigma \leq N$ this method effectively was utilized and provided the rapid convergence of iterative processes. With the use

of a gradient method of the search of initial conditions $p^{(0)}_{1,3}$ and of quadratic extrapolation for known sclutions $p^{(0)}_{1,3}(N_i)$ with i = 1, 2, 3 where N_i - assigned sizes of the g-force, was fulfilled the search of solution $p^{(0)}_{1,3}(N_4)$, which was being more precisely formulated then by Newton's method.

in practice during the numerical realization of problem by ETsVM instead of alternating/variable systems (1.2) were utilized $\bar{V}=\frac{V}{\sqrt{g_0 R}}$, $\bar{h}=\frac{h}{R}$, dimensionless variables $\bar{L}=\frac{L}{R}$

Page 81.

For an example let us give the optimum lines of descent in the vehicle in the atmosphere with the use of a lift-drag ratio. During calculations was accepted:

$$\frac{m}{S}=70\ кгс\cdot сек^2/м^2;\quad c_x=0{,}55+5c_y^2;$$
$$c_{y\max}=-c_{y\min}=0{,}4$$
(т. е. $K_{\max}\approx 0{,}302$ при $c_y\approx 0{,}331$);
$$V^{(0)}=7900\ м/сек;$$
$$h^{(1)}=0{,}00314\ R \text{ для } L^{(1)}\to\max;$$
$$h^{(1)}=10^{-9}R \text{ для } L^{(1)}\to\min;$$
$$\rho_0=0{,}125\ кгс\cdot сек^2/м^4;$$
$$\beta=0{,}000137\ 1/м;$$
$$h^{(0)}=0{,}0156\ R;$$
$$R=6371\cdot 10^3\ м;$$
$$g_0=9{,}80665\ м/сек^2.$$

Key: (1). kg•s²/m². (2). with. (2a). m/s. (3). for.

For the regularization of problem during the search of the regular optimum programs, close to irregular, it was accepted $\varepsilon = 0{,}01$.

During the calculation of zero functions p_1, $n_\Sigma = N$, $h = h^{(1)}$, $c_{y\,max,\,min} = c_y^*$ they were determined with an accuracy to 10^{-7}-10^{-8} and values $p_{1,3}^{(1)}$ were more precisely formulated during the solution of boundary-value problem to 10^{-4}-10^{-5}.

Fig. 2 and 3, give the results of the calculation of the optimum trajectories $I^{(1)} \to$ max. without limitation for overload. Let us focus attention on fracture curved max $n_\Sigma(\theta)$, that occurs at the value of the angle $\theta^{(0)}$, at which the height/altitudes of first and second maximum n_Σ coincide. From Fig. 3 it is evident that dependence $c_y(t)$ oscillates about value $c_y = 0{,}3$, which corresponds $c_y = c_y(K_{max})$. Let us note that fluctuations $c_y(t)$ contribute to damping fluctuations h(t) and $n_\Sigma(t)$.

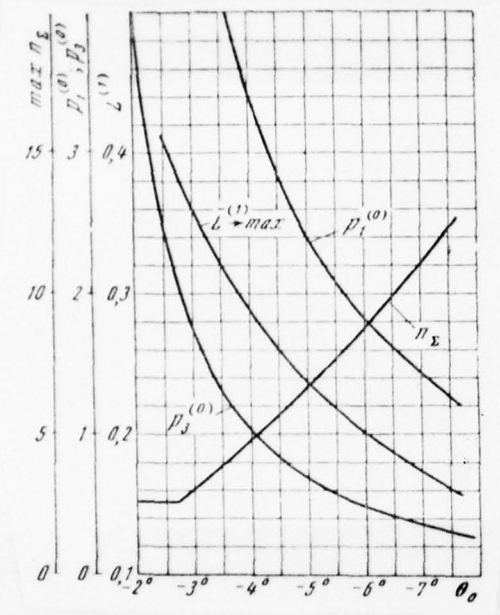

Fig. 2.

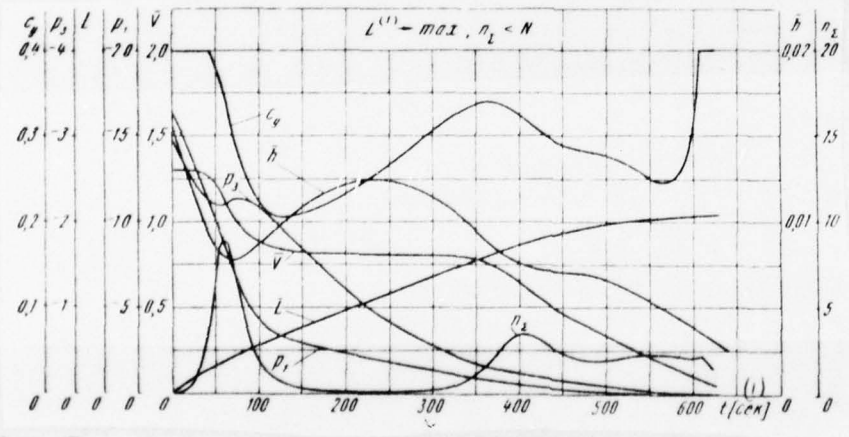

Fig. 3.

Key: (1). s.

Page 82.

The obtained solutions were used for the sclution of problem taking into account limitation $n \leq N$. Fig. 4, gives the results of calculations. It turned out that during decrease of N program $c_v(t)$ changed so that to some degree it compensated for the losses of distance from the action of limitaticn. When the possibilities of compensation were exhausted, beginning the noticeable decrease of distance.

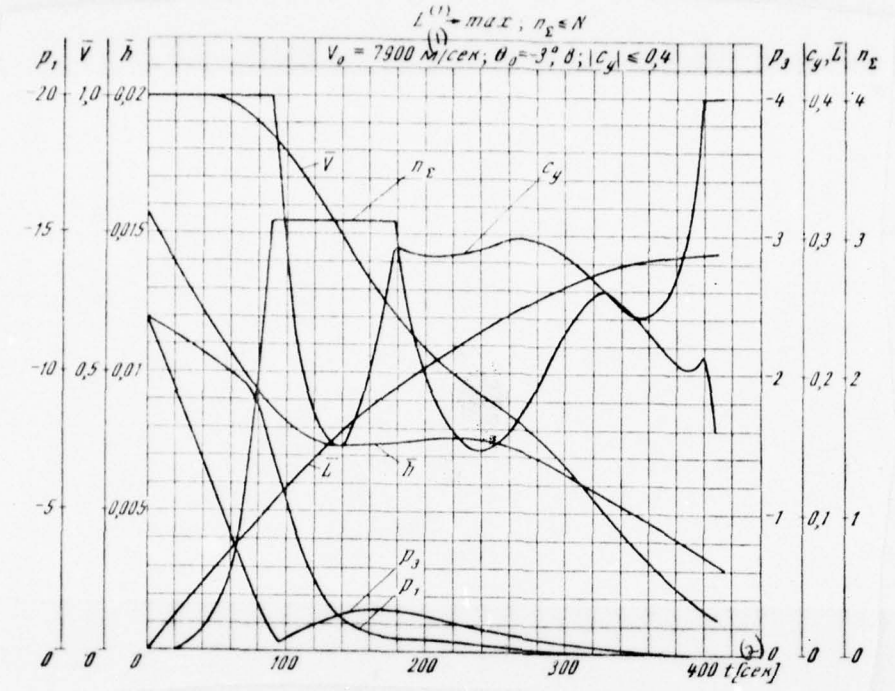

Fig. 4.

Key: (1). m/s. (2). s.

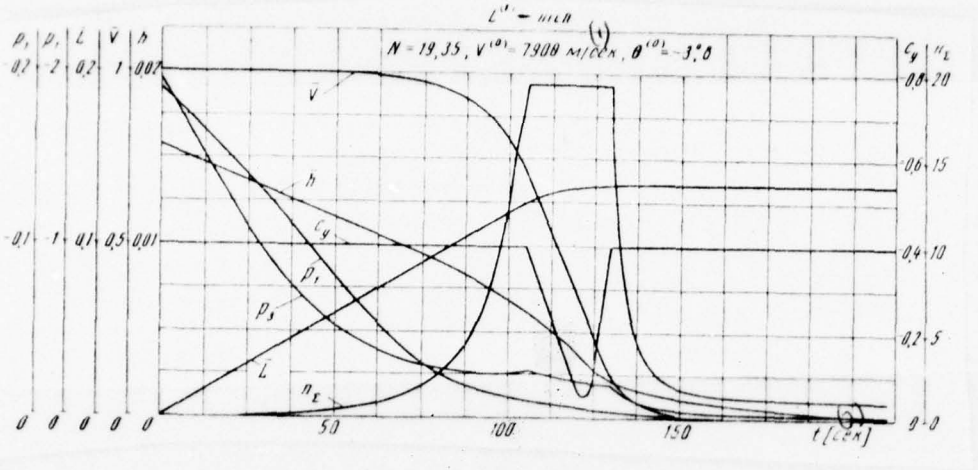

Fig. 5.

Key: (1). m/s. (2). s.

Page 83.

For the same parameters of vehicle, were determined solutions $L^{(1)} \to \min$ at different rates of entry $V^{(0)}$ and θ. Findings were used during the determination of solutions taking into account limitation to overload. Fig. 5, gives the optimum trajectory $L^{(1)} \to \min$, for which N = 19.35 with $V^{(0)}$ = 7900 m/s and $\theta^{(0)} = -3°.8$. It is evident that the possibilities of decreasing the overload by local variation in the control are almost exhausted; there is a maximum size of the g-force N_x, at which optimum trajectory still remains regular for a problem

on $L^{(1)}$ - min. With $N < N$, optimum trajectory will be irregular and this fact must be considered during the numerical solution of stated problem.

REFERENCES.

1. L. S. Pontriagin, V. G. Boltyanskiy, R. V. Gamkrelidze, Ye. F. Mishchenko. Mathematical theory of optimum processes. Fizmatgiz, 1961.

2. A. Ya. Dubovitskiy, A. A. Milyutin. Problems to extremum in the presence of limitations. The "journal of computational mathematics and the mathematician. of physics", 1965, No. 3.

3. A. Ya. Dubovitskiy, A. A. Milyutin. Necessary conditions of weak extremum in the problems of optimum control with the mixed limitations of the type of inequality. The "journal of computational mathematics and the mathematician. of physics", 1968, No. 4.

4. V. P. Anorov. Principle of maximum with presence of final communication/connections and the account of limitations to coordinates. "automation and telemechanics", 1967, No. 3 and 4.

5. E. R. Smol'yakov. Optimization of the corridor of entry in

the atmosphere. "space investigations", Vol. VI iss. 1, 1968.

The manuscript entered 28/IV 1969.

Page 84.

THERMOPLASTIC STRESSES AND DEFORMATIONS OF FUEL TANK IN THE PROCESS OF ITS EMPTYING.

V. M. Marchenko.

Is examined the quasi-stationary one-dimensional task of thermoplasticity: the determination of the stressed and of the states of strain of circular cylindrical shell duralumin fuel tank with horizontal axis, that appear during its uneven heating in the process of continuous emptying. Is considered the Bauschinger effect and the variability of plastic deformation (on space coordinate) during discharging. For the linear law of hardening obtained exact solution.

1. Formulation of the problem. Basic assumptions

The position of the current point on the circumference of the cross section of median surface of shell is assigned by angle φ, the position of the fuel level in tank - by angle ψ (Fig. 1).

The determination of deformations and stresses is conducted separately on the regions

$$0 \leqslant \varphi < \pi - \psi; \qquad (1.1)$$
$$\pi - \psi \leqslant \varphi \leqslant \pi. \qquad (1.2)$$

In each region to the assigned/prescribed and unknown values appropriates itself index i (i_i = 1, 2), that coincides with the number of this region, to relative and similar[1] values - a line above lettering.

FOOTNOTE [1]. Similar are, for example, boundary values ψ for elastic solution $(\psi = \psi_m;\ m = 1, 2, \ldots, 5)$ and boundary values ψ for elasto-plastic solution $(\psi = \psi_m;\ m = 1, 2, \ldots, 5)$ ENDFOOTNOTE.

Temperature T_i is assumed to be constant in the i region, moreover $T_2 > T_1$. Let us designate the moduli of elasticity through $E_i;\ E_2 < E_1 = e\, E_2$. Pure thermal deformation $\alpha_i \theta_i;\ \alpha_1 \theta_1 = 0;\ \alpha_2 \theta_2 = \alpha_2 (T_2 - T_1)$, where α_2 - coefficient of linear expansion.

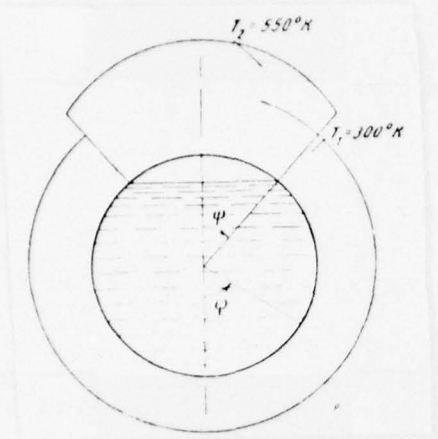

Fig. 1.

Page 85.

As a result of an abrupt change in the temperature on boundary of the region (1.1) and (1.2) (when $\phi = \pi - \psi$) all deformations: elastic $\varepsilon_{ei} = \frac{\sigma_i}{E_i}$, irreversible plastic ε_{pi}, ε_{pi}, pure/clean thermal $\alpha_i \theta_i$, and also thermal stresses σ_i and σ_i -- change abruptly.

The complete relative deformation of shell $\varepsilon(\psi, \varphi)$, continuous at all values ϕ, we set/assume by that obeying the law of the flat/plane sections:

$$\varepsilon(\psi, \varphi) = F(\psi) + \Phi(\psi)\cos\varphi \qquad (1.3)$$

[values $F(\psi)$ and $\Phi(\psi)$ are subject to determination].

It is accepted, that

$$\left.\begin{aligned} \bar{\varepsilon}(\psi, \varphi) &= \frac{\varepsilon(\psi, \varphi)}{D}; \quad D = |\varepsilon_{e2}(0, \pi)|; \\ \bar{\varepsilon}_{pi} &= \frac{\varepsilon_{pi}}{D}; \quad \bar{\sigma}_i = \frac{\sigma_i}{E_2 D} \end{aligned}\right\} \tag{1.4}$$

and that in each region

$$\epsilon(\psi, \varphi) = \varepsilon_{ei} + \varepsilon_{pi} + \alpha_i \theta_i. \tag{1.5}$$

Thermal stresses $\bar{\sigma}$ are subordinated to the conditions of self-balance to which it is convenient to give the form

$$\frac{1}{\pi}\int_0^{\pi} \bar{\sigma}(\psi, \varphi)\, d\varphi = 0; \quad \frac{2}{\pi}\int_0^{\pi} \bar{\sigma}(\psi, \varphi)\cos\varphi d\varphi = 0. \tag{1.6}$$

Integration in (1.6) is realize/accomplished separately on regions (1.1) and (1.2).

Equation (1.6), and also, therefore, the subsequent solution they dc not depend on radius and thickness cf shell (usual or given, if shell it is supported). Thermal stresses taking into account the power stresses, which depend on thickness, in this work on are examined.

The surfaces of the yield (or the plastic deformation [2]) for regions (1.1) and (1.2) they are accepted in the form

$$f(\sigma_i, \varepsilon_{pi}, T_i) \equiv \sigma_i \operatorname{sign} \sigma_i - \sigma_{si}(T_i) - E_i' \varepsilon_{pi} \operatorname{sign} \sigma_i = 0, \qquad (1.7)$$

where E_i' — the plastic module/moduli [slope tangents of straight lines, that connect points $(0, \sigma_{si})$ and $(\varepsilon_{pi}, \sigma_i)$];

σ_{si} — yield points for elongation ($-\sigma_{si}$ — for compression).

We will be restricted to the case when E_i' depend only on temperature, i.e., communication/connection (1.7) is linear.

With load accordingly (1.4) and (1.7).

$$\left.\begin{aligned} \bar{\varepsilon}_{pi} &= \frac{E_2}{E_i'}(\bar{\sigma}_i - \bar{\sigma}_{si} \operatorname{sign} \sigma_i); \\ \bar{\sigma}_{si} &= \frac{\sigma_{si}}{E_2 D}. \end{aligned}\right| \qquad (1.8)$$

Page 86.

The conditions under which occurs the resistive load $(d\varepsilon_{pi}/0)$ and discharging[1] $(d\varepsilon_{pi} = 0)$, if we ascribe the role of time to variable γ and

to consider that $T_i = \text{const}$, they are record/written as follows:

$$\left.\begin{array}{l} d\varepsilon_{pi} \neq 0, \quad \text{если } f = 0 \text{ и } \dfrac{\partial}{\partial \psi}\sigma_i \operatorname{sign}\sigma_i > 0; \\ d\varepsilon_{pi} = 0, \quad \text{если } f < 0 \text{ либо если } f = 0 \text{ и } \dfrac{\partial}{\partial \psi}\sigma_i \operatorname{sign}\sigma_i \leqslant 0. \end{array}\right| \qquad (1.9)$$

Key: (1). if. (2). and. (3). or if.

FOOTNOTE 1. Not only discharging, but also passive loading. ENDFOOTNOTE.

Differentials $d\varepsilon_{pi}$ quotients (on ψ).

Accordingly (1.9) during "discharging" variables ε_{pi} can be functions ϕ (but not ψ). The requiring in this case supplementary relationship/ratio for determination ε_{p2} in the case when $\varepsilon_{p2} < 0$ (which occurs in the beginning of unloading caused by emptying), let us introduce as follows.

Let the region

$$\pi - \gamma_i < \psi \leqslant \pi - \zeta \qquad (1.10)$$

is any of the regions of monotonicity ε_{p2}, wholly belonging (1.2), ψ when $\psi \geqslant \gamma_i$.

For these values of φ we assume that in (1.10)

$$\left.\begin{aligned} \bar{\varepsilon}_{p2}(\varphi) &= \nu \frac{\cos\eta_1 + \cos\varphi}{\cos\zeta - \cos\eta_1}, && \text{если } \bar{\varepsilon}_{p2}(\pi - \eta_1) = 0; \\ \bar{\varepsilon}_{p2}(\varphi) &= \nu \frac{\cos\zeta + \cos\varphi}{\cos\eta_1 - \cos\zeta}, && \text{если } \bar{\varepsilon}_{p2}(\pi - \zeta) = 0. \end{aligned}\right\} \quad (1.11)$$

Key: (1). if.

For values of φ, that are subordinated to inequality $\zeta \leqslant \varphi \leqslant \eta_1$, we assume that (1.11) it is correct only in the region

$$\pi - \varphi \leqslant \varphi \leqslant \pi - \zeta. \quad (1.12)$$

In both cases must be $\nu > 0$.

Let us assume also that determinations above the variable $\bar{\varepsilon}_{p2}$ satisfies (1.8) (condition f = 0) in boundary points of region (1.10).

Subsequently let us utilize the designations

$$\frac{E_i}{E_i + E_i'} = \lambda_i \ (i = 1, 2); \quad e(1 - \lambda_1) = \bar{e}; \quad \frac{\alpha_2 \theta_2 - \frac{\sigma_{s2}}{E_2}}{D} = \varkappa_2. \quad (1.13)$$

2. Equations for determining of F and Φ

As let us see, in certain range of change $\psi(\psi \geqslant 0)$ value $\varepsilon_{p1} = 0$, a ε_{p2} are defined for all φ in (1.2). For these values of ψ, accordingly (1.3) - (1.5), in ranges (1.1) and (1.2) respectively, must be

$$\left.\begin{aligned} D\,[F(\psi) + \Phi(\psi)\cos\varphi] &= \frac{\sigma_1(\psi,\ \varphi)}{e\,E_2}; \\ D\,[F(\psi) + \Phi(\psi)\cos\varphi] &= \frac{\sigma_2(\psi,\ \varphi)}{E_2} + \alpha_2\theta_2 + \varepsilon_{p2}(\varphi). \end{aligned}\right\} \qquad (2.1)$$

Page 87.

If $\psi = 0$, then of (2.1), (1.4), (1.6) it follows

$$\left.\begin{aligned} F(0) = \Phi(0) &= 0; \\ \sigma_1(0,\ \varphi) &= 0; \\ \sigma_2(0,\ \pi) &= -E_2\,[\alpha_2\theta_2 + \varepsilon_{p\,2}(\pi)]; \\ D &= \alpha_2\theta_2 + \varepsilon_{p\,2}(\pi). \end{aligned}\right\} \qquad (2.2)$$

On the other hand, accordingly (1.7),

$$\sigma_2(0,\ \pi) = -\sigma_{s\,2} + E_2'\varepsilon_{p\,2}(\pi).$$

Of two expressions for σ_2 (0, π) with the aid of designations (1.13) we will obtain

$$\left.\begin{aligned} \varepsilon_{p\,2}(\pi) &= -\lambda_2\left(\alpha_2\theta_2 - \frac{\sigma_{s\,2}}{E_2}\right); \\ D &= (1-\lambda_2)\,\alpha_2\theta_2 + \lambda_2\frac{\sigma_{s\,2}}{E_2}, \end{aligned}\right\} \qquad (2.3)$$

and therefore

$$\frac{\alpha_2 \theta_2}{D} = 1 + \lambda_2 \varkappa_2; \quad \bar{\sigma}_{s\,2} = 1 - (1 - \lambda_2)\varkappa_2. \tag{2.4}$$

Taking into account these relationship/ratios and (1.4) equalities (2.1) will be rewritten as follows:

$$\left.\begin{aligned} \bar{\sigma}_1 &= e\,(F + \Phi\cos\varphi); \\ \bar{\sigma}_2 &= F + \Phi\cos\varphi - 1 - \lambda_2\varkappa_2 - \bar{\varepsilon}_{p\,2}(\varphi). \end{aligned}\right\} \tag{2.5}$$

Introducing (2.5) in (1.6) and designating

$$\left.\begin{aligned} P &= \frac{1}{\pi}\int_{\pi-\psi}^{\pi} [\lambda_2\varkappa_2 + \varepsilon_{p2}(\varphi)]\,d\varphi; \\ Q &= \frac{2}{\pi}\int_{\pi-\psi}^{\pi} [\lambda_2\varkappa_2 + \varepsilon_{p\,2}(\varphi)]\cos\varphi\,d\varphi, \end{aligned}\right\} \tag{2.6}$$

let us arrive at the equations

$$\left.\begin{aligned} F\left[e - (e-1)\frac{\psi}{\pi}\right] + \Phi\,(e-1)\,\frac{\sin\psi}{\pi} &= \frac{\psi}{\pi} + P; \\ F\,2\,(e-1)\frac{\sin\psi}{\pi} + \Phi\left[e - (e-1)\left(\frac{\psi}{\pi} + \frac{\sin 2\psi}{2\pi}\right)\right] &= \\ = -\,2\,\frac{\sin\psi}{\pi} + Q. & \end{aligned}\right\} \tag{2.7}$$

Solving (2.7), let us find

$$\left.\begin{aligned} F(\psi) &= \frac{1}{R(\psi)}\left\{e\,\frac{\psi}{\pi} - (e-1)\,\Gamma(\psi) + \right. \\ &+ P\left[e - (e-1)\left(\frac{\psi}{\pi} + \frac{\sin 2\psi}{2\pi}\right)\right] - Q\,(e-1)\,\frac{\sin\psi}{\pi}\Big\}; \\ \Phi(\psi) &= \frac{1}{R(\psi)}\left\{-2e\,\frac{\sin\psi}{\pi} + Q\left[e - (e-1)\,\frac{\psi}{\pi}\right] - \right. \\ &\left. -2P(e-1)\,\frac{\sin\psi}{\pi}\right\}; \end{aligned}\right| \qquad (2.8)$$

here

$$\left.\begin{aligned} R(\psi) &= e^2 - e\,(e-1)\left(2\,\frac{\psi}{\pi} + \frac{\sin 2\psi}{2\pi}\right) + (e-1)^2\,\Gamma(\psi); \\ \Gamma(\psi) &= \frac{\psi^2}{\pi^2} + \frac{\psi\sin 2\psi}{2\pi^2} - 2\,\frac{\sin^2\psi}{\pi^2} \end{aligned}\right| \qquad (2.9)$$

Page 88.

Let us designate

$$\bar{\varepsilon}(\psi, \pi - \psi) \equiv F(\psi) - \Phi(\psi)\cos\psi \equiv \bar{\varepsilon}_\psi(\psi). \qquad (2.10)$$

Variable $\bar{\varepsilon}_\psi(\psi)$ plays important role during the determination of plastic deformations.

Let us note that accordingly (2.5), i.e., for it is sufficient

small ψ_*

$$\bar{\varepsilon}_\psi(\psi) = \frac{\bar{\sigma}_1(\psi, \pi - \psi)}{e}. \qquad (2.11)$$

To us is known the function $\bar{\varepsilon}_\psi(\psi)$. Let us designate through ψ_* the rçct of the equation

$$\bar{\varepsilon}_\psi(\psi_*) = \varkappa_1; \quad \varkappa_1 = \frac{\bar{\sigma}_{s1}}{e}. \qquad (2.12)$$

If when $0 \leqslant \psi \leqslant \psi_*$

$$\bar{\varepsilon}_\psi \leqslant \varkappa_1 \qquad (2.13)$$

and $\sigma_1(\psi, \pi - \psi)$ in range (1.1) is the greatest stress, then of (2.13) and (2.11) it follows that in range (1.1) $\varepsilon_{p1} = 0$. Under the formulated above conditicns of the formula cf this section, are valid for values ψ satisfying the inequality, entering in (2.13).

3. Purely elastic deformaticns and of the stress in shell.

This case, otherwise than in us, it was examined in work [1]. We will ctain it, after assuming $E_1 = \infty$. Then, accordingly (1.8), $\varepsilon_{pi} = 0$ with any σ_i, that means and in the zones of discharging. With this $\lambda_2 = 0$, $D = \frac{d^2}{d\varphi^2}\theta_2$, $P = Q = 0$ equation (2.8) is determined F and ϕ, but equations (2.5) - σ_i with $0 \leqslant \psi \leqslant \pi$.

Accordingly (2.5), (2.8) and (2.10)

$$\bar{\varepsilon}_{\psi}(\psi) = \frac{1}{R(\psi)}\left\{e\left(\frac{\psi}{\pi} + \frac{\sin 2\psi}{2\pi}\right) - (e-1)\Gamma(\psi)\right\} = \bar{\sigma}_2(\psi, \pi - \psi) + 1 = \frac{\sigma_1(\psi, \pi - \psi)}{e}. \quad (3.1)$$

Curve/graph $\bar{\varepsilon}_{\psi}(\psi)$ with e = 1.113; $\varepsilon_{p2} = P = Q = 0)$ is shown to by lower curve Fig. 2. This curve intersects from straight line $\bar{\varepsilon}_{\psi} = -\bar{\sigma}_{s2} + 1$ at the points for which $\psi = \psi_m$ (m = 1, 2, 4), and from straight line $\bar{\varepsilon}_{\psi} = \varkappa_1$ at pcint $\psi = \bar{\psi}_3$. Function $\bar{\varepsilon}_{\psi}$ (on lower curved) reaches the minimum with $\psi = \bar{\psi}_3 (\bar{\psi}_2 < \bar{\psi}_3 < \bar{\psi}_4)$.

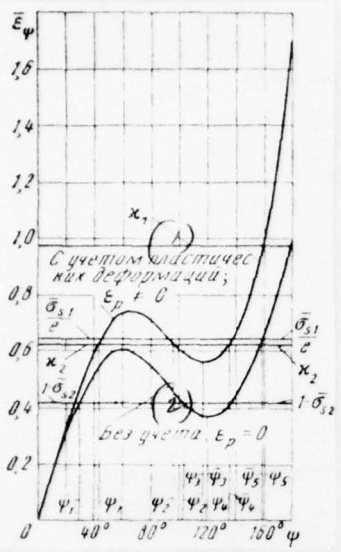

Key: (1). Taking into acccunt plastic defcrmaticns. (2). without acccunt.

Page 89.

From Fig. 2 and relationship/ratio (3.1) it follows

with $0 \leqslant \psi \leqslant \bar{\psi}_1$ and with $\bar{\psi}_2 \leqslant \psi \leqslant \bar{\psi}_4$

$$|\bar{\sigma}_2(\psi, \pi - \psi)| \geqslant \bar{\sigma}_{s2}; \tag{3.2}$$

when $\bar{\psi}_{3,4} \leqslant \psi < \pi$

$$\sigma_1(\psi, \pi - \psi) \geqslant \sigma_{s1}. \tag{3.3}$$

Consequently, with increase φ for its values, which correspond (3.2) or which exceed φ_1 (but it is later in the process of emptying, φ_4) in some parts of range (1.2), and with φ those correspond (3.3), in range (1.1) or its part they can arise the condition of forming the irreversible plastic deformations.

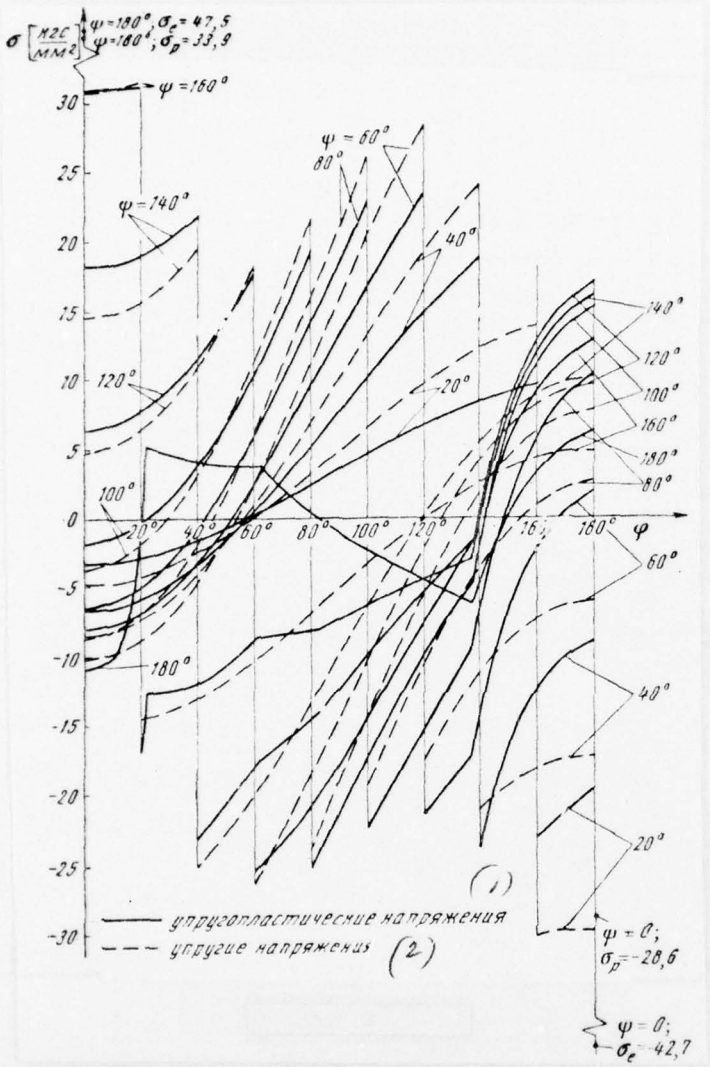

Fig. 3.

Key: (1). elastoplastic voltages. (2). elastic strains.

Page 90.

The curve/graphs of stresses σ_i found from formulas (1.4), (2.5), (2.8) when $\gamma_2 = \varepsilon_{p2} = 0$, are shown by broken lines by curves on Fig. 3. They testify that with increase of ψ in range (1.2) occurs the discharging, and in range (1.1), beginning from $\psi = \psi_5$, - load beyond yield point. From them it is evident also which $\sigma_1(\psi, \pi - \psi)$ in range (1.1) has great, and $\sigma_2(\psi, \pi - \psi)$ in range (1.2) - a small value. Then, as it follows from Fig. 2 and relationship/ratio (3.1), with $\bar{\psi}_1 \leqslant \psi \leqslant \bar{\psi}_2$ and with $\psi_1 \leqslant \psi \leqslant \psi_5$ occurs the inequality

$$|\bar{\sigma}_2(\psi, \pi - \psi)| \leqslant \bar{\sigma}_{s2}. \qquad (3.4)$$

a zone $\pi - \psi_2 \leqslant \varphi \leqslant \pi - \bar{\psi}_1$ and $\pi - \bar{\psi}_3 \leqslant \varphi \leqslant \pi - \bar{\psi}_4$ either their part when these zones or their parts belong (1.2), are knowingly free from plastic deformations $\bar{\varepsilon}_{p2}$.

The made analysis of elastic solution substantially facilitates finding the zones of plastic deformations.

4. Elasto-plastic deformations and of the stress in shell.

First case. Let us expand/develop the solution, obtained earlier for values of ψ satisfying inequality (2.13), at which $\varepsilon_{p1} = 0$. First let us construct ε_{p2}. According to results Section 1, it is possible

to expect the formation/education of three ranges of monotonicity $\bar{\varepsilon}_{p2}(\varphi)$:

$$\left.\begin{aligned} &\pi-\psi_1\leqslant\varphi\leqslant\pi;\\ &\pi-\psi_3\leqslant\varphi\leqslant\pi-\psi_2;\\ &\pi-\psi_4\leqslant\varphi\leqslant\pi-\psi_3 \end{aligned}\right\} \qquad (4.1)$$

and of two zones in which when $\pi-\psi_2\leqslant\varphi\leqslant\pi-\psi_1$ and when $\pi-\psi_5\leqslant\varphi\leqslant\pi-\psi_4$

$$\bar{\varepsilon}_{p2}(\varphi)=0. \qquad (4.2)$$

Let us designate through ψ_m ($m = 1, 2, 4$) values ψ, that satisfy condition $\bar{\varepsilon}_{p2}(\pi-\psi)=0$, through $\psi=\psi_3-$ to the conditions

$$\bar{\varepsilon}_{p1}(\psi_3,\ \pi-\psi_3)=0 \text{ (и/)} \bar{\varepsilon}_{\psi}(\psi_3)=\varkappa_1, \qquad (4.3)$$

Key: (1). and.

through $\psi=\psi_3-$ to conditions

$$\bar{\varepsilon}_{\psi}(\psi_3)=\min\bar{\varepsilon}_{\psi}(\psi)=\bar{\varepsilon}_3;\quad \frac{d\bar{\varepsilon}_{\psi}}{d\psi}(\psi_3)=0. \qquad (4.4)$$

For determination ψ_m let us note that $\bar{\sigma}_2=-\bar{\sigma}_{s2}$ when $\bar{\varepsilon}_{p2}(\pi-\psi_m)=0$, and then according to the second equations from (2.4) and (2.5), we will obtain

$$\bar{\varepsilon}_{\psi}(\psi_m)=\varkappa_2\ (m=1,\ 2,\ 4). \qquad (4.5)$$

Finding ψ_m from (4.5) makes sense only when $\varkappa_2 > 0 \left(\alpha_2 \theta_2 > \frac{\sigma_{s2}}{E_2}\right)$, when $\bar{\varepsilon}_{p2}$ real/actually there exists. When $\varkappa_2 < 0$ everywhere $\bar{\varepsilon}_{p2} = 0$.

As follows from Section 1 in the first of ranges (4.1) must appear dependence $\varepsilon_{p2}(\psi)$, corresponding to the first case from (1.11), moreover for it accordingly (4.1), (2.3) and (1.11) $\zeta = 0;\ \eta = \psi_1;\ \nu = -\bar{\varepsilon}_{p2}(\pi) = \lambda_2 \varkappa_2$.

Page 91.

In the second of ranges (4.1) it is necessary to expect the dependence $\bar{\varepsilon}_{p2}(\psi)$, corresponding to second case (1.11), for which $\zeta = \psi_2, \eta = \psi_3$ and accordingly (1.5), (2.4), (4.4) and (1.11) $\bar{\varepsilon}_3 = \bar{\sigma}_2(\psi_3, \pi - \psi_3) + 1 + \lambda_2 \varkappa_2 - \nu$.

On the other hand, from (1.8), (1.11) and (2.4) it follows

$$\bar{\sigma}_2(\psi_3, \pi - \psi_3) + 1 + \lambda_2 \varkappa_2 = \varkappa_2 - \frac{E_2^1}{E_2} \nu.$$

Thus, taking into account (1.13)

$$\nu = \lambda_2 (\varkappa_2 - \bar{\varepsilon}_3).$$

In the third of ranges (4.1), according tc that presented and (1.11), for the first case $\zeta = \psi_3;\ \eta = \psi_4;\ \nu = -\bar{\varepsilon}_{p\,2}(\psi_3) = \lambda_2(\varkappa_2 - \bar{\varepsilon}_3)$.

Consequently, for φ, that lie at ranges (4.1) and (4.2), when these ranges or at least their parts belong (1.2), function $\bar{\varepsilon}_{p\,2}(\varphi)$ necessary to assign thus:

$$\left.\begin{array}{ll}
\bar{\varepsilon}_{p\,2} = \lambda_2 \varkappa_2 \dfrac{\cos\psi_1 + \cos\varphi}{1 - \cos\psi_1} & \text{(1) при } \pi - \psi_1 \leqslant \varphi \leqslant \pi; \\
\bar{\varepsilon}_{p\,2} = 0 & \text{при } \pi - \psi_2 \leqslant \varphi \leqslant \pi - \psi_1; \\
\bar{\varepsilon}_{p\,2} = \lambda_2(\varkappa_2 - \bar{\varepsilon}_3)\dfrac{\cos\psi_2 + \cos\varphi}{\cos\psi_3 - \cos\psi_2} & \text{(1) при } \pi - \psi_3 \leqslant \varphi \leqslant \pi - \psi_2; \\
\bar{\varepsilon}_{p\,2} = \lambda_2(\varkappa_2 - \bar{\varepsilon}_3)\dfrac{\cos\psi_4 + \cos\varphi}{\cos\psi_3 - \cos\psi_4} & \text{(1) при } \pi - \psi_4 \leqslant \varphi \leqslant \pi - \psi_3; \\
\bar{\varepsilon}_{p\,2} = 0 & \text{(1) при } \pi - \psi_5 \leqslant \varphi \leqslant \pi - \psi_4.
\end{array}\right| \quad (4.6)$$

Key: (1). with.

Then consecutively it is possible to find everything ψ_m and ε_3, which will make it possible to completely sclve our task for $0 \leqslant \varphi \leqslant \psi_5$

It is real/actual, $0 \leqslant \varphi \leqslant \psi_1$. Then in field (1.2) we assign $\bar{\varepsilon}_{p\,2}$ acccrding to first equation (4.6) and cn (2.6) we compute $P = P_1(\psi)$ and $Q = Q_1(\psi)$ [P and Q it is convenient to assign the index, which

corresponds to the number of rows from (4.6), used for their determination]. On (2.8), we find F and Φ, on (2.10) $-\bar{\varepsilon}_\psi(\psi)$ and from (4.5) with m = 1 we determine ψ_1. Further similarly are located $P_2(\psi)$, $Q_2(\psi)$, F, Φ, $\bar{\varepsilon}_\psi$ also, from (4.5) ψ_2, that satisfies the condition

$$\psi_1 < \psi_2 < \pi. \tag{4.7}$$

With observance (4.7) we find $P_3(\psi)$, $Q_3(\psi)$, F, Φ, $\bar{\varepsilon}_\psi$ and from equations (4.4) ψ_3 and $\bar{\varepsilon}_3$. If it seems that $\bar{\varepsilon}_3 < \varkappa_2$, then we compute $P_4(\psi)$, $Q_4(\psi)$ and so forth, and from (4.5) ψ_4. Finally, through $P_5(\psi)$, $Q_5(\psi)$ we find F, Φ, $\bar{\varepsilon}_\psi$ also, from equation (4.3) ψ_5. If it seems that in region (4.7) there are no roots of equation (4.5), then it means that $\min \bar{\varepsilon}_\psi(\psi)$ it lie/rests above straight line $\bar{\varepsilon}_\psi = \varkappa_2$ and therefore $\bar{\varepsilon}_{p2} = 0$ everywhere, besides the first of regions (4.1).

If it turns out that $\bar{\varepsilon} = \varkappa_2$, then the mentioned straightline is tangent to $\bar{\varepsilon}_\psi(\psi)$ in the point of the $\psi_2 = \psi_3 = \psi_4$, $\bar{\varepsilon}_{p2} = 0$ everywhere except the first area (4.1).

Incidentally are calculated stresses σ_i.

Second case. If $\psi > \psi_5$, then in region (1.1) will arise deformations $\varepsilon_{p1} > 0$, in the process of emptying converting into region (1.2). For (1.2) they will become the deformations of discharging $\bar{\varepsilon}_{p2}(\bar{\varepsilon}_{p2} > 0)$.

That means that in the completely emptied tank when $0 \leq \varphi \leq \pi - \psi_5$

$$\bar{\varepsilon}_{p2} = \nu \frac{\cos\psi_5 + \cos\varphi}{1 + \cos\psi_5}. \tag{4.8}$$

Page 92.

According (4.8)

$$\bar{\varepsilon}_{p\,2}(\pi - \psi_5) = \bar{\varepsilon}_{p\,1}(\pi - \psi_5) = 0,$$

$$\bar{\varepsilon}_{p\,2}(0) = \nu = \bar{\varepsilon}_{p\,1}(0) = \frac{E_2}{E_1}\,[\bar{\sigma}_1(\pi,\ 0) - \sigma_{s\,1}]. \tag{4.9}$$

Let us designate

$$\bar{\varepsilon}_\psi(\pi) = F(\pi) + \Phi(\pi) = \bar{\varepsilon}_7 \tag{4.10}$$

and let us note that accordingly (1.5) and (4.9),

$$\bar{\varepsilon}_7 = \frac{\bar{\sigma}_1(\pi,\ 0)}{e} + \nu. \tag{4.11}$$

From (4.11) and (4.9) taking into acccant (1.13) we find that after which (4.8) it is copied as fcllcws:

when $0 \leq \varphi \leq \pi - \psi_5$

$$\bar{\varepsilon}_{p\,2} = \lambda_1(\bar{\varepsilon}_7 - \varkappa_1)\,\frac{\cos\psi_5 + \cos\varphi}{1 + \cos\psi_5}. \tag{4.12}$$

AD-A065 783 FOREIGN TECHNOLOGY DIV WRIGHT-PATTERSON AFB OHIO F/G 20/4
SCIENTIFIC NOTES FROM THE CENTRAL AEROHYDRODYNAMIC INSTITUTE.(U)
JUL 78
UNCLASSIFIED FTD-ID(RS)T-0680-78 NL

3 OF 3
AD
A065783

END
DATE
FILMED
5-79
DDC

Now for the completely emptied tank ($\psi = \pi$) we right to use the second of equations (2.5), and means by formulas (2.6)-(2.8). Taking into account (4.6) and (4.12) the deformation $\bar{\varepsilon}_{p2}(\varphi)$ is determined everywhere and computations using formulas (2.6) do not encounter difficulties. Computing by (2.6) $P(\pi)$ and $Q(\pi)$, and then on (2.8) $F(\pi)$ and $\Phi(\pi)$ (4.10) we will obtain linear equation relatively $\bar{\varepsilon}_1$ (when $\psi_5 < \pi$ must be $\bar{\varepsilon}_1 > \varkappa_1$). Let us return to case by $\psi < \pi$. The stresses $\bar{\sigma}_1(\psi, \varphi)$, examined in Section 3, and means in the case in question, with decrease φ, they decrease. Therefore with $\psi_5 \leqslant \psi \leqslant \pi$, generally speaking, not in entire region (1.1) $\bar{\varepsilon}_{p1} \neq 0$.

Let $\psi_6 (\psi_6 > \psi_5)$ be that value of parameter ψ, at which in (1.1) $\bar{\varepsilon}_{p1}(\varphi)|_{\varphi=0} \neq 0$; moreover $\varepsilon_{p1}(0) = 0$. Then for $\psi_6 \leqslant \psi \leqslant \pi$ with the aid of (1.5), (1.8), (2.4), (1.13) we obtain

$$\left.\begin{aligned} \bar{\sigma}_1(\psi, \varphi) &= \bar{e}(F + \Phi\cos\varphi) + \lambda_1 \bar{\sigma}_{s1}; \\ \bar{\sigma}_2(\psi, \varphi) &= F + \Phi\cos\varphi - 1 - \lambda_2 \varkappa_2 - \bar{\varepsilon}_{p2}(\varphi); \end{aligned}\right\} \tag{4.13}$$

moreover in region $\pi - \psi \leqslant \varphi \leqslant \pi - \psi_6$, by being part (1.2), $\bar{\varepsilon}_{p2}(\varphi)$ we assign on formula (4.11). With the aid of (4.13) and (1.6), again let us arrive at equations (2.7), if we in them replace e by $\bar{e}$ and to assume

$$\left.\begin{aligned} P(\psi) &= -\lambda_1 \bar{\sigma}_{s1}\left(1 - \frac{\psi}{\pi}\right) + \frac{1}{\pi}\int_{\pi-\psi}^{\pi} [\lambda_2 \varkappa_2 + \bar{\varepsilon}_{p2}(\varphi)]\, d\varphi; \\ Q(\psi) &= -2\lambda_1 \bar{\sigma}_{s1}\frac{\sin\psi}{\pi} + \frac{2}{\pi}\int_{\pi-\psi}^{\pi} [\lambda_2 \varkappa_2 + \bar{\varepsilon}_{p2}(\varphi)]\cos\varphi\, d\varphi. \end{aligned}\right\} \tag{4.14}$$

Consequently, as solution (2.7) for the case in question they also serve (2.8), (2.9), if we in them replace e by $\bar{e}$, and P and Q to calculate according to (4.14). Let us note that this solution with $\psi = \gamma$ leads to the same values of $F(\pi)$ and $\Phi(\pi)$, which enter in (4.10).

The first of equalities (4.13), with $\psi = 0$ and $\bar{\sigma}_1(\psi_0, 0) = \bar{z}_1$, reduces to the equation

$$F(\psi_6) + \Phi(\psi_6) = \varkappa_1. \qquad (4.15)$$

By the method presented it is possible to obtain equations for F, Φ, z_i and in the case $\psi_5 \leq \psi \leq \psi_6$. However, with ψ_{n-1} close to ψ_5 (which usually occurs), this interval/gap change it is possible not to examine.

Page 93.

The given formulas make it possible to solve state problem in

criterial form. Criterion $\varkappa_2 D = \alpha_2 \theta_2 - \frac{\sigma_{s2}}{E_2}$ makes it possible even before calculations to judge the possibility of the emergence of plastic deformations in tank. Criterion $\bar{\epsilon}_3$ solves the problem about the number of plastic flow areas during discharging.

Calculation was carried out by the author for stresses and strains of tank from D16AT with following by initial data: T_1 = 300°K; $\theta_2 = 250°$; $\alpha_2 \theta_2 = 6{,}53$; $\sigma_{s1} = 30{,}5$ кгс/мм²; $\sigma_{s2} = 25$ кгс/мм²; $E_2 = 6540$ кгс/мм²; $e = 1{,}113$; $E_1 = 1890$ кгс/мм²; $E_2 = 1615$ кгс/мм².

КГС = KG

The results of calculation are given tc Fig. 2 and 3.

The numerical values of the stresses and strains in region (1.2) satisfy the conditions of discharging (1.9). The account of plastic deformations leads to a noticeable reduction in the stresses.

REFERENCES

1. S. N. Kahn, S. I. Barashkov. To temperature of the stress in the housing of shell, by the partially filled liquid. XVAIVU, the transactions of school, iss. 128, 1958.

2. I. A. Birger, I. V. I. V. Dem'yanushko. Theories of

plasticity with nonisothermal loading. "mechanics of solid", 1968, No 6.

Received 4/VI 1969.

Page 94.

METHOD OF SUCCESSIVE APPROXIMATIONS IN PROBLEM OF TRANSIENT CREEP AND OF NONLINEAR ELASTICITY.

I. I. Pospelov.

In work is given the method of the solution of the problems of theory of creep that is the development of the method of elastic solutions [1]. Method allows physically the nonlinear task of the theory of creep to reduce to the sequence of linear tasks and to describe the redistribution of the stresses in construction in the process of creep. Unlike work [2] complete strain is represented in the form of the sum of instantaneous deformation, by nonlinear form voltage-sensitive, and creep strain, nonlinear voltage-sensitive and time.

The behavior of material during creep is described by the theory of flow. Is given an example of numerical computation.

1. Fundamental equations of the theory of creep.

It is assumed that the components of the deviator of complete strain e_{ij} are accumulated from the components of the deviator of instantaneous deformation e'_{ij} depending only on stresses, and creep strain p_{ij} that voltage-sensitive and the time:

$$e_{ij} = e'_{ij} + p_{ij} \quad (i, j = 1, 2, 3), \tag{1.1}$$

where $e_{ij} = \varepsilon_{ij} - \varepsilon\delta_{ij}$; here ε_{ij} — a strain tensor; $\delta_{ij} = 1$ with i = j and $\delta_{ij} = 0$ with $i \neq j$.

For describing the process of creep, are utilized the equations of the type

$$\dot{p}_{ij} = \frac{3}{2}\frac{\dot{p}_u}{\sigma_u} s_{ij}, \tag{1.2}$$

where s_{ij} — a stress deviator; $\dot{p}_{ij}$ — derivative of the strain deviator of creep on the modified time $\tau(t)$, which is the function of the physical time t; σ_u, $\dot{p}_u$ — the stress intensities to of the rates of creep strain, moreover

$$\sigma_u^2 = \frac{3}{2} s_{ij} s_{ij};$$

$$s_{ij} = \sigma_{ij} - \sigma\delta_{ij} \tag{1.3}$$

(here σ_{ij} — stress tensor; σ - average/mean stress).

Page 95.

The relationship/ratio between intensities of stresses and rates of creep strain and the time is accepted in the following form:

$$\dot{p}_u = f(\sigma_u). \tag{1.4}$$

During numerical computations is utilized $f(\sigma_u) = A\sigma_u^n$. Function $f(\sigma_u)$ and the modified time $\tau = \tau(t)$ are determined from the grid of curves of creep, obtained experimentally with elongation under conditions of constant temperature [2].

The components of the deviator of instantaneous deformation are determined by the equations

$$e'_{ij} = \frac{3}{2}\frac{e'_u}{\sigma_u} s_{ij}. \tag{1.5}$$

Communication/connection between intensities of instantaneous deformation and stresses

$$e_u' = \varphi(\sigma_u) \qquad (1.6)$$

let us accept in the form

$$e_u' = \frac{\sigma_u}{3\mu} + \left(\frac{\sigma_u}{\sigma^0}\right)^m, \qquad (1.7)$$

where μ - shear modulus; m, σ^0 - constants of material which can be determined from diagram $\sigma \sim \varepsilon$.

Communication/connection between the average/mean stress $\sigma = \frac{1}{3}\sigma_{ii}$ and the average/mean strain $\varepsilon = \frac{1}{3}\varepsilon_{ii}$ is expressed by the equation

$$\sigma = K\theta, \qquad (1.8)$$

where $K = \frac{E}{3(1-2\nu)}$, $\theta = 3\varepsilon$ (here E - Young's modulus, ν - Poisson ratio).

From equations (1.1), (1.2), (1.4)-(1.6) we will obtain

$$\frac{de_{ij}}{d\tau} = \frac{3}{2}\frac{d}{d\tau}\left[\frac{\varphi(\sigma_u)}{\sigma_u} s_{ij}\right] + \frac{3}{2}\frac{f(\sigma_u)}{\sigma_u} s_{ij}. \qquad (1.9)$$

Equations (1.9) describe the behavior of material both during instantaneous nonlinear deformation and transient creep. They not linear and their use during the solution of problems is connected

with considerable mathematical difficulties.

Page 96.

Equation (1.4) is convenient, isolating linear part, to present in the form

$$p_{и} = D\sigma_{и}(1 - \eta), \tag{1.10}$$

where

$$\eta = 1 - \frac{f(\sigma_{и})}{D\sigma_{и}}. \tag{1.11}$$

it is possible to subordinate to condition $0 \leqslant \eta < 1$ by selection of Key's constant

$$D \geqslant \frac{f(\sigma_{и\,max})}{\sigma_{и\,max}} \quad \left(\text{при} \quad \frac{df}{d\sigma_{и}} > 0;\right.$$

(1). with

here $\sigma_{и\,max}$ — certain conditional number.

In calculations D, it was calculated from the formula

$$D = \frac{f(\sigma_{и\,max})}{\sigma_{и\,max}}. \tag{1.12}$$

Analogous to equation (1.6) we represent in the form

$$e'_{и} = \frac{\sigma_{и}}{3\mu_{1}}(1 + \omega), \tag{1.13}$$

where

$$\omega = \frac{\varphi(\sigma_u) - \frac{\sigma_u}{3\mu_1}}{\frac{\sigma}{3\mu_1}} = \frac{\mu_1 - \mu}{\mu} + \frac{3\mu_1}{\sigma^0}\left(\frac{\sigma_u}{\sigma_0}\right)^{m-1} \qquad (1.14)$$

it is possible to subordinate to condition $-1 < \omega \leqslant 0$ by the selection

$$\mu_1 \leqslant \frac{1}{\frac{1}{\mu} + \frac{3}{\sigma^0}\left(\frac{\sigma_{u\,max}}{\sigma^0}\right)^{m-1}}.$$

For μ_1 it is possible to accept

$$\mu_1 = \frac{1}{\frac{1}{\mu} + \frac{3}{\sigma^0}\left(\frac{\sigma_{u\,max}}{\sigma^0}\right)^{m-1}}, \qquad (1.15)$$

which corresponds to secant module/modulus to the diagram $e'_u \sim \sigma_u$ for $\sigma_{u\,max}$, or

$$\mu_1 = \frac{1}{\frac{1}{\mu} + m\frac{3}{\sigma^0}\left(\frac{\sigma_{u\,max}}{\sigma^0}\right)^{m-1}}, \qquad (1.16)$$

that corresponds to the tangent modulus on diagram $e'_u \sim \sigma_u$ for $\sigma_{u\,max}$.

In the region where communication/connection between the stress

and the strain bears linear character,

$$\frac{3}{\sigma^0}\left(\frac{\sigma_{u\max}}{\sigma^0}\right)^{m-1} \approx 0 \quad (1) \quad \text{и} \quad \mu_1 = \mu.$$

Key: (1). and.

Taking into account (1.10) and (1.13) equation (1.9) let us present in the form

$$s_{ij} + 3\mu_1 D s_{ij} = 2\mu_1 e_{ij} - 2\mu_1 \varphi_{ij}. \tag{1.17}$$

or in the integral form

$$s_{ij} = 2\bar{\mu}e_{ij} + f_{ij} + \tilde{f}_{ij}, \tag{1.18}$$

where $\bar{\mu}z$ — a linear operator,

$$\bar{\mu}z = \mu_1 z - 3\mu_1^2 D e^{-3\mu_1 D(\tau-\tau_0)} \int_{\tau_0}^{\tau} z e^{3\mu_1 D(\tau'-\tau_0)}\, d\tau'; \tag{1.19}$$

$$f_{ij} = -2\mu_1 e^{-3\mu_1 D(\tau-\tau_0)} \int_{\tau_0}^{\tau} \varphi_{ij} e^{3\mu_1 D(\tau'-\tau_0)}\, d\tau', \tag{1.20}$$

$$\varphi_{ij} = -\frac{3}{2} D\eta s_{ij} + \frac{1}{2\mu_1}\frac{d}{d\tau}(s_{ij}\omega); \tag{1.21}$$

$$\tilde{f}_{ij} = [s_{ij}(\tau_0) - 2\mu_1 e_{ij}(\tau_0)]\, e^{-3\mu_1 D(\tau-\tau_0)}. \tag{1.22}$$

Page 97.

Equations (1.18) describe the behavior of material both during instantaneous nonlinear deformation and during creep. For the elastic

medium for which $\mu_1 = \mu$, $D = 0$, $\omega = 0$, $s_{ij}(\tau_0) = 2\mu e_{ij}(\tau_0)$ from equations (1.19)-(1.21) we have $f_{ij} - f_{ij} = 0$, $\mu = \mu$. ● For the linear medium, described by Maxwell's model, $\mu_1 = \mu$, $\gamma = 0$, $\omega = 0$ and from equations (1.18) we will obtain

$$s_{ij} = 2\mu e_{ij}. \tag{1.23}$$

From comparison (1.18) and (1.23) it is evident that the functions γ and ω when $\mu_1 = \mu$ characterize the deviation of the properties of body from the properties of Maxwell's model with the modified time $\tau = \tau(t)$.

If we place D = 0, then equations (1.18) will describe the plastic deformation of material during the active process of loading or the nonlinear elastic behavior of material. In this case τ, it can serve as the parameter of the loading of construction.

2. Equations of the theory of creep in displacement/movements.

From the equations of static equilibrium, expressed into stresses,

$$\frac{\partial \sigma_{ij}}{\partial x_j} + \rho F_i = 0 \quad (i, j = 1, 2, 3), \tag{2.1}$$

(where F_i – vector of mass forces), from Cauchy formula -

$$\varepsilon_{ij} = \frac{1}{2}\left(\frac{\partial u_i}{\partial x_j} + \frac{\partial u_j}{\partial x_i}\right), \tag{2.2}$$

(here u_i — displacement vector), and from equations (1.18) we will obtain the equations of equilibrium, expressed in displacement/movements, in the form of Lame:

$$\bar{\mu}\nabla^2 u_i + (\bar{\mu}+\bar{\lambda})\frac{\partial\theta}{\partial x_i} = -(\rho F_i + \Phi_i), \tag{2.3}$$

where $\bar{\lambda}z$ — linear operator, $\bar{\lambda}z = \left(K - \frac{2}{3}\mu\right)z$;

$$\Phi_i = \frac{\partial(f_{ij} + \tilde{f}_{ij})}{\partial x_j}. \tag{2.4}$$

The boundary conditions, expressed in the stresses

$$\sigma_{ij} l_j = F_{iv}, \tag{2.5}$$

(where l_j — direction cosines of normal to the surface; F_{iv} — forces, assign/prescribed on boundary surface with the use of relationship/ratios (1.18) and (2.2) they are converted to the form

$$\bar{\mu}\left(\frac{\partial u_i}{\partial x_j} l_j + \frac{\partial u_j}{\partial x_i} l_j\right) + \bar{\lambda}(\theta l_i) = F_{iv} - \Phi_{iv}. \tag{2.6}$$

where

$$\Phi_{iv} = (f_{ij} + \tilde{f}_{ij}) l_j. \tag{2.7}$$

For the elastic medium for which $\mu_1 = \mu$, $s_{ij}(\tau_0) = 2\mu e_{ij}(\tau_0)$, $D = 0$, and consequently, $\Phi_{iv} = \Phi_i = 0$, $\bar{\mu} = \mu$, $\bar{\lambda} = \lambda$, the system of equations (2.3) and (2.6) is reduced to the known equations of Lame and boundary conditions. Equations (2.3) and (2.6) formally coincide with the equations of the theory of small elastc-plastic deformations, to which let us use the method of elastic solutions.

The procedure of the calculation of the stressed and state of strain of body, which is located under conditions of transient creep, by the method of successive approximations, consists of following.

For determining the first approximation, we set/assume that $\eta^{(0)} = \omega^{(0)} = 0$. Then $\varphi_{ij}^{(0)} = f_{ij}^{(0)} = 0$, $\tilde{f}_{ij}$, $\Phi_i^{(0)} = \frac{\partial f_{ij}}{\partial x_j}$, $\Phi_{iv}^{(0)} = \tilde{f}_{ij} l_j$ ~~will~~ they be the known functions, determined by initial conditions and which are the solution either of elastic or nonlinear elastic problem. Equations (2.3) and (2.6) become the equations of the linear theory of viscoelasticity. The solution of these equations with the specified initial conditions $u_i^{(1)}$ we take for the first approximation. From equations (2.2) let us find that $\varepsilon_{ij}^{(1)}$, $e_{ij}^{(1)}$, of equations (1.18) $-s_{ij}^{(1)} = 2\mu e_{ij}^{(1)} + \tilde{f}_{ij}$, from equations (1.3), (1.11), (1.14), (1.21), (1.20), (2.4), (2.7) - respectively $\sigma_n^{(1)}$, $\eta_i^{(1)}$, $\omega^{(1)}$, $\varphi_{ij}^{(1)}$, $f_{ij}^{(1)}$, $\Phi_i^{(1)}$, $\Phi_{iv}^{(1)}$ and for the determination of the second approach/approximation $u_i^{(2)}$ we again

utilize a system of linear equations (2.3) and (2.6) with the converted right sides which can be interpreted as fictitious unsteady external forces. Continuing this the process of the solution of the sequence of the tasks of the linear theory of viscoelasticity with the introduction of fictitious external forces, we will obtain required the accuracy/precision of results. The rate of the convergence of the sequence of approach/approximations will decrease in the course of time; therefore for the purpose of the savings of machine time during the calculation that stressed and of states of strain one should utilize point-by-point method, i.e., at each space on time to solve system of equations (2.3) and (2.6) with initial conditions and constants D and μ_1, calculated on the preceding/previous space. Moreover for conditional value $\sigma_{u\,max}$ is used the maximum value of the stress intensity in body, calculated in the preceding/previous space: $\sigma_{u\,max}(x_1 x_2 x_3 \tau_0)$, multiplied on α, where $\alpha \geqslant 1$. On given one α in the process satisfying the inequality $\sigma^{(k)}_u(x_1 x_2 x_3 \tau) \leqslant \sigma_{u\,ma}$ we obtain process of the space $\Delta\tau$, for which $-1 < \omega \leqslant 0$, $0 < \tau_1 < 1$.

In general form a question concerning the convergence of the approach/approximations, obtained by the set-forth method, requires supplementary investigations. The examined below example of numerical computation testifies to the sufficiently high rate of the sequence of approach/approximations.

3. Elongation of rod with a given rate of deformation.

Let us examine the rod, which is deformed with speed $\frac{d\varepsilon_1}{d\tau} = c_1$. Then taking into account the incompressibility of material $\sigma_u = \sigma_1 \; \varepsilon_i = \varepsilon_1$, where σ_1 and ε_1 – stress and complete strain of rod, from equations (1.10), (1.11), (1.13) and (1.14) we obtain

$$\frac{d\sigma_1}{d\tau} + 3\mu_1 D\sigma_1 = 3\mu_1 c_1 + 3\mu_1 D\sigma_1\eta_1 - \frac{d}{d\tau}(\sigma_1\omega). \qquad (3.1)$$

The solution of equation (3.1) for the k iteration can be presented in the form

$$\sigma_1^{(k)}(\tau) = e^{-3\mu_1 D(\tau-\tau_0)}\left\{\sigma_1(\tau_0) + \frac{c_1}{D}\left(e^{3\mu_1 D(\tau-\tau_0)} - 1\right) + \right.$$
$$+ 3\mu_1 D\int_{\tau_0}^{\tau}(\sigma_1\eta_1)^{k-1}\, e^{3\mu_1 D(\tau-\tau_0)}\, d\tau - (\sigma_1\omega)^{k-1}\, e^{3\mu_1 D(\tau-\tau_0)} +$$
$$\left. + |\sigma_1\omega(\tau_0)|^{k-1} + 3\mu_1 D\int_{\tau_0}^{\tau} e^{3\mu_1 D(\tau-\tau_0)}(\sigma_1\omega)^{k-1}\, d\tau\right\}. \qquad (3.2)$$

where

$$\omega = \frac{\mu_1 - \mu}{\mu} + \frac{3\mu_1}{\sigma^0}\left(\frac{\sigma_1}{\sigma^0}\right)^{m-1},$$

$$\eta_1 = 1 - \frac{f(\sigma_1)}{D\sigma_1}.$$

This task allow/assumes the exact solution, expressed in quadratures,

$$\tau = \tau_0 + \int_{\sigma_1(\tau_0)}^{\sigma_1} \psi(\sigma_1)\, d\sigma_1, \qquad (3.3)$$

where

$$\psi(\sigma_1) = \frac{\dfrac{1}{3\mu} + \dfrac{m}{\sigma^0}\left(\dfrac{\sigma_1}{\sigma^0}\right)^{m-1}}{c_1 - f(\sigma_1)}, \qquad (3.4)$$

$$f(\sigma_1) = A\sigma_1^n.$$

The results of the calculation of a change in the stress in time, obtained on formulas (3.2) and (3.3) with $A = 0{,}16 \cdot 10^{-6}\left(\frac{кгс}{мм^2}\right)^{-n}\frac{1}{мин}$, μ = 9.9 = of 2117 kgf/mm², σ^0 = 46 kgf/mm² and n = 3.66, coincide and are represented in Fig. 1. For accelerating the process of the convergence of approach/approximations, the time interval in question was divide/marked off into the cuts with space $\Delta\tau$ = 0.02, in each of which the stress was determined from formula (3.2) with initial condition and constants D and μ_1, by determined equations (1.12) and (1.15) or (1.16), calculated on the preceding/previous cut. Conditional constant number σ_{max} was determined from formula $\sigma_{max} = \alpha\sigma(\tau_0)$. Was accepted α = 1.2.

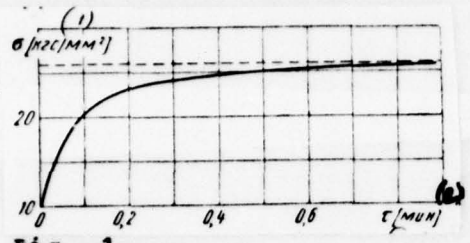

Fig. 1.

Key: (1). kgf/mm². (2). τ [min].

Page 100.

In the process of count, satisfying inequality $\sigma^{(k)}(\tau) < \sigma_{max}$ we determine the value of space $\Delta\tau$ via its fragmentation in such a way, that would be observed the conditions by $-1 < a \leq 0$, $0 \leq \eta < 1$. The results of calculation testify to the sufficiently high rate of the convergence of the sequence of approach/approximations. For the calculation of stresses with an accuracy to fifth significant digit, is not required more than eight approach/approximations.

REFERENCES

1. A. A. Il'yushin. Plasticity. State Technical Press, 1948.

2. A. A. Il'yushin, I. I. Pospelov. On the method of successive approximations in the problem of transient creep. "engineering journal", Vol. IV, iss. 4, 1964.

Received 23/V 1969.

Page 101.

EFFECT OF HEATING LOW-PRESSURE GAS IN A SHOCK TUBE ON INCREASE IN THE ATTAINABLE TEMPERATURE OF STAGNATION.

G. L. Grodzovskiy.

Is investigated the problem of an increase in the attainable temperature of stagnation of gas flow in shock tube. It is shown, that for this purpose is advisable heating low-pressure gas. Is carried out the analysis of the effect of heating low-pressure gas on the increase of the attainable temperature of stagnation in flow behind shock wave for the case of a one-diaphragm cylindrical shock tube.

To gas dynamics of flows in shock tubes devoted large number of investigations (for example, see [1] - [3]). Primary attention in these investigations is devoted to the problem of the achievement of maximum relation to the rate of the shock wave U to the speed of sound in the motionless gas before wave a_1:

$$M_1 = \frac{U}{a_1}.$$

where $a_1 = \sqrt{\varkappa_1 g R_1 T_1}$, T_1 - the static temperature of low-pressure gas in front of the wave, $\varkappa_1$ and R_1 - adiabatic index and the gas constant of this gas.

For the simplest cylindrical one-diaphragm shock tube (Fig. 1) maximum value of number M_1, as is known, is reached at an infinite pressure differential on the diaphragm:

$$M_{1\max} = \frac{(\varkappa_1 + 1) a_4}{(\varkappa_4 - 1) a_1} = \frac{\varkappa_4 + 1}{\varkappa_4 - 1} \sqrt{\frac{\varkappa_4 R_4 T_4}{\varkappa_1 R_1 T_1}}, \qquad (1)$$

where by index 4 are noted the parameters of high-pressure gas.

In accordance with relationship/ratio (1) number M_1 increases with an increase in the temperature of the high-pressure gas T_4 and with an increase in its gas constant R_4. Therefore considerable attention in works [1], [3] it is given to the problems of heating high-pressure gas with the use of high-pressure gases with light molecular weight. From these positions low-pressure gas (T_1) was examined cold.

By us is investigated the problem of an increase in the attainable temperature of stagnation T_0 of gas flow in shock tube. It

is shown, that for this purpose is advisable heating low-pressure gas. By calculation for final pressure differentials on diaphragm this effect was independently previously found by N. I. Khvostov. Lower on the basis of analytical solution is obtained the universal dependence of the attainable temperature of stagnation of gas flow in shock tube on temperature of low-pressure gas.

Let us give analysis for the simplest diagram of shock tube for the perfect gases (see Fig. 1). The obtained results can be common for the cases of more compound circuits and for gases.

Page 102.

The temperature of stagnation T_0 of gas flow in region 2 (behind shock wave), it is logical, it depends on the rate of flow $u_2 = u_3 = V$ and the parameters of low-pressure gas. The limiting value of the velocity of the gas flow V is reached at an infinite pressure differential on diaphragm, value V_{max} depends only on the parameters of the high-pressure gas:

$$V_{max} = \frac{2}{\varkappa_4 - 1} a_4 = \frac{2}{\varkappa_4 - 1} \sqrt{\varkappa_4 g R_4 T_4} \qquad (2)$$

For the fixed value of V, we come to the task of the maximum attainable temperature of stagnation T_0 in flow behind shock wave in the gas, compressed driving/moving at a rate of V by the piston (rcle

of piston performs contact surface, see Fig. 1).

From the equations of shock wave propagation, it is possible to obtain the following expression for the relative rate of flow behind the shock wave:

$$\frac{V}{a_1} = \frac{V}{\sqrt{\varkappa_1 g R_1 T_1}} = M_1 \left[1 - \frac{2\left(1 + \frac{\varkappa_1 - 1}{2} M_1^2\right)}{(\varkappa_1 + 1) M_1^2} \right] = \Phi(M_1). \qquad (3)$$

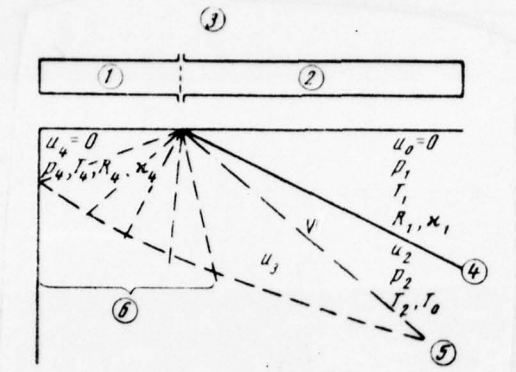

Fig. 1. 1 - high-pressure chambers; 2 - low-pressure chamber; 3 - diaphragm; 4 - shock wave; 5 - contact surface; 6 - centered rarefaction wave.

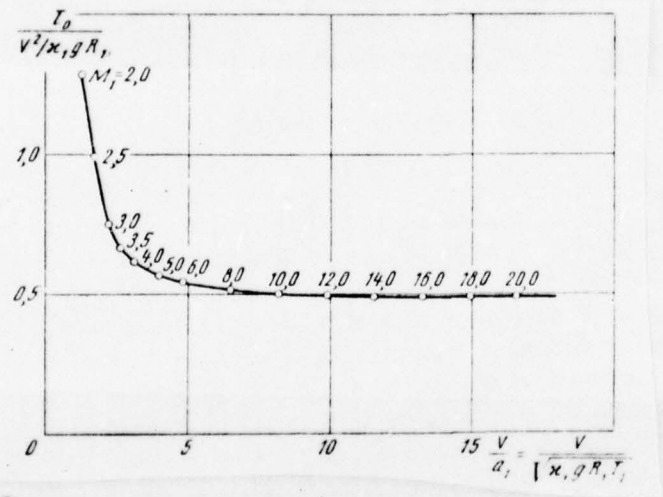

Fig. 2.

Page 103.

A jump/drop in the static temperatures T_2T_1 on shock wave is determined by the known relationship/ratio

$$\frac{T_2}{T_1} = \frac{\left(\varkappa_1 M_1^2 - \frac{\varkappa_1 - 1}{2}\right)\left(\frac{\varkappa_1 - 1}{2} M_1^2 + 1\right)}{\left(\frac{\varkappa_1 + 1}{2}\right)^2 M_1^2} = f(M_1). \tag{4}$$

Respectively the ratio of the unknown temperature of stagnation T_0 in flow behind shock wave to the static temperature of the low-pressure gas T_1 is possible write in the form

$$\frac{T_0}{T_1} = f(M_1) + \frac{\varkappa_1 - 1}{2} \Phi^2(M_1). \tag{5}$$

whence one should expression for the dimensionless value of the temperature of stagnation in flow the shock wave

$$\bar{T}_0 = \frac{T_0}{V^2/(\varkappa_1 g R_1)} = \frac{f(M_1)}{\Phi^2(M_1)} + \frac{\varkappa_1 - 1}{2}. \tag{6}$$

One should consider that according to equation (3) to each value of parameter M_1 corresponds the specific value of the relative velocity of flow behind shock wave (piston speed) V/a_1.

Fig. 2, gives a change in the dimensionless value of the temperature of stagnation $\bar{T}_0$ depending on the relative speed V/a_1. It is evident that at the assigned/prescribed value of velocity v of flow behind shock wave (piston speed), an increase in the temperature

of the low-pressure gas T_1 leads to an increase in the attainable temperature of stagnation T_0. Thus, for instance, if parameter M_1 was located in the range $10 \leqslant M_1 \leqslant 20$, then during heating of low-pressure gas in shock tube it is possible it is more than to twice raise the temperature of stagnation T_0 in flow behind shock wave.

REFERENCES.

1. "Shock tubes". Coll. of article. Publ. foreign lit., 1962.

2. E. V. Stupochenko, S. A. Layev, A. I. Osipov. Relaxation processes in shock waves. M., "science", 1965.

3. H Oertel. Shock tubes. Springer-Verlag, Wien-New York, 1966.

Received 30/IV 1969.

Page 104.

BASE PRESSURE AFTER RECTANGULAR STEPS WITH DIFFERENT RATIOS OF HEIGHT TO THE WIDTH OF STEP.

G. N. Lavrukhin.

Are given the results of the experimental investigation of base pressure after rectangular steps with different ratios of height/altitude to the width of step at subsonic and supersonic speed of external flow.

Is given the empirical formula for determining the base pressure after rectangular steps, which considers the effect of the relative height/altitude of steps and Mach number of the incident flow.

At present is investigated in sufficient detail base pressure after axisymmetric and flat/plane steps [1] - [3]. As showed these investigations, in the case of turbulent boundary layer base pressure after the axisymmetric step higher than base pressure after flat/plane step on 10-15o/o with subsonic and on 30-40o/o at supersonic speeds of external flow. However, the information about base pressure after the steps of some "transitional" forms - oval,

rectangular with different ratios of height/altitude to the width of step and the like - is virtually absent.

Theoretical studies of base pressure after such steps encounters great difficulties due to the need for considering transverse overflowing for separation zones.

Article gives the results of the experimental investigation of base pressure after rectangular steps with different ratios of height/altitude to width. Investigations were conducted with Mach numbers of external flow 0-84-2.76.

Reynolds numbers changed in the range Re = 4.5-14•10⁶ as a result of a change both the length of the model and the total pressure in external flow.

Were investigated the models of two combinations (wedge - parallelepiped and cone - cylinder). The basis of model was central drain/vented plate 1, establish/installed on holding pylons 2 (Fig. 1). With the aid of interchangeable rectangular plates 3 and segmental extensions 4, fastened to central plate, they were compose/collected the body of combinations indicated above.

The width of rectangular steps remained for all models of

constant (b = of 70 mm). The relative height/altitude of step $\bar{h}$ (all linear dimensions are referred to the width of step) changed from 0.143 to 1.0. The relative length of models $\bar{l}$ changed from 3.43 to 5.15. The half-angle of the wedge of the nose section of the models was equal to 17°.

The model of combination cone - cylinder, that was being intended for the joining the results to known data, had diameter of the bottom section/shear D = of 70 mm, semiapex angle of cone of 17° and $\bar{l}$ = 3.43.

Models were establish/installed near the section/shear of two-dimensional nozzle of 5 wind tunnels with the open test section. In the process of experiment, was measured the base pressure, static pressure and Mach number in external flow. The location of static-pressure probes and the eleven receivers of base pressure is shown on Fig. 1.

Page 105.

Measurements showed that the static pressure on both sides of models virtually coincides and it is close to the static pressure external flow. This indicates the absence of the angle of attack of models and that at the selected length of the models of

disturbance/perturbation from spcut of bottcm section/shear they virtually attenuate.

A change of Re number (one and a half times) as a result of changing the length of model $\bar{l}$ from 3.43 to 5.15 with this Mach number of external flow did not virtually influence the value of base pressure. Apparently, and for the transitional forms of steps there is a region of self-similarity according to Re number, discovered for the axisymmetric and flat/plane steps (for example, see [4]).

Fig. 2, depicts the diagram/curves of pressure on the end/face of models with Mach number = 0.84. With the large Mach numbers, the form of diagram/curve is retained, changes only the level of base pressure. For the models, close in form to the flat/plane step (with value of $\bar{h} < 0.5$), is noted certain pressure increase on the edges of step, connected, apparently, with the emergence of intense tip vortexes. With an increase $\bar{h}$ during transition to step with square section/shear, the increase of base pressure in the edges of step becomes less noticeable. In the middle part of the steps, the base pressure is retained constant.

Subsequently during the analysis of test results for value $\bar{p}_s$ is accepted the base pressure, averaged on the height/altitude of step. Fig. 3, gives the averaged values of base pressure after

rectangular steps with diferent ratios of height/altitude to width. Here corrected values of base pressure for flat/plane step $\bar{p}_n^0$ and for axisymmetric step $\bar{p}_v^0$ averaged on the data of works [2] and [3].

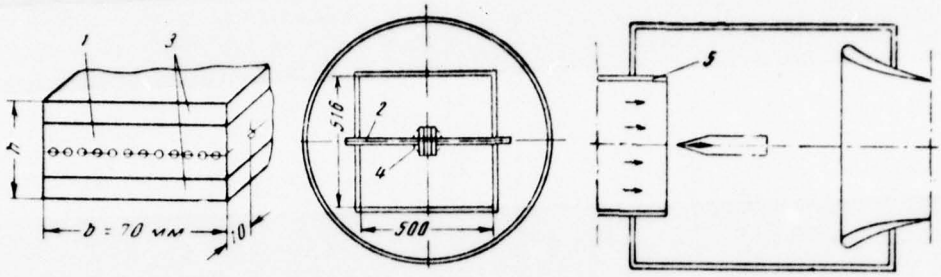

Fig. 1.

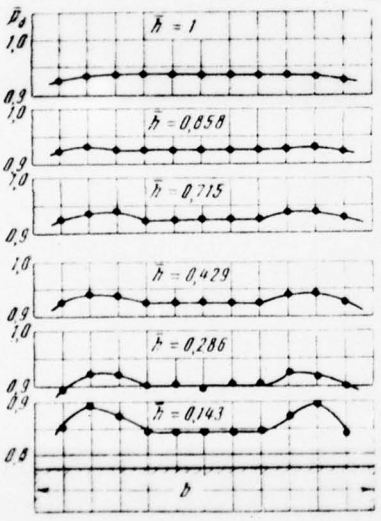

Fig. 2.

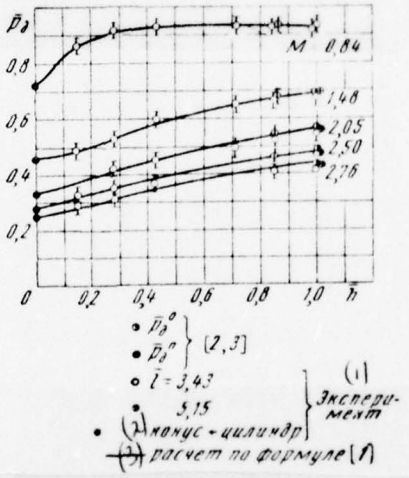

Fig. 3.

Key: (1). Experiment. (2). cone - cylinder. (3). calculation according to formula [1].

Page 106.

The experimental values of base pressure, obtained by the author on cylindrical model, are close to value p_1^0 for an axisymmetric step, which can serve as indirect proof of the fact that the pylons, which support models, were arrange/located at this distance from the bottom section/shear when their effect on the value of pressure virtually disappeared. The values of the base pressure cylindrical model and model with square bottom section/shear ($\bar{h} = 1.0$) virtually coincided with all Mach numbers of external flow.

With the decrease of the relative height/altitude of rectangular step, the base pressure decreases from the value of base pressure after axisymmetric step p_1^0 to the value of base pressure after flat/plane step p_1^n, moreover with an increase in Mach number of external flow the law of this change ever more approaches linear (curves for Mach numbers = 2.50 and 2.76; Fig. 3).

The values of base pressure after rectangular steps with the

relative height/altitude of step $\bar{h}$ and Mach number of external flow, obtained on the proposed empirical dependence

$$\bar{p}_1 = \bar{p}_1^0 - (\bar{p}_1^0 - \bar{p}_1^n)(1 - \bar{h}^{1,1})^m. \qquad (1)$$

where

$$m = 1,4 - \frac{1}{0,01 + M^{10}},$$

satisfactorily will agree with experimental values.

REFERENCES.

1. Korst H. H. A theory for base pressures in transonic and supersonic flow. Journal of Appl. Mech., 23, No. 4, pp. 593–600, 1956.
2. Chapman D. R. An analysis of base pressure at supersonic velocities and comparison with experiment. Report NACA, 1951, No. 1051.
3. Chapman D. R., Kuehn D. M., Korst H. H. Analysis and experiments of separated flow in supersonic and subsonic streams. IX Congress International de mecanique uppliquee, t. II, 1957.
4. Gadd G. E., Holder D. W., Regan J. D. Base pressure in supersonic flow. ARC C. P., 1956, No. 271.

Received 21/III 1969.

Page 107.

THE STRUCTURE OF POWERFUL SHOCK WAVE.

A. L. Stasenko.

It is proposed to find density profile in plane shock wave in the form of two branches of smooth function, which asimptotically tend for density values at infinity (before the wave and after it) with the dyne of the relaxation of the order of local mean free path. With arbitrary viscosity-temperature dependence, the task is reduced to quadratures, and for rigid and Maxwellian molecules it is solved in elementary functions. Is conducted the comparison with the results, obtained by other methods, which shows that the proposed examination is reasonable with Mach numbers of the incident flow on the order of three and it is above.

The proposed simple method of calculation of the parameters according to shock wave thickness can render/show useful for the rough estimates, for example, during the study of the passage of small solid particles, driving/moving in jet, through shock waves or during the determination of the effect of the strongly spraying jet, which escapes into evacuated space, on the macroscopic bodies whose

size/dimensions are comparable with the thickness of wave.

Let X-axis be perpendicular to shock wave, point x = 0 corresponds to the position of hydrodynamic discontinuity/interruption. Let us search for density distribution n(x) in the form continuous functions, with two branches:

$$\left.\begin{aligned} \frac{n-n_1}{n_0-n_1} &= \exp\left[\int_0^x \frac{dx}{\lambda(x)}\right], \quad x<0; \\ \frac{n_2-n}{n_2-n_0} &= \exp\left[-\int_0^x \frac{dx}{\lambda(x)}\right], \quad x>0. \end{aligned}\right| \tag{1}$$

where

$$\lambda = l\frac{u+\langle c\rangle}{\langle c\rangle} \qquad \left(l=\frac{2\mu}{mn\langle c\rangle}\right) \tag{2}$$

there is a mean free path of molecule in the system, connected with wave; l - mean free path in gas, determined through the coefficient of ductility/toughness/viscosity μ; m - molecular mass; u, $\langle c\rangle$ - macroscopic and average/mean thermal of gas velocity. Factor $(u+\langle c\rangle)/\langle c\rangle$ describes passage from one system to another: in the case of an intense shock wave, it is of the order of number M_1 in the incident flow before wave $(\langle c_1\rangle \gg u_1)$ and the order of one - for a wave $(\langle c_2\rangle \gg u_2)$. Indices by 0, 1, 2 are related to conditions in the "center" of wave, in the flow before the wave and after it at infinity.

Ductility/toughness/viscosity can be the arbitrary function of temperature T.

Page 108.

In relationship/ratios (1) are taken into account the conditions, by which must satisfy function r(x) at infinity and in zero: with $x \to -\infty$ we have $n \to n_1$, with $x \to +\infty$ we have $n \to n_2$ (asymptote), with $x \to \pm 0$ we have $n \to n_0$ (continuity).

From (1) after differentiation we obtain

$$\left.\begin{aligned} \frac{dv}{dx} &= \frac{v-1}{r} \quad (x<0); \\ \frac{dv}{dx} &= \frac{v_2-v}{r} \quad (x>0); \quad v=\frac{n}{n_1}. \end{aligned}\right\} \tag{3}$$

Requiring another equality the derived both branches of function $v(x)$ [or n(x)] at point x = 0, we obtain [taking into account continuity $v(x)$ and $\lambda(x)$] $v_0 - 1 = v_2 - v_0$, whence

$$v_0 = \frac{1}{2}(1+v_2). \tag{4}$$

Constructed thus function belongs to class C_1, since its second derivative at point x=0 suffers the discontinuity/interruption (analogous situation occurs, for example, in the case of the artificial ductility/toughness/viscosity of Neumann-Rikhtmayler, in

which second derivative of velocity profile is disruptive on the front/leading and rear boundaries of wave).

The thickness of wave from Prandtl is determined by the expression

$$L = \frac{v_2 - 1}{\left(\frac{dv}{dx}\right)_{max}} = \frac{v_2 - 1}{v_0 - 1} l_0. \qquad (5)$$

With $M \to 1$ the order of the tendency of values v_2 and v_0 toward unity is identical; consequently, the thickness L, limited by relationship/ratio (5), approaches final limit. This means that relationship/ratios (3) or equivalent to them relationship/ratios (1) are wrong for weak waves.

From the law of conservation of mass, we have

$$\rho u = \rho_1 u_1 = \rho_2 u_2. \qquad (6)$$

The law of conservation of energy let us accept in the form, analogous to Bernoulli's integral in the theory of the steady flow:

$$c_p T + \frac{u^2}{2} = c_p T_1 + \frac{u_1^2}{2} = c_p T_2 + \frac{u_2^2}{2}, \qquad (7)$$

where c_p - the heat capacity at a constant pressure.

This relationship/ratio is fulfilled at any point of wave only in the case of Prandtl's number Pr = 3/4; the latter is most close to

the value of number Pr for two- and triatomic molecules. In real/actual, according to Eucken's formula, number $Pr = \frac{4\varkappa}{9\varkappa - 5}$, where $\varkappa$ - relation heat capacity of gas, so that ratio 4Pr/3 is equal for such molecules 56/57 and 64/63 respectively. For monatomic gases Pr = 2/3 and the relation indicated is equal to 8/9.

Utilizing relationship/ratios (6), (7) and taking into account that

$$\varepsilon_2 = \frac{n_2}{n_1} = \frac{\frac{\varkappa+1}{2} M_1^2}{1 + \frac{\varkappa-1}{2} M_1^2},$$

let us knowingly satisfy all laws of conservation at infinity before and after wave.

Page 109.

From relationship/ratios (2), (6) and (7) we have

$$x = l_1 \left(\frac{\rho}{\rho_1}\right)^{\frac{1}{\nu+2}} \frac{\sqrt{\frac{\pi\varkappa}{8}} M_1 + \nu\sqrt{\theta}}{\theta}, \tag{8}$$

$$\theta = \frac{T}{T_1} = \left(1 + \frac{\varkappa-1}{2} M_1^2\right)^{\frac{1}{\nu+2}} \left[\varepsilon^{\nu} - \frac{\frac{\varkappa-1}{2} M_1^2}{1 + \frac{\varkappa-1}{2} M_1^2}\right], \tag{9}$$

where l_1 - mean free path in the gas before the wave. Substituting (8) in (3), we will obtain ordinary differential equations for two branches of the function of reverse/inverse to $v(x)$, solved in quadratures.

At least, for two cases - rigid ($\mu \sim \sqrt{T}$) and Maxwellian ($\mu \sim T$) molecules - quadratures for $x(\nu)$ can be expressed in the elementary functions:

for rigid molecules, $\mu/\mu_1 = \sqrt{\theta}$,

$$\left.\begin{aligned} \frac{x}{l_1} &= \left(I_1 + \frac{b}{a} I_2 - \frac{b}{\sqrt{1-a^2}} I_3\right)_{\nu_0}^{\nu}, \quad x \leq 0, \quad \nu \leq \nu_0; \\ \frac{x}{l_1} &= \left(\frac{1}{\nu_2} I_1' - \frac{b}{a\nu_2} I_2 + \frac{b}{\nu_2\sqrt{\nu_2^2 - a^2}} I_3'\right)_{\nu_0}^{\nu}, \quad x \geq 0, \quad \nu \geq \nu_0. \end{aligned}\right| \qquad (10)$$

for Maxwellian molecules, $\mu/\mu_1 = \theta$,

$$\left.\begin{aligned} \frac{x}{l_1 q} &= (bI_1 - aI_2 - \sqrt{1-a^2} I_3 + I_4)_{\nu_0}^{\nu}, \quad x \leq 0, \quad \nu \leq \nu_0; \\ \frac{x}{l_1 q} &= \left(\frac{b}{\nu_2^2} I_1' + \frac{a}{\nu_2^2} I_2 + \frac{\sqrt{\nu_2^2 - a^2}}{\nu_2^2} I_3' + \frac{a}{\nu_2^2} I_4\right)_{\nu_0}^{\nu}, \quad x \geq 0, \quad \nu \geq \nu_0; \end{aligned}\right| \qquad (11)$$

here

$$I_1 = \ln \frac{\nu - 1}{\nu};$$

$$I_1' = \ln \frac{\nu}{\nu_2 - \nu};$$

$$I_2 = \arcsin \frac{a}{\nu};$$

$$I_3 = \ln \frac{\sqrt{(1-a^2)(\nu^2-a^2)} + \nu - a^2}{\nu - 1};$$

$$I_3' = \ln \frac{\sqrt{(\nu_2^2-a^2)(\nu^2-a^2)} + \nu\nu_2 - a^2}{\nu_2 - \nu};$$

$$I_4 = \frac{b + \sqrt{\nu^2 - a^2}}{\nu};$$

$$a^2 = \frac{\frac{1}{2}(\varkappa - 1) M_1^2}{q^2};$$

$$b = \frac{\sqrt{\frac{\pi\varkappa}{8}} M_1^2}{q};$$

$$q^2 = 1 + \frac{1}{2}(\varkappa - 1) M_1^2.$$

Fig. 1 and 2, give the airfoil/profiles of shock waves for the case of rigid molecules, designed on formulas (10), and the airfoil/profiles, designed in work [1] according to Navier-Stokes equations, the method of Motte-Smith and Monte-Carlo. In Fig. 3, are constructed the density profiles and temperatures for the case of Maxwellian molecules on formulas (11) of present article and the airfoil/profiles, designed in work [2] according to Navier-Stokes equations, Motte-Smith's method and with the aid of elliptical (two-temperature) the distribution functions of molecules according to speeds.

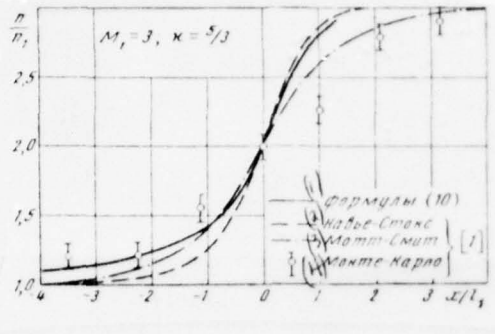

Fig. 1.

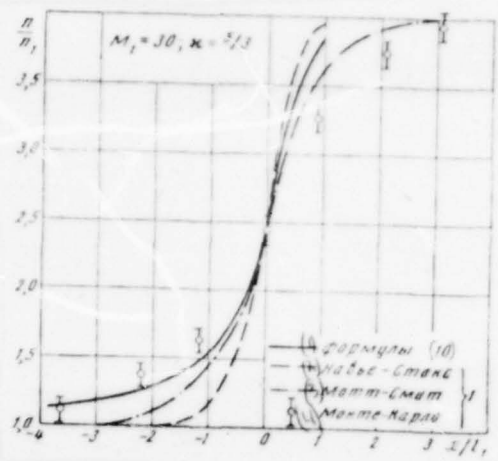

Fig. 2.

Fig. 1.

Key: (1). Formulas (10). (2). Navier-Stokes. (3). Motte-Smith. (4). Monte Carlo.

Fig. 2.

Key: (1). Formulas (10). (2). Navier-Stokes. (3). Motte-Smith. (4). Monte Carlo.

Page 110.

From the given curve/graphs it is evident that for the powerful

shock waves ($M \geqslant 3$) of the difference between the density profiles and temperatures, obtained by the enumerated methods (including proposed in this article) of one order. Furthermore, is noticeable powerful asymmetry (relative to the "center" of wave) obtained simple, is noticeable powerful asymmetry (relative to the "center" of wave) of the obtained density profile which was noted both in theoretical and in experimental [3], [4] investigations. In particular, Fig. 4 gives experimental data on the measurement of density distribution in shock wave by the method of electron beam [3]. Shock wave was obtained in air ($\varkappa = 1,4; M_1 = 6, p^1 = 10$ mm Hg) during the flow around disk and sphere by diameter $1.5 \cdot 10^{-2}$ m (white and black small circles respectively). In Fig. 4, are plotted also the results of the calculation of the airfoil/profile of wave, carried out by the author of work [3] according to Motte-Smith's method (dot-dash line). Unbroken curve - calculation according to formulas (11) for the Maxwellian molecules: in the range of temperatures $T_1 = 35^\circ K < T < 288^\circ K = T^\circ$ in flow the dependence of the ductility/toughness/viscosity of air on temperature is close to straight line $\mu \sim T$, moreover $\mu_1 = 2.5 \cdot 10^{-6}$ $kg \cdot m^{-1} \cdot s^{-1}$, whence mean free path in gas is obtained equal to $l_1 \approx 0.37 \cdot 10^{-3}$ to m. Fig. 4, shows that the convergence experimental data and theoretical results, obtained on the basis of the proposed method, sufficiently good.

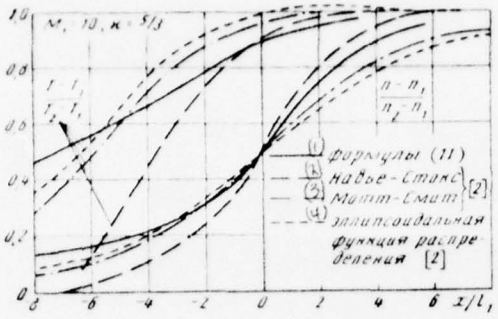

Fig. 3.

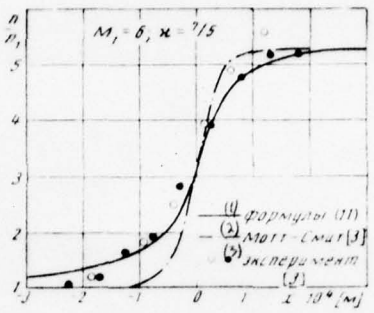

Fig. 4.

Fig. 3.

Key: (1). Formulas (11). (2). Navier-Stckes. (3). Motte-Smith. (4). ellipsoidal function of distributicn [2].

Fig. 4.

Key: (1). Formulas (11). (2). Motte-Smith. (3). experiment.

REFERENCES.

1. G A Bird. Shock-wave structure in a rigid sphere gas. Rarefied Gas Dynamics, Fourth Symp., vol. I, Acad. Press, 1965.

2. L H Holway. The effect of collisional models upon shock-wave structure. Rarefied Gas Dynamics, Fifth Symp., vol. I, Acad. Press, 1968.

3. A. V. Ivanov. The experimental determination of density distribution before the blunted bodies, streamlined with supersonic low-density flow. "appl. mat. and tech. phys.", 1964, No. 6.

4. I. V. Skokov, A. I. Akimov, G. I. Kremskiy. Determination of the airfoil/profile of shock wave by interferometric method. "Bull. of MGU", physics and astronomy, 1967, No. 1.

Received 21/III 1969.

BALLISTIC TUBE FOR DRAG MEASUREMENT ON MODELS IN FREE FLIGHT AT HYPERSONIC SPEEDS

L. P. Gur'yashkin, A. P. Krasil'shchikov, and V. P. Podobin

A brief description is given of a ballistic wind tunnel, the operating principle of which is based on the firing of models towards the supersonic flow in the wind-tunnel working section. The installation is intended for the measurement of the drag coefficient and for studying flow fields of axially symmetrical bodies in the range of supersonic and hypersonic flight velocities.

The range values of the M number in the ballistic wind tunnel is equal to 1.5-15. High resulting M numbers are obtained, in the first place, as a result of the firing of models towards the flow, and, in the second place, as a result of the lowering in the speed of sound in the working section of the supersonic wind tunnel by means of cooling of the air in transit through the nozzle. For the resulting M number the following expression is correct:

$$M = M_n + \frac{V}{a}.$$

where V - the speed of flight of the model relative to earth;

a - speed of sound in the flow;

M_n - number of M flow.

The values of the Reynolds number are obtained considerably higher than in wind tunnels at the same M number. The expression for the Reynolds number can be written in the form

$$Re = \frac{dV_n \rho}{\mu} + \frac{dV\rho}{\mu},$$

where d - the diameter of the midsection of the model;

V_n - flow velocity;

ρ - air density in the flow;

μ - viscosity of air in the flow.

The first term corresponds to the Re number of the model at zero velocity of the firing, and the second term - to the Re number during motion relative to earth. The Re numbers realized in the ballistic wind tunnel under various conditions of the experimentation are of the order of 10^6-10^7.

In ballistic installations the stagnation temperature increases with an increase in speed of the flight of the model [1]. The maximum stagnation temperature in the described installation is equal to ~2800°K.

Figure 1 gives a diagram of a ballistic wind tunnel which consists of three basic elements: the wind channel, rifle stand and electron optical equipment.

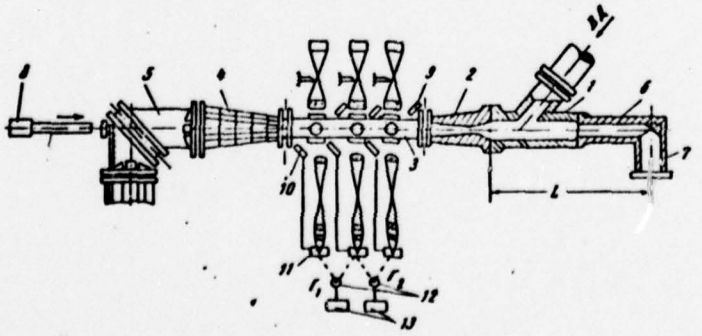

Fig. 1.

The wind tunnel is supersonic and operates in air of high pressure without preheating. The pressure in the antechamber 1 can reach 200 atm. The wind tunnel has interchangeable nozzles 2 calculated for numbers M_n = 2.5, 3 and 3.5. For the purpose of providing for the compensation of the boundary layer, the nozzles have an octahedral cross section. The inlet section of the working section 3, whose length is 24 gauges, has the shape of a correct octahedron with the diameter of an inscribed circle of 74.5 mm. In proportion to the distance from the inlet, the cross section of the working section increases because of a decrease in the area of the angular inserts, which accomplish a junction from the octahedral cross section to the square. In this case two pairs of opposite walls of the working section of the wind tunnel remain in parallel to each other. Installed on these walls are optical windows for photographing the model. The working section is closed by a subsonic diffuser 4 which is connected with a turning elbow 5.

The braking of model after the flight of the working section occurs in the high-pressure air in the phase of trajectory L, which consists of the internal cavity of the antechamber and tube 6 with the collector of the model 7 deflected 90°. The velocity of the model in this section decreases approximately 5-10 times.

The models were fired from smooth and threaded barrels 8 of the caliber 14.5 mm with flight velocities of 500-2000 m/s. The firing was conducted with Dural steel or brass models.

For the test work in the range of the low supersonic M numbers, the aerodynamic circuit of wind tunnel, i.e., the nozzle, working section and diffuser, was dismantled and in its place a thermal chamber was installed where the pressure could change from 1 to 15 atm. The inlet of the model into the thermal chamber with increased pressure was accomplished with the help of an explosive film gate.

The ballistic wind tunnel was equipped with three identical measuring stations for photographing the model and measuring the time between the moments of photographing. Each station is shadow system with a parallel light beam.

In a direction perpendicular to the optical axis of the shadow system, in the center of the photographing field there passes the plane of photoblocking, which is a slotted parallel light beam which goes from source 9 to the photoelectric pickup 10. To prevent the illumination of the photographic film by diffuse scattered light, the source is equipped with a light filter which displaces the spectrum of light into the region insensitive for photographic film. The model, flying through the working section, consecutively intersects the light beams of the photoblockings of three stations. The signal, which appears in the photosensitive device at the intersection of the light ray by the model, enters into the control unit of the spark light source 11. There occurs an intense light flash, and the model is fixed on the film of the camera of the first station. Simultaneously the impulse of the light of the spark source falls on photoelectric head Γ_1 12, which consists of the vacuum phototube STsV-4 and cathode follower. The electrical signal of the photoelectric head starts the first electronic chronometer 13. The second station works similar to the first with the only difference being that simultaneously there occurs the stopping of the first chronometer and the starting of the second one, which is stopped from the flash of the light source at the third station.

The thus obtained space-time dependence of the flight of the model was used for the calculation of the drag coefficient [2]. The accuracy of the measurement of time by the electronic chronometer is equal to $0.25 \cdot 10^{-6}$ s, and the accuracy of the measurement of the position of the model on the trajectory is equal to 0.2 mm.

Given below for an example are some experimental results obtained on the installation described.

Figure 2 depicts depending on the M number the values of the drag coefficient of the axisymmetric model with the conical expanding panel half-angle of aperture of which is equal to 35°. The head section of the model represents a cone with the half-angle of aperture equal to 15°. The length of the cylindrical part of the model is equal to 1.5d, and the ratio of the diameter of the cylindrical part to the diameter of the midsection of the model d/D = 0.565. A decrease in the drag coefficient in the range of M numbers of 1.5 to ~8 are caused by the change in the pattern of flow of the model. With a further increase in M number the drag coefficient does not change.

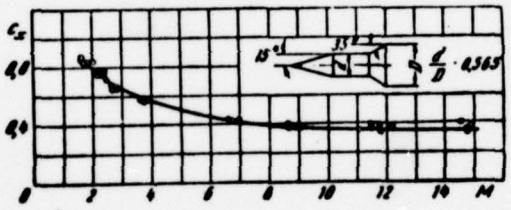

Fig. 2.

Figure 3 shows the changes in the drag coefficient of the ellipsoids of revolution at the fixed M numbers depending on the ratio of the semiaxis. (a - horizontal semiaxis, b - vertical semiaxis). An equidistant displacement of this dependence with a change in the M number is observed.

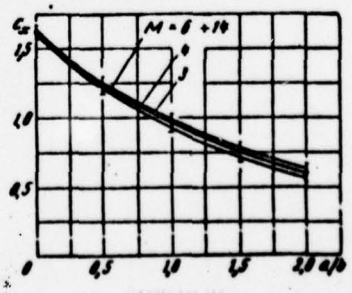

Fig. 3.

The development of the width of the turbulent nucleus of the wake behind the sphere of up to 3500 gauges in air at atmospheric pressure is shown on Fig. 4 in the form of dependences of $\bar{\delta}$ on $\bar{x}$ where $\bar{\delta} = \delta/d$ is the width of the turbulent nucleus referred to in the diameter of the midsection of the model, and $\bar{x} = d/x$ is the distance from the model to the place of the measurement of the width of the wake referred to the diameter of the midsection of the model. The turbulent wake behind the sphere in its near part at m = 2.8 and Re = 10^5 is shown on Fig. 5. For a comparison Fig. 4 shows test data from works [3] - [5] and the theoretical dependence [6] for M = 8.5. Despite the great difference in velocities all the test data agree well with each other. In the interval of the gauges from 30 to 3500 the development of the width of the turbulent wake can be approximated by empirical relation $\bar{\delta} = 0.2084\bar{x}^{-1/2}$.

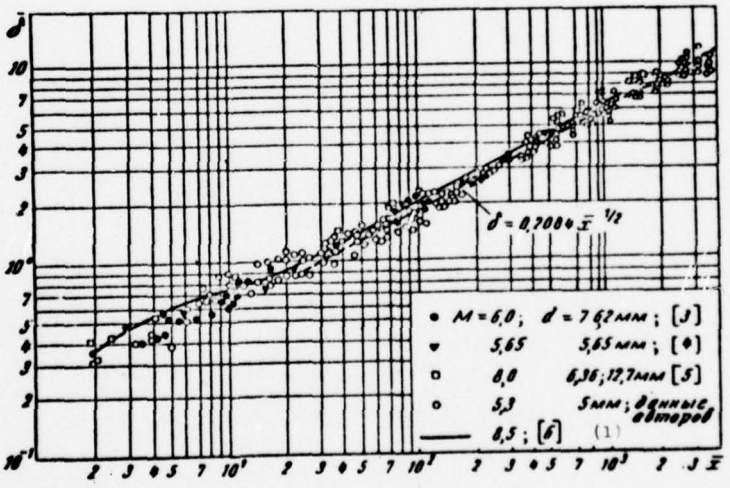

Fig. 4.
KEY: (1) Data of authors.

Fig. 5.

Bibliography

1. Seiff A. A. Free-flight wind tunnel for aerodynamic testing at hypersonic speeds. NACA Peport, 1922, 1955.

2. Красильщиков А. П., Подобин В. П. Экспериментальное исследование аэродинамических характеристик шара в свободном полете до чисел M = 15. Изв. АН СССР, Механика жидкости и газа, 1968, № 4.

3. Knystautas R., Growth of the turbulent juner wake behind 3-in Ciam spheres. AIAA Journ., vol. 2, No. 8, 1964.

4. Dana T. A., Short W. W. Experimental study of hypersonic turbulent wakes. Convair, San-Diego, Calif. Z. P.h. — 103 (May 1963).

5. Slattery R. E. Clay W. G. Width of the turbulent trail behind a hypervelocity spheres. „Phys. Fluids", 1961, 4, 1199 — 1201.

6. Lees L., Hromas L. Turbulent diffusion in the wake of a blunt-nosed body at hypersonic speeds. J. Aerospace sci., 1962, 29, p. 976—993.

Page 115.

THE EFFECT OF THE PROCESS OF OVERCHARGING ON THE EFFECTIVENESS OF IONIC SOURCE WITH VOLUMETRIC IONIZATION.

Yu. E. Kuznetsov, V. P. Rudakov.

Is examined the flat/plane model of ionic source with the distributed over its length neutral component of plasma.

It is shown, that the process of overcharging whose intensity is determined by the physical properties of gas (atomic weight, the section of overcharging and ionization) and by electron temperature, limits the value of the overall efficiency of the use of a mass.

The effectiveness of the work of ionic source is characterized by the value of the coefficient of the use of mass η (ratio of ion flow in by output/yield section to the consumption of the work substance, expressed in unity of equivalent ion current). Comparatively high effectiveness have sources with the ionization of

neutral particles by electron collision [1] - [5]. The maximum effectiveness of such sources is examined in work [6], in this case the process of overcharging in the volume of discharge is not examined.

Unlike the conditions of the accelerator of the plasma where the process of the distributed overcharging plays positive role [7], under conditions of ionic source this process can become barrier/obstacle for achievement of the high values of the coefficient of the use of a mass, since the rapid neutral particles, formed as a result of overcharging, have the low ionization probability.

In the present work are approximately examined the processes, which occur in the camera/chamber of ionization, taking into account overcharging.

The camera/chamber of ionization is considered plane. The neutral and ionic components of plasma move along coordinate x, perpendicular to chamber walls which are found under the potential, negative with respect to the potential of plasma. Is examined the case, when the potential difference near the electrode is greater than the electron temperature, expressed in electron volts. Through the left wall (Fig. 1a) occurs the inleakage of working

medium/propellant. The density of the incoming flow of work substance n_0 just as the densities of the flows of neutral particles in the camera/chamber, it will be expressed in unity of equivalent ion current, i.e., in amperes to square centimeter.

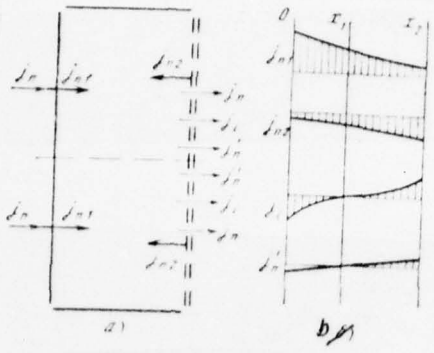

Fig. 1.

Page 116.

The discharge of ionic and neutral component occurs through the right wall - to riding-crop with transparency $\gamma = \frac{S_\infty}{S_к}$, where S_∞ - area of opening/apertures, $S_к$ - common/general/total area of chamber end. For ions and neutral particles, the effective transparency of grid is accepted identical and equal geometric transparency γ.

Neutral component let us consider consisting of three parts (Fig. 1b):

1) the flow of "cold" neutral particles with a density of $j_{n1}(x)$, driving/moving of left wall to the right (always positive).

2) the flow of "cold" neutral particles with a density of $f_{n2}(x)$, driving/moving from right wall to the left (always positive).

3) the flow of rapid neutral particles with a density of $f_n'(x)$, formed as a result of overcharging.

The first two unidirectional flows are characterized by certain average constant thermal velocity v_n, determined by the temperature of walls the third - by velocity v_n' whose average value the order of the velocity of ions v_i is determined by electron temperature.

High velocity and the light portion of the flow of rapid neutral particles in comparison with velocity and flow of cold neutral particles makes it possible to disregard in equations the terms, which consider secondary overcharging and the ionization of rapid neutral particles.

Let us consider that the ions move from certain section x_0 within the camera/chamber to the left and right walls (as this follows from work [8]), moreover on both walls ion currents are equal and are determined by Bohm's formula [9].

The neutral particles, which were being formed because of overcharging, move to the side of the action of ionic flows, i.e., on the left side of the camera/chamber to the left, and in the right side of the camera/chamber to the right (see Fig. 1b). In section x_1, the flow of these neutral particles is equal to zero.

Are accepted the following assumptions: in any section x, all ions have identical velocity $v_i(x)$, which depends only on x, moreover $v_i(x) = \frac{j_i(x)}{en_e}$; the mean free path of neutral particle before collision with neutral particle and with ion is much more the distance between the walls of source; electronic concentration and the distribution function of electrodes along X-axis are constant.

Within the framework of the adopted assumptions, the ion flows and rapid neutral particles, through the arbitrary section x taking place, are determined only by their generation and are expressed respectively by the following dependences:

$$dj_i(x) = en_e n_n \sigma_i v_e \, dx; \tag{1}$$

$$dj_n'(x) = en_e n_n \sigma_{\text{nep}} |v_i(x)| \, dx, \tag{2}$$

where n_n - a concentration of cold neutral particles,

$$n_n = \frac{j_{n1}(x) - j_{n2}(x)}{ev_n};$$

$\sigma_{\text{nep}} = \text{const}$ - the section of overcharging, accepted by constant in value in each section x [1];

$\overline{\sigma_i v_e}$ - averaged according to distribution function product of ionization cross section to the velocity of electrons.

FOOTNOTE 1. According to the estimation of the authors, introduced by this assumption error into the flow value of the recharged neutral particles, for the majority of work substances and in the real speed range of ions does not exceed 20o/c as a result of the logarithmic dependence of the section of symmetrical resonance overcharging on the module/modulus of relative velocity. END FOOTNOTE.

The flows of cold neutral particles, driving/moving from left to right and from right to left, are expressed by the respectively given below dependences and represent by themselves the loss/depreciation of neutral particles as a result of ionization and overcharging:

$$dj_{n1}(x) = -en_e n_n \overline{\sigma_i v_e}\, dx - en_e n_n \sigma_{\text{пер}} |v_i(x)|\, dx; \quad (3)$$

$$dj_{n2}(x) = en_e n_n \overline{\sigma_i v_e}\, dx + en_e n_n \sigma_{\text{пер}} |v_i(x)|\, dx. \quad (4)$$

Page 117.

Equations (1) - (4) for determining the constants it is necessary to supplement by the following boundary conditions:

$$j_n = j_{n1}(0) + j_{n2}(0) + j_i(0) + j_n'(0) \quad (x = 0); \tag{5}$$

$$j_n = j_{n1}(x_1) + j_{n2}(x_1) \quad (x = x_1); \tag{6}$$

$$-j_{n2}(x_2) = (1 - \gamma_i)[j_{n1}(x) + j_i(x_2) + j_n'(x_2)] \quad (x = x_2); \tag{7}$$

$$\gamma_i = \frac{j_i(x_2)}{j_n'(x_2) + j_i(x_2) + j_{n1}(x_2)} \quad (x = x_2). \tag{8}$$

The physical sense of expressions (5)-(7) is clear: the total flow of all particles is equal to consumption, and in section x_1, the ion flows and rapid neutral particles are equal to zero [see (5) and (6)]. From grid in section x_2 the neutral particles reflected and neutralized ions give counterflow of cold neutral particles (7). Condition (8) determines the coefficient of the use of a mass.

We will be restricted to the examination of the Maxwellian distribution function of electrons. Let us introduce the designations:

$\bar{\sigma}_i = \frac{\overline{v_e \sigma_i}}{v_e}$ - ionization cross section, averaged according to the Maxwellian distribution function of electrons.

$\bar{v}_e$ - the mean arithmetic velocity of electrons.

$j_i(0) = j_i(x_2) = kn_e v_e$ - Bohm's formula [9], in which $k \approx 0{,}2 \sqrt{\frac{\pi m_e}{M_i}}$

(where $\frac{m_e}{M_i}$ - ratio of the mass of electron to the mass of ion).

$A = \frac{k\sigma_{пер}}{e\sigma_i}$ - the parameter of overcharging.

Under flows $j_{n1}(x)$, $j_{n2}(x)$, $j_n'(x)$, $j_i(x)$ let us subsequently understand their relation to the module/modulus of the maximum strength of ion current $j_{i\infty}$ while under independent the variable x let us understand the dimensionless quantity, which represents by itself the ratio of longitudinal coordinate to the mean free path of neutral particle to the ionization:

$$l_i = \frac{v_n}{n_n v_e \sigma_i}.$$

Latter makes sense when the effectiveness of ionization does not depend on coordinate.

In the adopted designations we obtain the following system of differential equations:

$$dj_i(x) = [j_{n1}(x) - j_{n2}(x)]\,dx; \tag{9}$$

$$dj_n'(x) = A|j_i(x)|[j_{n1}(x) - j_{n2}(x)]\,dx; \tag{10}$$

$$dj_{n1}(x) = -j_{n1}(x)[1 + A|j_i(x)|]\,dx; \tag{11}$$

$$dj_{n2}(x) = j_{n2}(x)[1 + A|j_i(x)|]\,dx; \tag{12}$$

with the boundary conditions

$$j_n = j_{n1}(0) + j_{n2}(0) + j'_n(0) - 1 \quad (x=0); \tag{13}$$

$$j_n = j_{n1}(x_1) + j_{n2}(x_1) \quad (x = x_1); \tag{14}$$

$$-j_{n2}(x_2) = (1-\gamma)[j_{n1}(x_2) + 1 + j'_n(x_2)] \quad (x = x_2); \tag{15}$$

$$\gamma_1 = \frac{1}{j_{n1}(x_2) + 1 + j'_n(x_2)} \quad (x \geqslant x_2). \tag{16}$$

Page 118.

Solving together (9) and (10), let us have

$$\left.\begin{aligned} j'_n(x) &= \frac{A j_i^2(x)}{2} \quad \text{при} \quad j_i(x) > 0, \\ j'_n(x) &= -\frac{A j_i^2(x)}{2} \quad \text{при} \quad j_i(x) < 0. \end{aligned}\right| \tag{17}$$

Key: (1). with.

Then is determined the value of the current of rapid neutral particles on the boundaries:

$$\left.\begin{aligned} j'_n(x_2) &= \frac{A}{2} \quad (x = x_2); \\ j'_n(0) &= -\frac{A}{2} \quad (x = 0). \end{aligned}\right| \tag{18}$$

Let us replace of the differential of independent variable in equations (11) and (12) by the expression, obtained from (9),

$$dx = \frac{dj_i(x)}{j_{n1}(x) - j_{n2}(x)} \tag{19}$$

let us introduce the designations

$$\left.\begin{aligned} j_{n1}(x) + j_{n2}(x) &= y \\ j_{n1}(x) - j_{n2}(x) &= z. \end{aligned}\right\} \tag{20}$$

We will obtain the system of the differential equations

$$\left.\begin{aligned} dy &= -[1 + A|j_i(x)|]\,dj_i(x); \\ dz &= -\frac{y}{z}[1 + A|j_i(x)|]\,dj_i(x). \end{aligned}\right\} \tag{21}$$

Its solution taking into account boundary conditions and (18) takes the form:

in field $j_i(x) > 0$

$$\left.\begin{aligned} y &= j_n - j_i(x) - \frac{Aj_i^2(x)}{2}; \\ z &= \sqrt{2C_1 - 2j_n j_i(x) + (1 + Aj_n) j_i^2(x) + Aj_i^3(x) + \frac{A^2 j_i^4(x)}{4}}; \end{aligned}\right\} \tag{22}$$

in field $j_i(x) < 0$

$$\left.\begin{aligned} y &= j_n + j_i(x) + \frac{Aj_i^2(x)}{2}; \\ z &= \sqrt{2C_1 + 2j_n j_i(x) + (1 + Aj_n) j_i^2(x) + Aj_i^3(x) + \frac{A^2 j_i^4(x)}{4}}, \end{aligned}\right\} \tag{23}$$

where

$$C_1 = \frac{j_n^2}{2}\left(\frac{2}{\gamma} - 1\right)^2 - 2j_n\left(1 + \frac{A}{2}\right)\left(\frac{1}{\gamma} - 1\right).$$

Function z, proportional to the concentration of cold neutral particles, represents by itself their relative distribution along the length of the camera/chamber of ionization.

The fourth integral of systems (9)-(12) will be located during the solution of differential equation (9), written in the form

$$dx = \frac{dj_i(x)}{z}, \tag{24}$$

which it is necessary separately to integrate in two fields of the camera/chamber where $j_i(x) > 0$ and $j_i(x) < 0$.

Page 119.

Relative value of the consumption of working medium/propellant j_n in (22) and (23) can be expressed by dependence $j_n = \frac{\gamma}{\gamma_1}$, which ensues from the determination of the coefficient of the use of a working medium/propellant.

The results of numerical count for two different values and in different parameters of overcharging A are given to Fig. 2 and 3.

A system of differential equations (9)-(12) can be utilized for the case of the overlap of working medium/propellant from the side of grids.

In this case, will change only boundary conditions:

$$j_{n1}(0) = j_{n2}(0) + 1 + \frac{A}{2} \quad (x = 0); \tag{25}$$

$$j_{n1}(x_1) + j_{n2}(x_1) = 0 \quad (x = x_1); \tag{26}$$

$$-j_{n2}(x_2) = (1 - \gamma)\left[j_{n1}(x_2) + 1 + \frac{A}{2}\right] + j_n \quad (x = x_2); \tag{27}$$

$$\gamma_1 = \frac{\gamma}{j_{n1}(x_2) + 1 + \frac{A}{2}} \quad (x > x_2). \tag{28}$$

Respectively will change the integrals of the system:

in field $j_i(x) > 0$

$$\left.\begin{aligned} y &= -j_i(x) - \frac{A j_i^2(x)}{2}; \\ z &= \sqrt{j_i^2(x)\left[1 + \frac{A}{2} j_i(x)\right]^2 + 2C_2}; \end{aligned}\right| \tag{29}$$

in field $j_i(x) < 0$

$$\left.\begin{aligned} y &= j_i(x) + \frac{A j_i^2(x)}{2}; \\ z &= \sqrt{j_i^2(x)\left[1 + \frac{A}{2} j_i(x)\right]^2 + 2C_2}, \end{aligned}\right| \tag{30}$$

where

$$C_2 = \frac{2j_n}{\gamma}\left(\frac{j_n}{\gamma} - 1 - \frac{A}{2}\right).$$

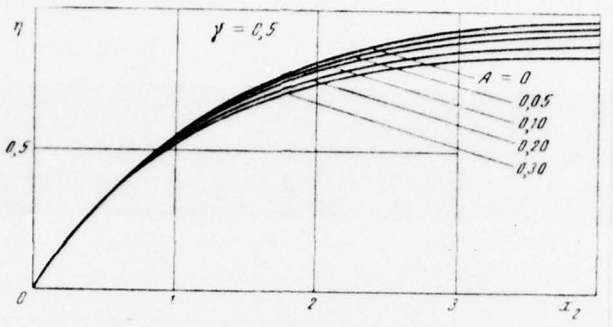

Fig. 2.

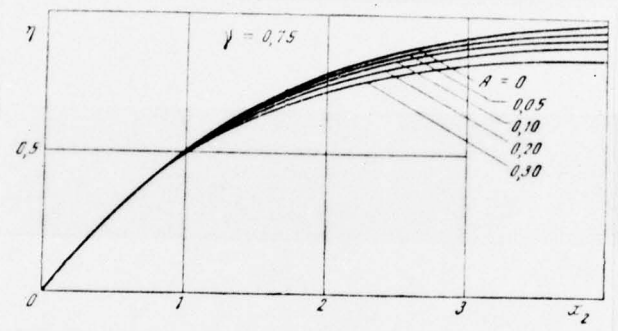

Fig. 3.

Page 120.

Value $\eta = f(x_2)$, obtained for this case, does not detect dependence on the transparency of grid (Fig. 4).

From (18) follows the interesting universal dependence: the ratio of the flow of the recharged neutral particles to ion current

on the boundary of plasma (in the examined one-dimensional case) is always equal to value A/2.

Recall that the constant A depends only on the physical properties of gas (atomic weight, the section of overcharging and ionization) and of electron temperature and, that very substantially, directly it does not depend on the value of the camera/chamber.

From (16) and (28) it is evident that the upper limit of the value of the coefficient of the use of a mass even for the sufficiently long camera/chambers is the expression

$$\eta = \frac{1}{1 + \frac{A}{2}}. \qquad (31)$$

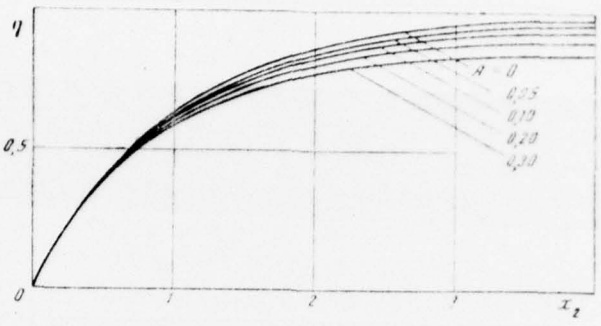

Fig. 4.

REFERENCES

1. P. M. Morozov, E. N. Makov, M. S. Joffe. Source of polyvalent ions for a cyclotron. "atomic energy", 1957, No 3.

2. P. M. Morozov, L. N. Pigul'nov. Source of molecular hydrogen ions for installation "Ogra [Огра - Soviet thermonuclear mirror machine]". Journal technical physics", Vol. XXXIII, iss. 470, 1963.

3. M. D. Gabovich. Plasma ion sources. Kiev, "Scientific Thought", 1964.

4. H R Kaufman, P D Beader. Experimental performance of ion

rocket employing electron-bombardment ion source. Progr. Astron. Rocketry, Vol. 5, 1961.

5. P. D. Reader. Scall effects on ion rocket performance. ARS-J., Vol. 5, 1962.

6. G. I. Slobadenyuk. Calculation of the maximum effectiveness of ionic sources with ionization by electron collision. The "Jour. of Technical Physics", Vol. XXXVIII, iss. 1182, 1968.

7. J. White, U. D. de. Use of the distributed overcharging in the accelerators of plasma. In the collection "applied magnetchydrodynamics". M., "peace/world", 1965.

8. O. B. Firsov. Current of positive ions to the electrodes of vacuum arc. The "Journal of Technical Physics", Vol. XXVI, iss. 445, 1956.

9. D Bohm. The characteristics of Electrical Discharges in Magnetic Fields, Edited by Guthrie, Wakerling, N. Y., 1949.

The manuscript will enter 12/V 1969.

THE VERSION OF DISPERSION METHOD AND THE TASKS OF BOUNDARY LAYER STABILITY.

V. M. Lutovinov.

Is examined the version of dispersion method for the systems of the differential second order equations. Is noted its communication/connection with the task of the factorization of linear differential expression. Is shown the possibility of applying the method for the numerical solution of the tasks of boundary layer stability within the framework of linear theory.

Let us examine the solution of boundary-value problem for the system of the differential equations of the second order

$$\vec{\Psi}'' - A\vec{\Psi} = \vec{F}. \qquad (1)$$

Let on one of the ends of the cut of integration ab, for example, with y = b the boundary conditions be arbitrary relatively $\vec{\Psi}$ and $\vec{\Psi}'$; but on other - with y = a they take the form

$$\vec{\Psi}' + K\vec{\Psi} = \vec{\gamma};$$

here

$$\vec{\Psi} = \vec{\Psi}(y) = \begin{Vmatrix} \Psi_1 \\ \cdot \\ \cdot \\ \cdot \\ \Psi_n \end{Vmatrix}; \quad \vec{\Psi}' = \frac{d}{dy}\vec{\Psi}; \quad \vec{\gamma} = \begin{Vmatrix} \gamma_1 \\ \cdot \\ \cdot \\ \cdot \\ \gamma_n \end{Vmatrix}; \quad \vec{f} = \begin{Vmatrix} f_1 \\ \cdot \\ \cdot \\ \cdot \\ f_n \end{Vmatrix}; \qquad (1)$$

$$A = A(y) = \begin{Vmatrix} a_{11} \cdots a_{1n} \\ \cdot \quad\quad \cdot \\ \cdot \quad\quad \cdot \\ a_{n1} \cdots a_{nn} \end{Vmatrix}; \quad K = \begin{Vmatrix} k_{11} \cdots k_{1n} \\ \cdot \quad\quad \cdot \\ \cdot \quad\quad \cdot \\ k_{n1} \cdots k_{nn} \end{Vmatrix};$$

a_{ij} and k_{ij} - complex numbers (i, j = 1, ..., n).

On the basis of the ideas of the dispersion method of Gelfand and Lokutsiyevskiy [1], let us search for matrix/die B = B(y) and vector $\vec{\Phi} = \vec{\Phi}(y)$, where

$$B = \begin{Vmatrix} b_{11} \cdots b_{1n} \\ \cdot \quad\quad \cdot \\ \cdot \quad\quad \cdot \\ b_{n1} \cdots b_{nn} \end{Vmatrix}; \quad \vec{\Phi} = \begin{Vmatrix} \Phi_1 \\ \cdot \\ \cdot \\ \cdot \\ \Phi_n \end{Vmatrix},$$

which satisfy

$$\vec{\Psi}' + B(y)\vec{\Psi} = \Phi; \qquad (2)$$

$$B(a) = K; \quad \vec{\Phi}(a) = \vec{\gamma}. \qquad (3)$$

Page 122.

Differentiating (2) and utilizing (1) and (2), we will obtain $\vec{\Psi}'' + (B' - B^2)\vec{\Psi} = \vec{\Phi} - B\vec{\Phi}$. Since $\vec{\Psi}$ is solution (1) and satisfies (1'), matrix/die B vector function $\vec{\Phi}$ they must satisfy

$$B' - B^2 = -A; \tag{4}$$

$$\vec{\Phi}' - B\vec{\Phi} = \vec{F}; \tag{5}$$

$$B(a) = K; \quad \vec{\Phi}(a) = \vec{\gamma}. \tag{6}$$

Integrating systems (4), (5) with initial conditions (6), we will obtain at point y = b of conditions, which are missing for the investigation of the solvability of boundary-value problem. After determining, if this is possible, $\vec{\psi}(b)$, let us find via reverse/inverse screw die $\vec{\psi}(y)$, solving the problem of Cauchy for equation (2).

It is possible to show that

$$B = -\left(\frac{d}{dy}U\right)U^{-1}; \tag{7}$$

here $U = \|\vec{\varphi}_1 \dots \vec{\varphi}_n\|$, $\vec{\varphi}_i$ there is n of the linearly independent solutions $\vec{\phi}'' - A\vec{\phi} = 0$, which satisfy $\vec{\phi} + K\vec{\phi} = 0$ with y=a; U^{-1} - matrix/die, reverse/inverse U.

The described method, as other dispersion methods, can be obtained from the theorem about the factorization of linear differential expression [2]. From this same theorem follows the continuous differentiability of matrix elements B.

During the study of boundary layer stability within the framework of linear theory, it is necessary for the equation of Orr-Sommerfeld

$$\varphi^{IV} - 2\alpha^2\varphi'' + \alpha^4\varphi = i\alpha R[(v-c)(\varphi'' - \alpha^2\varphi) - v''\varphi] \tag{8}$$

with the boundary conditions

$$\left.\begin{aligned}&\varphi''' + \alpha\varphi'' - \beta^2(\varphi' + \alpha\varphi) = 0;\\ &\varphi''' + \beta\varphi'' - \alpha^2(\varphi' + \beta\varphi) = 0\end{aligned}\right\} \text{при } y = \delta; \tag{9}$$

$$\varphi = \varphi' = 0 \quad \text{при} \quad y = 0 \tag{10}$$

Key: (1). with

to determine among eigenvalues R, α, $c = c_r + ic_i$ of boundary-value problem (8)-(10) the field where there exist $c_i > 0$.

Equation (8) and boundary conditions (9) can be presented in the form

$$\tilde{\Psi}'' - A\tilde{\Psi} = 0; \tag{11}$$

$$\tilde{\Psi}' + K\tilde{\Psi} = 0 \quad \text{with} \quad y = \delta; \tag{12}$$

here

$$\tilde{\Psi} = \begin{Vmatrix} \varphi \\ \varphi'' - \alpha^2\varphi \end{Vmatrix};$$

$$A = \begin{Vmatrix} \alpha^2 & 1 \\ -i\alpha R v'' & \alpha^2 + i\alpha R(v - c) \end{Vmatrix};$$

$$K = \begin{Vmatrix} \alpha & \dfrac{1}{(\alpha + \beta)} \\ 0 & \beta \end{Vmatrix}.$$

Page 123.

The dispersion method in question is led in this case to the integration of the system

$$B' = B^2 - A \tag{13}$$

with the initial conditions

$$B(3) = K. \qquad (14)$$

The investigation of a question concerning the affiliation/accessory of the values of parameters R, α, c, with the number of its own is reduced taking into account (10) to checking of condition $b_{12}(0)=0$. The presence of communication/connection (7) gives grounds to rely on the stability of the process of integration (13). This is confirmed by numerical experiments.

Let us note that the method in question can be used also to the stability analysis of jets.

REFERENCES

1. L. S. Berezii, N. P. Zhidkov. Methods of calculations. T. 2. Fizmatgiz, 1959.

2. V. F. Zhdanovich. On the factorization of linear differential expression. The "successes of math. sciences", Vol. XVI, iss. 4 (100), 1961.

The manuscript will enter 12/V 1969.

DISTRIBUTION LIST

DISTRIBUTION DIRECT TO RECIPIENT

ORGANIZATION		MICROFICHE
A205	DMATC	1
A210	DMAAC	2
B344	DIA/RDS-3C	9
C043	USAMIIA	1
C509	BALLISTIC RES LABS	1
C510	AIR MOBILITY R&D LAB/FIO	1
C513	PICATINNY ARSENAL	1
C535	AVIATION SYS COMD	1
C591	FSTC	5
C619	MIA REDSTONE	1
D008	NISC	1
H300	USAICE (USAREUR)	1
P005	ERDA	1
P005	CIA/CRS/ADB/SD	1
NAVORDSTA (50L)		1
NASA/KSI		1
AFIT/LD		1

ORGANIZATION		MICROFICHE
E053	AF/INAKA	1
E017	AF/RDXTR-W	1
E403	AFSC/INA	1
E404	AEDC	1
E408	AFWL	1
E410	ADTC	1
E413	ESD	2
	FTD	
	CCN	1
	ASD/FTD/NICD	3
	NIA/PHS	1
	NICD	2